

Urban stormwater infiltration: assessment and enhancement of pollutant removal.

[DNR-102] 1992

Armstrong, David E.; Cowell, Susan E.

Madison, Wisconsin: Wisconsin Department of Natural Resources, 1992

<https://digital.library.wisc.edu/1711.dl/O3IEEQKAXC5PQ8H>

<http://rightsstatements.org/vocab/InC/1.0/>

For information on re-use see:

<http://digital.library.wisc.edu/1711.dl/Copyright>

The libraries provide public access to a wide range of material, including online exhibits, digitized collections, archival finding aids, our catalog, online articles, and a growing range of materials in many media.

When possible, we provide rights information in catalog records, finding aids, and other metadata that accompanies collections or items. However, it is always the user's obligation to evaluate copyright and rights issues in light of their own use.

172681

Urban Stormwater Infiltration:
Assessment and Enhancement of
Pollutant Removal

Water Resources Center
University of Wisconsin - ~~MADISON~~
1975 Willow Drive
Madison, WI 53706

112
UNIVERSITY
of
\$175

Urban Stormwater Infiltration: Assessment and

Enhancement of Pollutant Removal

Water Resources Center
University of Wisconsin - MSN
1115 Willow Drive
Madison, WI 53706

Principal Investigator: Dr. David Armstrong

Research Assistant: Sue Cowell

Table of Contents

List of Tables	vii
List of Figures	viii
I. Introduction	
Stormwater	1
Overview of Problem	1
Stormwater Compositions	1
Stormwater Management	13
II. Background	17
Contaminant Transport during Stormwater Infiltration.	17
Saturated and Unsaturated Flow	17
Proposed Models	22
Subsurface Fate of Organic Contaminants	37
Subsurface Fate of Metal Contaminants	44
III. Research Objective	49
IV. Materials and Methods	50
Soils	50
Simulated Stormwater	53
Batch Experiments	54
Organic Contaminant Batch Experiments	54
Metal Contaminant Batch Experiments	60
Column Experiments	63
V. Results and Discussion	67
Organic Contaminants	67
Partitioning in Batch Systems	67
Metal Contaminants	105
Partitioning in Batch Systems	105
Partitioning and Transport in Soil Columns	121
VI. Conclusions	141

VII.Recommendations for Future Research	143
References	145

List of Tables

1-1	Contaminants Found in Wisconsin Stormwater.	3
1-2a	Various Metal Concentrations in the <63 um Size Fraction of Street Sweepings (Wilber and Hunter, 1979).	4
1-2b	Exchangeable Metals Levels in Street Sweepings	4
1-3	Particle Size Distribution of Street Solids from Chicago Illinois	4
1-4	Ranges of Calcium, Magnesium, Sodium, Chloride, Ionic Strength and pH in Wisconsin Stormwaters	7
4-1	Soil Physical and Chemical Characteristics	24
4-2	Simulated Stormwater	25
4-3	Chemical Properties	27
5-1	Soil Characteristics	32
5-2	Sparta Soil Column Specifications	47, 71
5-2	Sparta Soil Column Specifications	50
5-3	St Charles Silt Loam Column Specifications	100

List of Figures

1-1	Generic Stormwater Contaminant Concentration History	11
2-1	Illustration of 1D Advection/Dispersion v Retardation	26
2-2	Peclet Number and Dominant Transport Processes	29
2-3	Nonequilibrium Sorption	32
2-4	Ionization of Organic Contaminants	39
4-1	Chemical Structures of Atrazine, Phenanthrene and Fluoranthene	55
4-2	Column Apparatus	64
5-1	Sparta Sand Atrazine Partitioning Kinetics	70
5-2	Sparta Sand DOC Versus Atrazine Kd	72
5-3	Sparta Sand PAH Sorption Kinetics	73
5-4	Sparta Sand PAH Versus Dissolved Atrazine	74
5-5	Sparta Sand Atrazine Desorption Kinetics	78
5-6	Sparta Sand Phenanthrene Desorption Kinetics	79
5-7	Sparta Sand Fluoranthene Desorption Kinetics	81
5-8	St Charles Silt Loam Atrazine Partitioning Kinetics	83
5-9	St Charles Silt Loam PAH Partitioning Kinetics	84
5-10	Pals Grove Silt Loam Atrazine Partitioning Kinetics	86
5-11	Pals Grove Silt Loam PAH Partitioning Kinetics	88
5-12	Atrazine Experimental Kd Value Correlation With Soil Characteristics	91
5-13	Bromide Tracer Concentration History	92
5-14	Sparta Sand Atrazine Concentration History	95
5-15	Sparta Sand Cumulative Atrazine Mass	96
5-16	St Charles Silt Loam Column Tritium Concentration History and Cumulative Mass	101
5-17	St Charles Silt Loam Column Bromide Concentration Profile	102
5-18	St. Charles Silt Loam Column Atrazine Concentration History and Cumulative Mass	103
5-19	Zinc and Copper Stormwater Speciation	106
5-20	Zinc (50 $\mu\text{g/L}$) and Copper (20 $\mu\text{g/L}$) Partitioning Kinetics	108
5-21	Dissolved Zinc and Copper Versus DOC	109
5-22	Zinc (100 $\mu\text{g/L}$) and Copper (40 $\mu\text{g/L}$) Versus Zinc (50 $\mu\text{g/L}$) and Copper (20 $\mu\text{g/L}$) Partitioning	111

5-23	Zinc and Copper Kd Values for All Three Soils . . .	114
5-24	Zinc Log Kd Value Versus Soil Silt, Clay and Organic Matter	116
5-25	Copper Log Kd Value Versus Soil Silt, Clay and Organic Matter	117
5-26	Soil Organic Matter and Silt Content	118
5-27	Zinc and Copper Log Kd Value Versus Soil Organic Matter	119
5-28	Copper Log Kd Value Versus Soil Calcium	120
5-29	Sparta Sand Continuous Input Column pH, DOC, and Conductivity	122
5-30	Sparta Sand Continuous Input Column Colloid Production	125
5-31	Sparta Sand Continuous Input Column Effluent Calcium, Magnesium and Sodium	127
5-32	Sparta Sand Continuous Input Column Effluent Zinc and Copper	128
5-33	Sparta Sand Continuous Input Column Conservative Tracer	130
5-34	Sparta Sand Continuous Input Zinc Transport	131
5-35	Sparta Sand Slug Input Column Effluent pH, DOC and Conductivity	134
5-36	Sparta Sand Slug Input Column Colloid Production	135
5-37	Sparta Sand Slug Input Column Effluent Calcium, Magnesium and Sodium	137
5-38	Sparta Sand Slug Input Column Effluent Zinc and Copper	138
5-39	Sparta Sand Slug Input Column Zinc and Copper Transport	139

I. Introduction

A. Stormwater

1. Overview of Problem

Urban stormwater contains a variety of organic and inorganic chemical "pollutants". Thus, discharge of stormwater to surface water, a common practice, raises concern over the impact on water quality of the receiving waters (lakes and streams). One alternative is treatment of stormwater in municipal wastewater treatment plants, but large variations in stormwater loadings creates problems with plant capacity. Infiltration through soil is another alternative for stormwater disposal. Adsorption, degradation, and other processes may remove pollutants, allowing "clean" water to recharge the groundwater system. However, if pollutants migrate into the groundwater, infiltration may be an unacceptable method of stormwater management. Availability of sites for infiltration is another important limitation.

In order to understand the advantages and disadvantages of infiltration as a stormwater management practice, information

on stormwater composition and alternative management methods is briefly reviewed.

The term "stormwater" is used in this report to encompass runoff water in urban areas derived from water from rainfall events, snowmelt, combined sewer overflows and dry weather baseflow. Both stormwater quantity and quality can cause adverse environmental impacts and are regulated directly or indirectly through several state and federal statutes. Although stormwater quantity may be a very pertinent concern, this report will focus solely upon stormwater quality.

State and federal statutes are requiring states and municipalities to minimize stormwater environmental impacts. Several Wisconsin state statutes apply directly to stormwater management. The stormwater permit program (Clean Water Act, section 402(p)) requires permits for discharges from municipal separate stormwater sewers for large (greater than 250,000), medium (greater than 100,000) urban areas, and for industrially-related stormwater discharges. Permits may also be required for stormwater discharges on a case-by-case basis (Prey et al., 1994). Other state statutes relating to the

quality of surface and groundwater may indirectly influence stormwater discharge management.

2. Stormwater Compositions

Stormwater routinely contains a myriad of contaminants (Table 1-1) which vary with land use and season of the year. Particulates, nutrients, oxygen demanding material, bacteria, trace metals, pesticides, and toxic chemicals (such as polycyclic aromatic hydrocarbons or PAHs) have been identified by the Wisconsin Department of Natural Resources as contaminants of concern in stormwater (Prey et al., 1994).

Table 1-1 Frequently Detected Contaminants in Wisconsin
Stormwater Armstrong and Llena, 1992).

PAHs, PCBs, Phthalates Pesticides

Group 1 - Pollutants Exceeding Surface and Groundwater Criteria

Lead (2)	Fluoranthene (3)
Bacteria (2)	Pyrene
	Phenanthrene
	Benzo(ghi)Perylene
	Benzo(a)Anthracene
	Indeno(1,2,3) Pyrene
	Benzo(b) Fluoranthene
	Benzo(k) Fluoranthene
	Fluorene
	Anthracene
	Acenaphthlene
	PCBs (3)

Group 2 - Pollutants Exceeding Groundwater Enforcements Standards

Chromium	Bis(2-ethylhexyl)phthalate (3)
Chloride	

Group 3 - Pollutants Exceeding Groundwater Preventive Action Limits

Cadmium	Cyanazine
Arsenic	Metolachlor
Selenium	2,4-D
Antimony	Chlordane
Nitrate	

Group 4 - Pollutants Exceeding Only Surface Water Criteria

Zinc	Malathion (4)
Copper	Diazinon (4)

Group 5 - Pollutants Not Exceeding Any Criteria

Nickel (3)	Pentachlorophenol
	Metoxychlor
	Dicamba
	Dacthal Metabolites (5)

Notes

- (1) All pollutants listed occurred in 10 % or more of the samples.
- (2) Pollutants exceeding enforcement standard for groundwater.
- (3) Based on acute toxicity levels - criteria not available.
- (4) Not analyzed in the sample set.

While contaminants are the major concern, the stormwater matrix (major components) should also be considered when assessing contamination potential. Contaminant concentrations also vary with stormwater quantity and storm duration.

Many metals and hydrophobic organic contaminants are partly associated with particulate phases (Shaw and Berndt, 1990; Dean, 1993; Herrin, 1994) and may be concentrated within certain size fractions of these particulate materials (Michelbach and Wohrle, 1992). Table 1-2a lists various metals associated with street sweeping particulates, whereas Table 1-2b illustrates the percent of the total particulate metal which is considered "available", where available metal is defined as the fraction exchangeable with ammonium acetate at pH 7. Table 1-3 compares particulate size distributions in stormwater from urban and industrial areas. In addition to providing transport for contaminants, particulate matter can decrease aesthetic values of streams and alter fish populations. Phosphorus is the primary stormwater nutrient of concern, since phosphorus may promote weed and algae growth in freshwater lakes and streams. Land use may be a ~~a~~ very

Table 1-2a Various Metal Concentrations in the <63 μm Size Fraction of Street Sweepings
(Wilber and Hunter, 1979).

Concentrations mg/kg

	Pb	Zn	Cu	Ni	Cr	Mn	Fe
Residential	2110	464	75	36	43	301	27500
Industrial	2520	2580	3170	9840	1450	1450	128000
Traffic Intersection	8300	1110	500	51	69	331	38000

Table 1-2b Exchangeable Metals Levels in Street Sweepings Wilber and Hunter, 1979)

Exchangeable Metal (% of Total Metal)

	Pb	Zn	Cu	Ni	Cr	Mn	Fe
Residential	38.88	26.10	7.7	18.48	4.41	10.71	0.04
Industrial	1.85	5.68	16.19	0.42	0.24	2.50	0.004
Traffic Intersection	28.32	24.39	3.91	17.66	0.47	3.80	0.02

Table 1-3 Particle Size Distribution of Street Solids from Chicago Illinois (Klemetson, 1985)

Percent Distribution by Weight

Size range (μm)	Commercial	Industrial	Average
2000	5.8	3.4	4.6
1190-2000	7.8	7.0	7.0
840-1190	5.2	6.4	5.8
590-840	6.6	12.8	9.7
840	74.5	70.4	72.5

important indicator of phosphorus contamination potential. Average phosphorus concentrations amounts in urban land runoff were reported to be twice that found in runoff from rural land (Shaw and Berndt, 1990). Nitrogen compounds in stormwater may be converted to nitrate in soil and pose a threat to groundwater quality (Pitt et al, 1993).

Oxygen demanding materials, such as leaf litter, may influence water quality by depleting oxygen in receiving waters. Sudden fish kills may occur if large pulses of oxygen demanding material are flushed into a waterway. Oxygen depletion may also influence concentrations and forms of chemical contaminants by causing associated changes in chemical reactions and speciation.

Fecal coliforms are used as indicators of bacterial contamination. Bannerman et al. (1993) reported fecal coliform counts in stormwater ranging from 20 to 40 times above swimming health standard levels. In addition, enteric bacteria and viruses are also routinely found in stormwater (Pitt et al, 1993).

Common trace metals in stormwater include lead, zinc, copper, chromium and cadmium (Prey et al., 1994). Vehicular traffic is a primary source for these metals, although roof top materials may be sources of zinc and copper (Prey et al., 1994; Bannerman et al., 1993).

Pesticides are frequently detected in stormwater. Even some agricultural pesticides such as atrazine which are not commonly used in urban areas are detected in urban stormwater (Prey et al., 1994). Apparently, volatilization and wind-blown soil lead to transport by air and subsequent deposition in urban area through precipitation and/or dry deposition.

A wide array of toxic contaminants may be found in stormwater. The two primary classes of organic compounds identified by the Wisconsin Department of Natural Resources (Prey et al., 1994) in stormwater are polychlorinated biphenyls (PCBs) and polycyclic aromatic hydrocarbons (PAHs). PCBs are persistent organic chemicals which tend to bioaccumulate in aquatic foodwebs. Though widespread use in electric capacitors, and transformers, hydraulic fluids, and other commercial products, PCBs have become distributed world-

wide through transport by air and water. PAHs identified in surface and groundwater are benzo-a-pyrene, benzo-ghi-perylene, chrysene, pyrene, fluoranthene and phenanthrene (Prey et al., 1994). A primary source of PAHs is incomplete combustion of organic compounds because combustion with insufficient oxygen which forms C-H free radicals which can polymerize to form various PAHs (EPA, 1980).

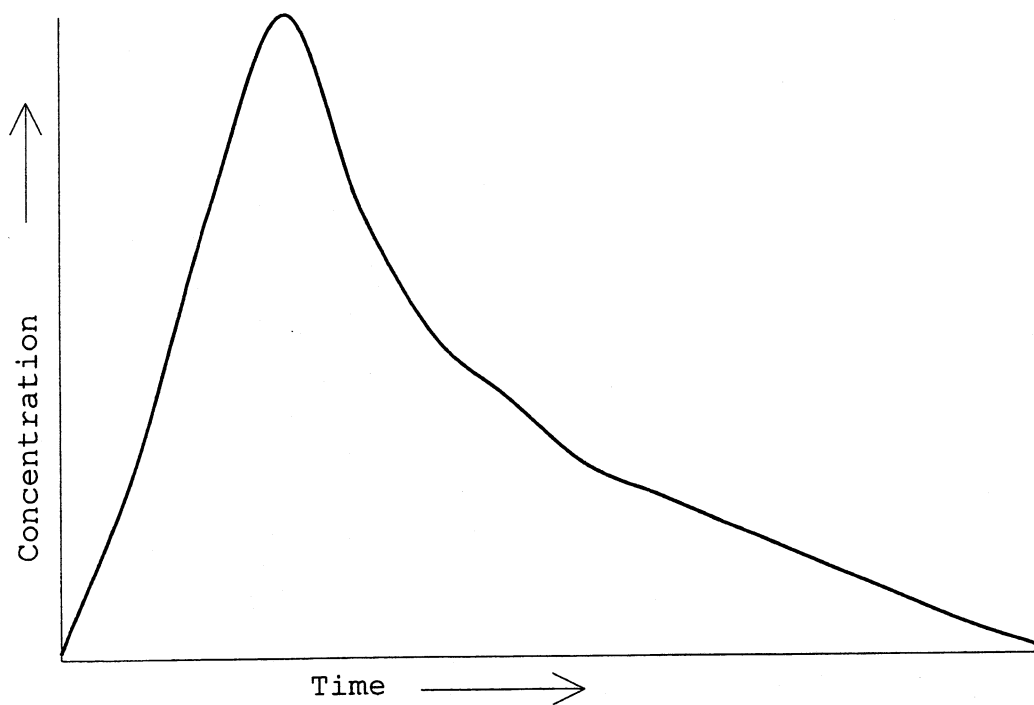
"Representative" metals and organic chemicals chosen for this study were zinc, copper, atrazine, phenanthrene and fluoranthene. Selections of these chemicals were based on the following criteria:

- 1) The chemicals should be routinely present in stormwater
- 2) The chemicals should be representative of the range in chemical properties and associated leacheability potentials of stormwater pollutants.
- 3) The chemicals should be compatible with available analytical methods and amenable to the experimental design.

Contaminant concentrations in stormwater vary widely, depending in part on the intensity and duration of the storm event. The time between storm events is also related to pollutant concentrations in stormwater. Typically, contaminant concentration in runoff is proportional to the storm volume and intensity and varies during the duration of the storm event (Shaw and Berndt, 1990). In fact, contaminant concentration history profiles often may take the shape illustrated in Figure 1-1. Reported concentrations are often flow weighted, or composites of the concentration profile.

Concentrations of major cations and anions can also influence stormwater quality. Matrix components, such as calcium, magnesium, sodium, chloride, ionic strength and pH, may not be as important as contaminants such as metals and PAHs when assessing contamination potential. These matrix components, however, influence the overall fate of metal and organic contaminants. Calcium and magnesium, often reported as water hardness, can compete with trace metals for soil sorption sites (Zelmanowitz, 1992; Zhu and Alva, 1993; Wood,

Figure 1-1 Generic Stormwater Contaminant Concentration History



1985). Calcium, magnesium and sodium also function as cation exchangers for "natural" cations in soils. Chloride can significantly alter the transport of metals by forming complexes (Donner, 1978). Metals speciation, and therefore transport, is dependent on solution ionic strength and pH (Xian and Shokohifard, 1989; Zhu and Alva, 1993). For these reasons, approximate hardness (calcium and magnesium), sodium, chloride, ionic strength and pH values "typical" of Wisconsin stormwater (Table 1-4) were used for preparing a simulated stormwater matrix in this investigation.

Certainly other stormwater matrix components, particularly dissolved organic carbon, affect transport and fate of metal and organic contaminants. However, due to the complexity and large variations in all matrix components, only major cations and anions, ionic strength and pH were included in a synthetic stormwater. While characteristics of the stormwater are important, the soil also exerts a major influence on the composition of waters percolating through the soil during infiltration.

Table 1-4 Ranges of Calcium, Magnesium, Sodium, Chloride, Ionic Strength and pH in Wisconsin Stormwaters (Bannerman, Shaw and Berndt, 1990, USGS Report 94)

	Approximation	Range
Hardness (mg/L)	40	11 to 168
Chloride (mg/L)	16.8	11
Sodium (mg/L)	10.9	28 to 988
Ionic Strength*	0.01	0.001 to 0.09
pH	7.5	5.6 to 8.81

* Ionic strength estimated from the approximation Conductivity ($\mu\text{mhos/cm}$)* $1.6\text{e-}5$ (Snoeynick and Jenkins, 1980).

3. Stormwater Management

Other than source control, seven basic stormwater management practices were identified by Wisconsin Department of Natural Resources (Prey et al., 1994). The alternate methods include wet detention ponds, constructed stormwater wetlands, infiltration basins, infiltration trenches, porous pavement, street sweeping and catchbasin cleaning.

Wet detention ponds may be lined with an impermeable material to protect groundwater. Settling of particulate matter is probably the most important effect of a detention pond. In addition, certain contaminants which associate with particulate matter, such as metals, will also be removed from the water column, depending on the fraction adsorbed to particles. Possible negative aspects of detention ponds include long term maintenance and increased temperatures of downstream receiving water (Prey et al., 1994).

A constructed stormwater wetland is an attempt to simulate observed pollutant removals associated with natural wetlands. While particulate and "dissolved" contaminant concentrations may be reduced, the exact mechanisms of pollutant removal are poorly understood. Thus, removal efficiency is difficult to predict. This lack of knowledge coupled with warming of outflow waters, availability of wetland areas, and possible environmental impact on adjacent surroundings detract from the potentials benefits of this management option.

Infiltration basins attenuate contaminant transport by allowing stormwater to collect and infiltrate through the

bottom and sides of the structure. While helping to maintain stream baseflow and colder receiving water temperatures, infiltration basins have a limited lifespan, pose the potential for groundwater pollution, and also may cause flooding if the groundwater table increases dramatically above stream levels (Prey et al., 1994).

Infiltration trenches consist of excavated trenches lined with a coarse layer of material covered with a pervious soil layer. A perforated pipe may be used to carry water which has infiltrated through the subsoil to the groundwater table or to a receiving surface water. According to the Wisconsin Department of Natural Resources, over half of these structures in North America failed within 5 years of installation (Prey et al., 1994).

Porous pavement is a lattice-like structure of permeable asphalt and exposed soil. It allows stormwater to infiltrate through the soil and subsoil to groundwater. Like infiltration basins, porous pavement allows maintenance of stream baseflow and colder receiving water temperatures. Maintenance requirements of stormwater pretreatment to remove

settleable solids may preclude widespread use.

Street sweeping is touted as a method for reducing suspended solids in residential outflow stormwater by 1 to 11 % (Prey et al., 1994). The factors affecting solids reduction include street sweeping equipment, street moisture, particle sizes and loadings, and parked car conditions (Pitt, 1993). Certainly, as previously indicated in Table 1-2a, street solids are an important source of metals, and removal should reduce metal loadings in stormwater runoff.

Catchbasin cleaning twice a year can reduce total solids and lead by 10 and 25 percent and also lower loadings of COD, total Kjeldahl nitrogen, total phosphorus and zinc (Prey et al., 1994).

Several stormwater management practices involve infiltration of stormwater through soil and subsoil to attenuate contaminant transport. If attenuation is inadequate, alterations of the infiltration basin to provide increased attenuation of stormwater contaminants may be possible. Enhancements might include the incorporation of materials such as peat (attenuate organics) or clay, fly ash

and diatomaceous earth (attenuate metals), or even municipal compost (W & H Pacific, 1992) with natural soil. Management would be required to maintain soil permeability, perhaps involving periodic replacement of the surface soil layer.

II. Background

A. Contaminant Transport during Stormwater Infiltration

1. Saturated and Unsaturated Flow

Alternating periods of saturated and unsaturated conditions occur in stormwater infiltration basins.

The driving force for water movement under saturated or unsaturated conditions may be described by equation 2-1 (Dragun, 1988).

$$E_p = E_m + E_s + E_g + E_a + E_{hs} \quad (2-1)$$

where

E_p = water potential or driving force for water movement

E_m = matric potential or attraction of soil surfaces for water

E_s = solute potential or attraction of solutes for water

E_g = gravitational potential or downward pull of water by gravity

E_a = pneumatic potential or atmospheric pressures on soil water

E_{hs} = hydrostatic potential or liquid water pressure (also termed pressure head).

Inherent to the familiar Darcy equation describing saturated flow, (equation 2-2) are gravitational (described by dh/dl) and hydrostatic potentials (encompassed in K). The remaining potential terms in equation 2-1 may be considered negligible under saturated conditions.

$$Q = -KA(dh/dl)$$

(2-2)

where

Q = groundwater discharge

K = hydraulic conductivity

A = cross-sectional flow area

dh/dl = hydraulic gradient or the pressure head difference
over a distance l

Differences between saturated and unsaturated flow arise because of the changing magnitudes of each contributing potential (equation 2-1). Prediction of water movement in the unsaturated zone requires consideration of all potential terms and how each term, particularly hydraulic conductivity, changes during infiltration. As infiltration proceeds, the magnitude of the matric and pneumatic potentials (E_m and E_a) decrease and the contribution of gravitational potential (E_g) increases. Using Dragun's terminology, an equation for unsaturated flow may be written (equation 2-3).

$$Q = K_c A ((h_c - z)/z) \pm (dh/dl) \quad (2-3)$$

where

Q = water discharge

K_c = hydraulic conductivity (dependent on water content in the unsaturated zone)

$((h_c - z)/z)$ = gradient due to surface tension forces

(dh/dl) = gradient due to gravity

Hydraulic conductivity is dependent upon soil moisture content. Also, the maximum hydraulic conductivity is the saturated hydraulic conductivity. This, however, is not the maximum rate of infiltration, rather the final steady state infiltration rate after soil saturation has been reached. When initial soil moisture is lower than saturation, the initial rate of infiltration may exceed saturated hydraulic conductivity. The initial infiltration rate and time to reach the infiltration rate predicted by the saturated hydraulic conductivity are both dependent on initial soil moisture content.

Because of the difficulties in predicting unsaturated flow, primarily due to the changing hydraulic conductivity, this investigation focused on saturated transport. Furthermore, saturation is common at infiltration sites following storm events. Although unsaturated transport does occur, it is assumed that most contaminant transport in stormwater infiltration basins occurs under saturated conditions.

2. Proposed Models

Saturated transport of contaminants in groundwater is routinely described by the one-dimensional advection/dispersion equation (eq 2-4) (Freeze and Cherry, 1979 Domineco and Schwartz, 1990).

$$D_x(\delta^2 C / \delta x^2) - (v_x(\delta C / \delta y)) = \delta C / \delta t \quad (2-4)$$

where

D_x = coefficient of hydrodynamic dispersion in the x direction

C = concentration in the dissolved phase

v_x = average pore water velocity in the x direction

t = time

The dispersion coefficient (D_x) describes contaminant spreading due to molecular and mechanical diffusion (eq 2-5).

$$D_x = D_d + D_m \quad (2-5)$$

where

D_d = effective molecular dispersion

$$D_d = tD_o$$

t = tortuosity of the medium

an approximation is often made is $t = (\pi \cdot d)/2$,

which is the distance around an soil grain

D_o = solution diffusion coefficient

D_m = mechanical dispersion coefficient

$$= \alpha \cdot v$$

α = dispersivity parameter

v = pore water velocity

The mechanical diffusion coefficient encompasses diffusion due to velocity variations within a soil pore, differing pore geometries along a flow path and divergence of flow around soil grains (Freeze and Cherry, 1979; EPA, 1989). Laboratory-scale dispersion coefficients generally range from 0.0001 to 0.01 meters, whereas dispersion coefficients obtained from field experiments using conservative tracers range from 10 to 100 meters. This scale dependence has been attributed to aquifer heterogeneity and/or chemical reactions which alter contaminant transport (EPA, 1989). The basic one dimensional

equation may be modified to include the effects of adsorption (eq 2-6).

$$D_x(\delta^2 C / \delta x^2) - (v_x(\delta C / \delta x) + (\rho_b/n)(\delta S / \delta t)) = \delta C / \delta t \quad (2-6)$$

where

ρ_b = solid dry bulk density

n = porosity

S = concentration sorbed to the solid phase

Disregarding dispersion, equation (2-6) may be simplified and arranged to predict the adjective velocity of a contaminant relative to average pore water velocity (eq 2-7).

$$v_x/v_c = 1 + (\rho_b/n)K_d \quad (2-7)$$

where

v_x = average pore water velocity in the x direction

v_c = contaminant velocity in the x direction

K_d = distribution coefficient

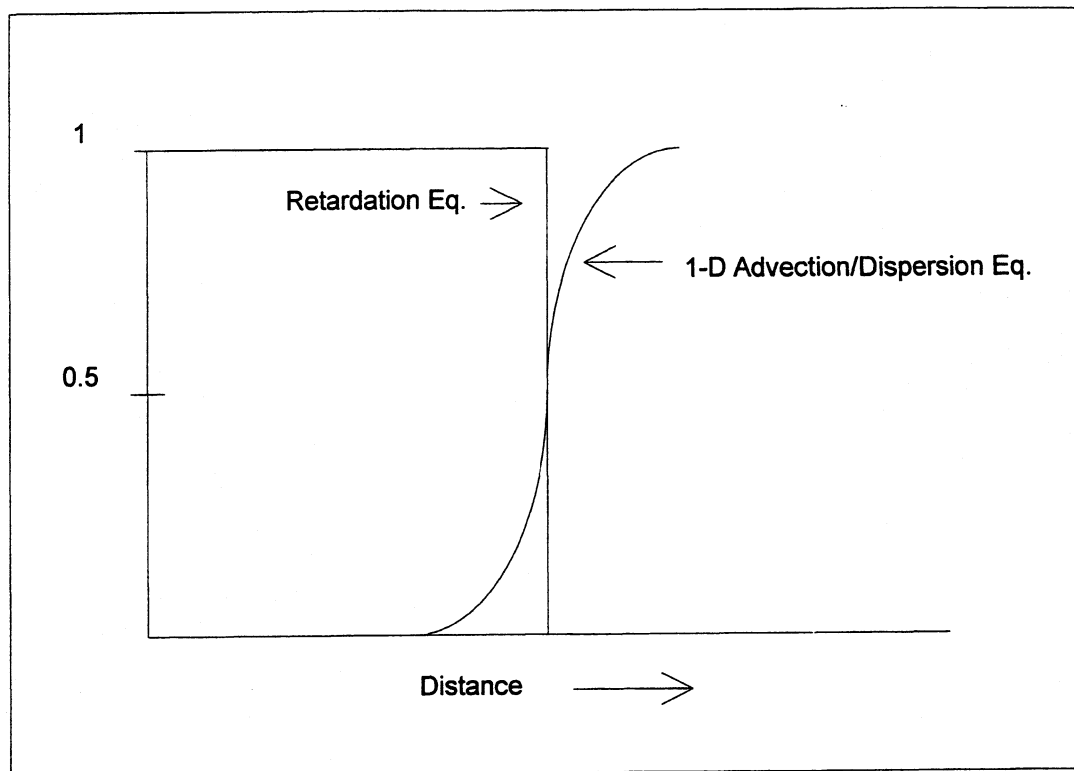
$$K_d = S/C$$

S = mass of contaminant per unit weight of solid

C = mass concentration of contaminant in liquid phase

Thus, the units of K_d are volume of liquid per mass of solid, e.g., L/kg. Equation 2-7 is often referred to as the retardation equation (Freeze and Cherry, 1979 Domenico and Schwartz, 1990). The term $1+(\rho_b/n)K_d$ is also denoted as the retardation factor. This "factor" accounts for adsorption reactions which retard the contaminant and slow transport. Figure 2-1 illustrates the predictive capability of the one dimensional advection dispersion equation versus the less stringent retardation equation. Despite its apparent limitations, the retardation equation is often used to predict contaminant migration because of its simplicity and minimal data requirements. Expanded retardation equations have also been proposed to include the effects on transport of sorption to colloids (eq 2-8a) or to colloids and DOC (eq 2-8b) (Dean, 1992).

Figure 2-1 Illustration of 1D Advection/Dispersion v Retardation



$$R_f^* = 1 + (\rho_b/n) [K_{soil} / (1 + K_{coll} * SCM)] \quad (2-8a)$$

where

K_{soil} = partition coefficient for the bulk soil

K_{coll} = partition coefficient for colloids

SCM = colloidal concentration

$$R_f^* = 1 + (\rho_b/n) [K_{soil} / (1 + K_{coll} * SCM + K_{doc} * DOC)] \quad (2-8b)$$

where

K_{doc} = partition coefficient to DOC

DOC = DOC concentration

Many assumptions are inherent to the basic retardation equation (eq 2-7) and its development from the one dimensional advection dispersion (eq 2-4). The assumptions include:

1. Transport occurs only under saturated conditions.
2. Only transport in the longitudinal direction is described.
3. Porosity and pore water velocity are constant.
4. Dispersion is considered negligible.
5. All water is involved in transport, there are no dead end pore spaces.
6. Adsorption is described by a single K_d (a linear isotherm).

7. Equilibrium (sorption and desorption) is reached throughout the soil.
8. There is no chemical or biological removal of contaminants.

As previously discussed, only saturated flow will be considered due to the complexity of predicting unsaturated transport. In addition, it is assumed that transport, neglecting preferential flow, will occur mainly during contaminant loading and subsequent stormwater infiltration through the saturated soil.

The assumption that transport occurs only in a longitudinal direction is based upon the anticipated hydraulic properties of soils at infiltration sites. In order to accommodate massive pulses of stormwater, an infiltration basin must contain soil which allows rapid infiltration. Dominant transport processes, advective or diffusive, may be described through graphical examination of the Peclet number (eq 2-8) versus the ratio of dispersive to diffusive coefficients (Figure 2-2).

$$vd/D^*$$

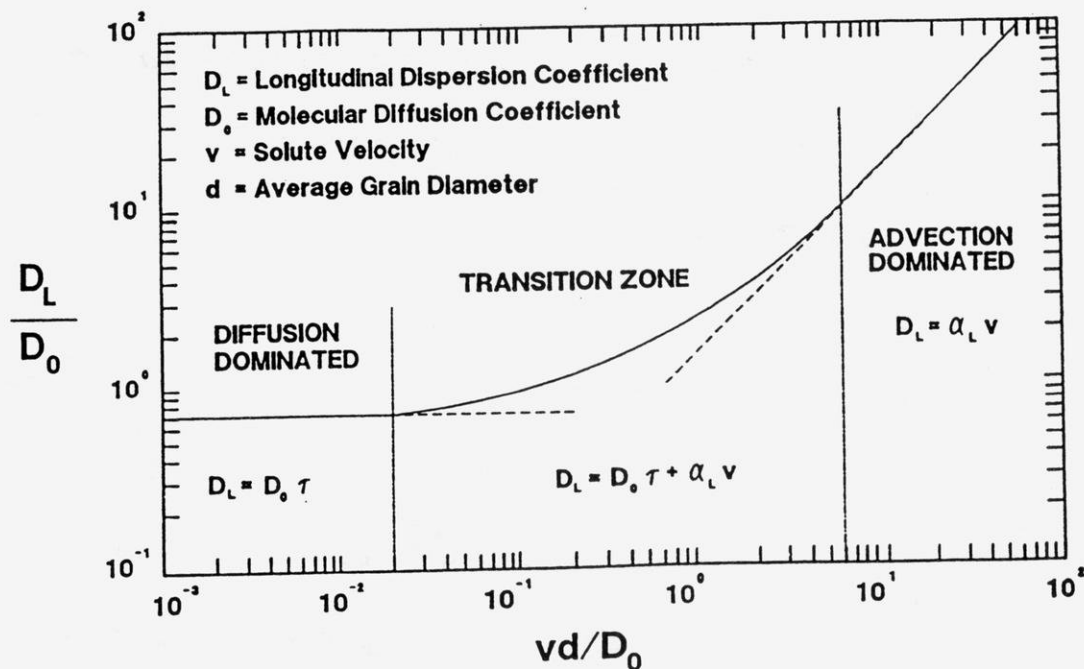
where

v = average linear pore water velocity

d = average grain diameter

D^* = diffusion coefficient

Figure 2-2 Peclet Number and Dominant Transport Processes



Considering the nature of stormwater, especially particulate matter loads and ionic strength, the assumption of constant porosity and pore water velocity is poor. It is very likely that clogging of the upper soil zone will occur

due to deposition of stormwater particulate matter and accumulation of dissolved salts during periods of drying. Salts may also enhance flocculation of small (colloidal) particles. Use of the assumption of constant porosity and pore water velocity would be conservative under these conditions. However, transport of contaminants may also be enhanced by colloids (organic, mineral or bacterial). Often, colloids move faster than the bulk pore water. Since bulk soils usually possess a net negative charge, and colloids also are often negatively charged, ion repulsion excludes colloids from some soil pores and causes them to travel faster than average bulk pore water.

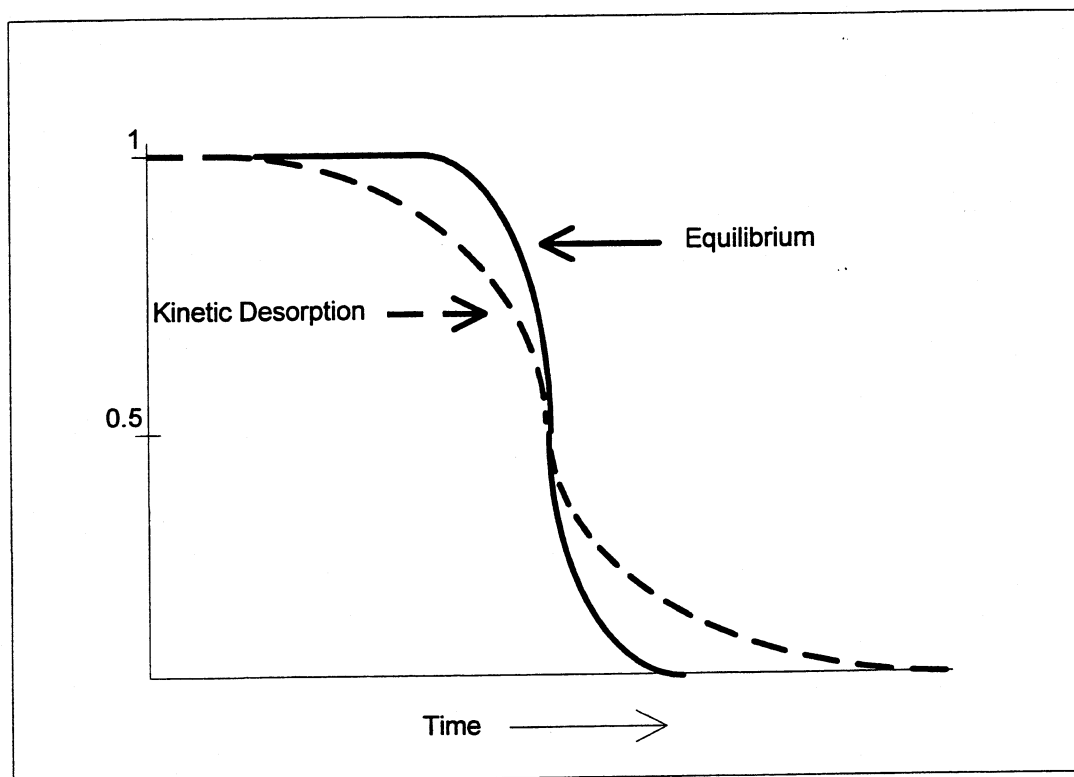
Dispersion, as previously discussed, serves to spread contaminants. Examination of the Peclet number with estimates of the longitudinal dispersion coefficient and molecular diffusion coefficient can be used to determine the contribution of diffusion to transport. Again, assuming a hydraulically suitable material such as sand, diffusion should be minimal.

Loss of contaminant mass in dead-end pores may be significant in some soils. For example, clay soils may have porosities between 0.4 to 0.7, but effective porosities (interconnected pores) may be considerably less (Freeze and Cherry, 1979). Porosity and effective porosities for sandy soils are nearly equivalent, so contaminant loss due to dead-end pores should be negligible in a hydraulically-efficient infiltration basin.

Nonlinear sorption often results in less sorption at higher concentrations than predicted by a single K_d (Armstrong and Llena, 1992). This could lead to gross underestimates of contaminant transport. Linearity of sorption isotherms for contaminants over the range anticipated to occur in infiltrating water should be examined before applying a linear sorption model.

Nonequilibrium sorption could also cause underestimation of contaminant transport by increasing dispersion, as shown by Figure 2-3.

Figure 2-3 Nonequilibrium Sorption



Observations of increased dispersion have been attributed to nonequilibrium conditions and aquifer heterogeneity (Valocchi, 1989 and EPA, 1989). As Valocchi indicates, the equilibrium assumption is probably valid when adsorption reactions are faster than pore water advection and dispersion. This assumption will likely be violated for soils having suitable hydraulic characteristics for infiltration sites, since infiltration rates may be faster than partitioning kinetics.

The assumption in the retardation equation that chemical and/or biological removal of contaminants are unimportant is conservative, since removal of contaminants would decrease the concentrations transported in the subsurface.

The distribution coefficient (K_d) is the key contaminant-specific parameter in the retardation equation. Models have been developed to predict K_d values for organic contaminants. Most models used to predict hydrophobic organic contaminant adsorption are of the form of equation 2-9 (Karickhoff et al, 1979; Chiou et al, 1979).

$$K_d = K_{oc} * f_{oc}$$

(2-9)

where

K_{oc} = organic carbon partition coefficient

f_{oc} = weight fraction of organic carbon

Since K_{oc} values are not always known, predictive equations such as eq 2-10a and 2-10b have been proposed using K_{ow} or aqueous solubility parameters often more readily available than K_{oc} values for a range of organic chemicals (Dragun, 1988).

$$\log K_{oc} = \log K_{ow} - 0.21 \text{ (for \%OC } 0.09 - 3.29) \quad (2-10a)$$

$$\log K_{oc} = -0.551 \log S + 3.64 \quad (2-10b)$$

While these equations may predict the behavior of some nonionic organic compounds to soil organic matter, other relationships are needed to describe sorption to mineral phases. The importance of sorption to mineral surfaces becomes increasingly important as the organic matter content of the

soil decreases. Furthermore, mineral phase sorption is an inverse function of the hydrophobicity of the solute for some classes of polar compounds (Grundl and Small, 1993), tending to increase with increasing solute polarity. However, for nonpolar solutes, mineral phase adsorption tends to increase with hydrophobicity and becomes important when the fraction of soil organic carbon is low. Armstrong and Llena, 1992 suggested the use of equation 2-11 to estimate adsorptive contributions from the mineral fraction from limited information on soil properties. Grundl and Small (1993) developed a similar equation to model adsorption studies of atrazine and alachlor (eq 2-12).

$$K_d = K_{oc}f_{oc} + K_{io}f_{io} \quad (2-11)$$

where

K_{oc} = partition coefficient

f_{oc} = fraction of soil organic carbon

K_{io} = inorganic partition coefficient

$$= (SS/200) (K_{ow})^{0.16}$$

SS = soil specific surface area

$$= 0.005(\% \text{ sand}) + 0.4(\% \text{ silt}) + 2(\% \text{ clay})$$

K_{ow} = octanol water partition coefficient

f_{io} = fraction soil inorganic matter

$$K_d = K_{oc}f_{oc} + K_m(cm)$$

(2-12)

where

cm = fractional soil clay content

K_m = intrinsic partition coefficient to clay surfaces
 $= K_m^{\circ}f_m$

K_m° = intrinsic partition coefficient to clay surfaces

f_m = sorptively active portion of cm

While these equations provide a basis for prediction of K_d values, the uncertainty in predicted values may be large. Measured K_d values should be considerably more accurate. Batch and column experiments are the two commonly used methods to measure partitioning behavior. Laboratory packed and intact column techniques are preferable to batch experiments because they more accurately represent field behavior (Herrin, 1994 and Dean, 1993). However, use of natural groundwater velocities may lead to unacceptably long experimentals. Batch experiments offer a faster alternative, but sacrifice true representation of field behavior. Descriptions of the batch technique may be found in Chapter IV. Partition coefficients for batch experiments may deviate from partitioning under field conditions, because particle abrasion and dispersion

during batch equilibration increase the amount of soil surface area exposed to contaminants (Spurlock and Biggar, 1993; Burglsser et al, 1993).

B. Subsurface Fate of Organic Contaminants

Prediction of the fate of organic contaminants in the subsurface begins with assessment of the chemical properties of the contaminants and the linkages between properties and fate (MacKay, 1991; Saltzman and Yaron). Various chemical, biological and physical processes dictate the fate of organic contaminants. Important processes include cosolvation, complexation, chemical degradation, biodegradation, volatilization, complexation, adsorption and advection and dispersion.

Chemical structure influences key chemical-physical properties of organic contaminants, including water solubility, octanol-water partition coefficient, affinity for solids, molecular volume and biodegradability. Structural fragments containing C, H, Br, Cl and I contribute to a

contaminants hydrophobicity whereas fragments containing N, S, O and P contribute to hydrophilicity (Dragun, 1988).

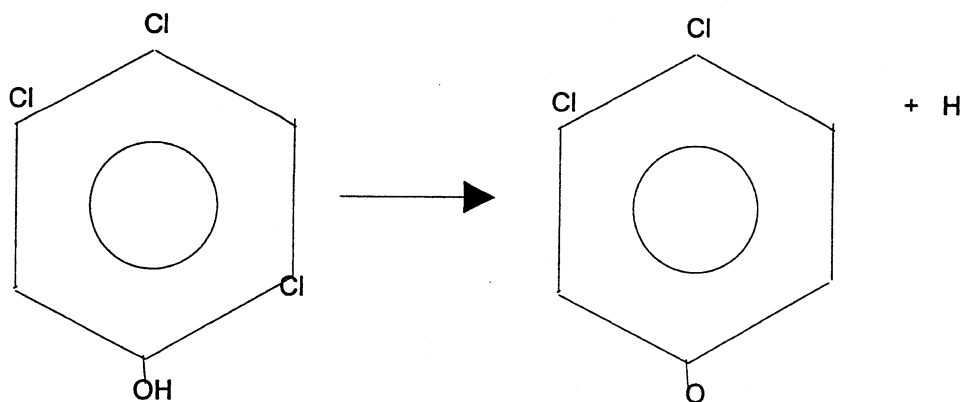
Molecular volume, molecular surface area, and hydrophobicity (K_{ow}) have been linked to the degree of partitioning into organic material (Brusseau and Rao, 1991). In general smaller, less complex structures are more readily biodegraded.

Cosolvents increase organic contaminant solubility through organic contaminant/solvent interactions (EPA, 1989). If solvent concentrations are high enough to cause phase separation, cosolvents can extract the contaminants from the aqueous phase. Thus, cosolvents tend to decrease contaminant sorption. Boyd and Sun (1989) showed that residual oil components have approximately ten times more sorptive capability than natural organic matter. Although oil and grease are routinely found in storm water (Bannerman, 1992), unless high concentrations (approximately >1% by volume) are contained in runoff, the cosolvent effect is likely negligible.

Complexation with dissolved ligands, particularly dissolved organic carbon (DOC) can increase transport by increasing "solubility" (Dean, 1993), although the mechanisms are different than those occurring with cosolvents.

If acidic organic contaminants ionize in solution, the anions formed, due to their charge, are water soluble (EPA, 1989). An example of this is the ionization of phenol illustrated in Figure 2-4.

Figure 2-4 Ionization of Organic Contaminants



Large numbers of diverse microorganisms exist in the upper soil layers (Sims et al., 1990). Therefore, biodegradation of organic contaminants is an important removal process in the subsurface. Factors which affect biodegradation include temperature, pH, dissolved oxygen, Eh, salinity, concentrations of suitable bacteria, competing bacteria, organic contaminant, and toxic contaminants (Newson, 1985). Degradation may progress to complete mineralization (conversion to CO_2 and inorganic components) or may produce refractory degradation products which may be less, equal or more toxic than the original parent contaminant. An example is the degradation of tetrachloroethylene to vinyl chloride (EPA, 1989). In addition, these degradation products could be more mobile than the parent contaminant. Differences between aerobic and anaerobic conditions may also be important. For instance, atrazine degradation half lives measured for aerobic, anaerobic and alternating aerobic/anaerobic conditions were 556, 2632 and 669 days respectively (Obenhuber, 1988).

Clearly, the runoff process can facilitate volatilization

of selected organic contaminants depending on runoff turbulence and contaminant air-water partition coefficient. Volatilization in the subsurface is dependent on the exposure area between the contaminant and unsaturated zone air, contaminant vapor pressure and diffusion rate (EPA, 1989). Because soil particles are usually wet or hydrated, air-water partition coefficients and soil-water partition coefficients are key parameters in defining contaminant distribution between soil particles and soil air (Mackay, 1991). Assuming the contaminant is dissolved in water, the exposure area would be the retained, or hygroscopic, water on soil grains. Actual vapor movement may be described by Fick's law (equation 2-13).

$$D_e (\partial^2 C / \partial x^2) = \partial C / \partial t \quad (2-13)$$

where D_e = effective diffusion coefficient
 = $D_a t$
 D_a = free air diffusion coefficient
 t = tortuosity factor

The effective diffusion coefficient is also influenced by soil-air partitioning (Mackay, 1991).

Adsorption of hydrophobic organic contaminants is believed a two stage process (Gamerding et al., 1990). The first stage is rapid removal of the organic contaminant from water to a hydrophobic surface. Slow diffusion into the matrix of the solid is considered the second stage of hydrophobic adsorption. It is this slow diffusion into the solid matrix which many contribute to sorption nonequilibrium (Lee et al., 1991). Hydrophobic adsorption is driven by a combination of weak van der Waals forces and large entropy changes (Schlautman, 1993). The entropic contribution is from the destruction of an ordered water shell around the organic solute and the movement of the solute to a hydrophobic surface (Dragun, 1988). This hydrophobic surface may be bulk soil matter (both organic and mineral) or colloidal material. It should also be recognized that partitioning to humic material is not only a function of hydrophobicity but is also dictated by the organic contaminant's size and its ability to fit into the humic material's hydrophobic cavities in humic material

(Schlautman, 1993). As previously discussed, the adsorption of nonpolar hydrophobic contaminants is closely related to the fraction of soil organic carbon (Karickhoff et al, 1979; Chiou et al, 1979). Mineral surfaces also provide adsorption sites (Grundl and Small, 1993; Armstrong and Llena, 1992) and should be included in predictive equations. Mineral surface adsorption is especially important for polar organic contaminants and for hydrophobic organic contaminants in soils with low organic carbon content (Newsom, 1985; Dean, 1993). Other factors influencing adsorption include temperature, soil moisture content, pH, and ionic strength (Dao and Lavy, 1978; Lee et al., 1991). Finally, the adsorption of hydrophobic organic contaminants to colloids may have a significant source of transport (Dunnivant et al, 1992; Liu and Amy, 1993; Armstrong et al, 1991). Colloids serve as contaminant sorptive phases and, if stable, smaller than the effective pore size of soil or aquifer material, and mobile can greatly increase contaminant mobility. McCarthy et al. (1993) demonstrated this mobility via a direct injection of natural organic matter into an aquifer. Initially, small-sized (less

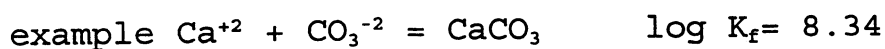
than 3000 MW), hydrophilic components of natural organic matter were transported faster than the larger, more hydrophobic components. However after a "steady state" was achieved, all natural organic matter components traveled unretarded through the aquifer.

C. Subsurface Fate of Metal Contaminants

Dissolution and weathering of minerals in addition to chemicals contained in the influent water determine the composition of unsaturated zone and saturated zone water. Thus, subsurface waters contain "background" concentrations of metals and naturally available ligands. However, it is the chemical form, or particular metal species which dictates the ultimate fate of metal contaminants in the subsurface (EPA, 1989). Important processes influencing concentration and speciation include precipitation/coprecipitation, complexation, adsorption, and change in redox potential.

All soils contain metals in mineral phases which are subject to dissolution or exchange reactions. Metals may occur as free ions, insoluble species, soluble metal complexes/chelates, "adsorbed" species or as species with differing oxidation states.

Precipitation can occur when activities of the ions involved exceed the ion activity product of the least soluble mineral phase in equilibrium with the ions. Disregarding competing ions, the equilibrium formation constant of a mineral may be used to predict precipitation. The ion activity product (IAP) (example below) is often used to describe solution status with regard to precipitation.



$$\text{IAP} = (\text{Ca}^{+2}) * (\text{CO}_3^{-2}) / (10^{8.34}) \quad (\text{Stumm and Morgan, 1981})$$

If the IAP value is greater than 1, precipitation is likely to occur since the solution is supersaturated. IAP values less than one indicate that the mineral phase is undersaturated. It should be recognized that the IAP approach is

oversimplified primarily because it is representative of equilibrium conditions and does not consider the effects of competing ions or complexes. Natural precipitation of some minerals may not occur unless there is an influx of a limiting mineral component. Generally, unless conditions radically change, precipitation removes the affected contaminants from solution. However, transport may still occur if the precipitates are of a colloidal size, or if in-situ conditions change to favor mineral dissolution. Coprecipitation refers incorporation of a dissolved species as a minor component of a precipitating mineral (Drever, 1988). For purposes of this discussion chelates, which are complexes involving multidentate ligands, will be considered equivalent to complexes. Complexation generally increases solubility and therefore the potential for transport. Sometimes however, complexation by organic ligands has been reported to decrease adsorption to oxide and silicate surfaces by forming a ternary metal-ligand surface complex (Drever, 1988). Common metals in order of complexation strength are: Fe(III), Hg, Cu, Pb, Ni, Zn, Cd, Fe(II), Mn, Ca and Mg. Common ligands include humic

materials, OH, Cl, SO₄, CO₃, S, F, NH₃, PO₄, CN and polyphosphates (EPA, 1989). Adsorption occurs via coordination bonding of metals (or anions) to specific surface sites. The surfaces of oxides and hydroxides (commonly aluminum, iron and manganese) often provide adsorption sites for metals. Changes in pH and metals concentration can have significant effects on sorption. The solution pH, while potentially altering the metal speciation can also change the net surface charge on minerals affecting adsorption affinity for certain ions and also the adsorption bond strength. Since metals adsorption is thought to be site specific, the concentration of metals competing for limited adsorption sites is important. Adsorption of metals is often described by the Freundlich or Langmuir equations.

Freundlich $S = KC^n$

where

S = concentration of sorbed contaminant
K = freundlich coefficient
C = concentration of dissolved phase
n = fitting parameter

Langmuir $S = S_{\max} (KC / 1 + KC)$

where

S = concentration of sorbed contaminant

S_{\max} = maximum amount that can be adsorbed

C = concentration in the dissolved phase

While not defining particular sorption mechanisms, sorption data for metals often can be fit to these equations. Ion exchange may be considered as a type of adsorption reaction. Ion exchange refers to the process where ions are held by electrostatic forces rather than by coordination bonding. This process is exhibited by clay minerals where exchange involves inner layer and external surface cations.

Changes in oxidation state can alter speciation of a particular metal and also lead to mineral dissolution. Examples of oxidation state change and associated environmental ramifications include $\text{Fe(III)}/\text{Fe(II)}$ and $\text{Cr(VI)}/\text{Cr(III)}$. Fe(III) precipitates under slightly alkaline

to acidic conditions as a adsorptive solid phase (ferric hydroxide). Conversely, Fe(II) is very soluble and reduction of Fe(III) to Fe(II) not only releases ferrous ions but also species adsorbed to the ferric hydroxide. Similarly, Cr(III) is a strong absorber, whereas Cr(VI) is not only soluble but also toxic (EPA, 1989).

III. Research Objective

The purpose of this investigation was to determine whether stormwater infiltration through soil would be effective in attenuating trace metal and nonionic organic contaminants. Batch experiments were conducted to obtain equilibrium soil-water partition coefficients for selected soils and contaminants and to measure rates of approach to equilibrium. A retardation equation was used to model expected transport rates during infiltration under saturated flow. Subsequently, column experiments were performed to compare predicted and observed transport rates.

to acidic conditions as a adsorptive solid phase (ferric hydroxide). Conversely, Fe(II) is very soluble and reduction of Fe(III) to Fe(II) not only releases ferrous ions but also species adsorbed to the ferric hydroxide. Similarly, Cr(III) is a strong absorber, whereas Cr(VI) is not only soluble but also toxic (EPA, 1989).

III. Research Objective

The purpose of this investigation was to determine whether stormwater infiltration through soil would be effective in attenuating trace metal and nonionic organic contaminants. Batch experiments were conducted to obtain equilibrium soil-water partition coefficients for selected soils and contaminants and to measure rates of approach to equilibrium. A retardation equation was used to model expected transport rates during infiltration under saturated flow. Subsequently, column experiments were performed to compare predicted and observed transport rates.

IV. Materials and Methods

A. Soils

Batch equilibration experiments were conducted using three different soils. Sparta sand consists of water-deposited sand formed on low stream terraces along the Wisconsin river under prairie vegetation (Iowa County Soil Survey, 1978). This soil was collected from the University of Wisconsin Agricultural Research station in Arena Wisconsin. The St. Charles silt loam was obtained from private property near Sun Prairie Wisconsin. This soil formed in deep loess and loamy glacial material on glaciated uplands under a mixed hardwood forest environment (Dane County Soil Survey, 1978). Finally, the Pals Grove silt loam was collected from the University of Wisconsin Agricultural Research station located near Lancaster Wisconsin. All soils were sampled to a depth of approximately one foot and, with the exception of the St. Charles silt loam, collected from undisturbed sites. The St. Charles silt loam was collected adjacent to an agricultural test field plot which had not been subjected to atrazine application for at

least ten years. Soils were stored in plastic bags in the dark at 4°C until use. Physical and chemical characteristics of the soils measured by the University of Wisconsin Soil and Plant Analysis Laboratory are listed in Table 4-1. Soil samples for field dry bulk density analysis were collected by driving a stainless steel column section into the soil. After the soil column dimensions were measured, the soil was removed and then dried to a constant mass in an oven at 110°C. Equation 4-1 was used to calculate field dry bulk density, and an estimate of field porosity was calculated with equation 4-2 (Freeze and Cherry, 1979).

$$\rho_b = \text{g dried soil/cm}^3 \text{ soil volume} \quad (4-1)$$

$$n = 1 - (\rho_b/2.65) \quad (4-2)$$

Table 4-1 Soil Physical and Chemical Characteristics

Soil	pH	% OM	CEC								
Sparta Sand	6.1	1.3	1								
St Charles Silt Loam	7	2.3	10								
Pals Grove Silt Loam	7.2	2.4	10.5								
Bulk Soil	P	K	Ca	Mg	S	mg/kg Zn	Mn	Fe	Cu	Al	Na
Sparta Sand	245.6	281.45	328.75	453.2	47.755	5.6825	159.15	3494	<2.5	3926.5	3.5865
St Charles Silt Loam	488.9	1647	2493.5	2623	176.25	55.42	1217.5	14393	9.3605	13176	97.15
Pals Grove Silt Loam	419.1	1597	2362	2628.5	217.75	69.225	1386.5	14253.5	12.165	14800.5	<61.2

B. Simulated Stormwater

Recognizing the diversity in composition of stormwater, a simplified simulated stormwater matrix was created to approximate some basic chemical components. Chemicals added to MilliQ water are listed in Table 4-2. While not containing the full range of stormwater constituents, the simulated stormwater represents major inorganic components of a "typical" stormwater.

Table 4-2 Simulated Stormwater

Chemical Constituent	Concentration (mg/L)
$\text{CaCl}_2 \cdot 2\text{H}_2\text{O}$	37.4
$\text{MgCl}_2 \cdot 6\text{H}_2\text{O}$	32.0
NaCl	27.7
KBr	724.3
KOH	11.1

C. Batch Experiments

1. Organic Contaminant Batch Experiments

Organic contaminant batch experiments were conducted with atrazine, fluoranthene and phenanthrene. Their chemical structures are illustrated in Figure 4-2, and some important chemical properties are listed in Table 4-3. These contaminants were chosen based on expected sorptive behavior, ranging from a polar compound (atrazine) to more hydrophobic compounds (phenanthrene and fluoranthene), while still maintaining experimental feasibility. Chemical parameters measured in the batch experiments included dissolved and sorbed concentrations of the added contaminants and dissolved

Table 4-3 Chemical Properties

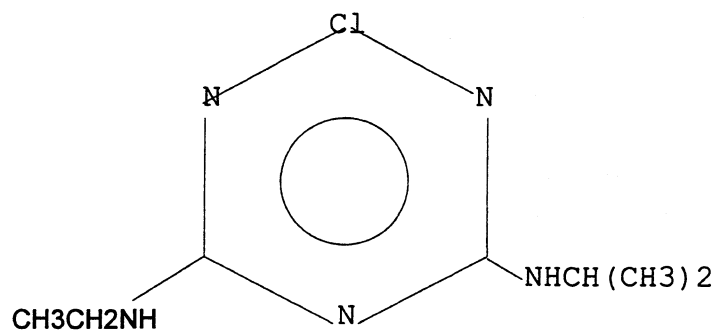
Property	Atrazine	Phenanthrene	Fluoranthene
Chemical Formula	$C_8H_{14}ClN_5$	$C_{14}H_{10}$	$C_{16}H_{10}$
Molecular Weight	215.7	178	202
Aqueous Solubility	70 ppm	0.1 ppm	0.2 ppm
Log K_{ow}	2.33*	4.57*	4.90*
Log K_{oc}	2.21*	4.37*	4.82*
Vapor Pressure	40 mPa		

*Values from Armstrong and Llena (1992)

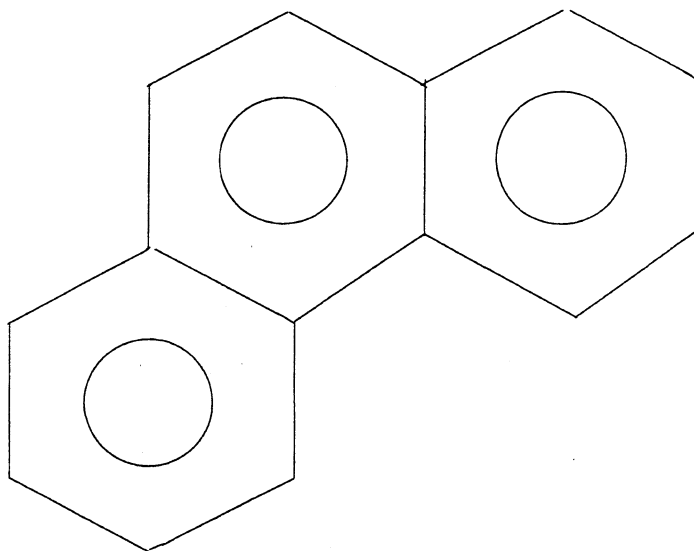
organic carbon (DOC). Sorbed concentrations and dissolved concentrations were summed to obtain total experimental recoveries of phenanthrene and fluoranthene. In K_d calculations, dissolved concentrations were corrected for phenanthrene volatilization during the vacuum filtration step used to separate dissolved and particulate fractions. This correction was needed, since sorbed concentrations could not be accurately determined for the silt loam soils because the extraction procedure did not fully recover sorbed contaminants. K_d values for the Sparta sand soil were calculated using only the sorbed concentrations, thus avoiding an "average volatilization" correction.

Figure 4-2 Chemical Structures of Atrazine, Phenanthrene and Fluoranthene

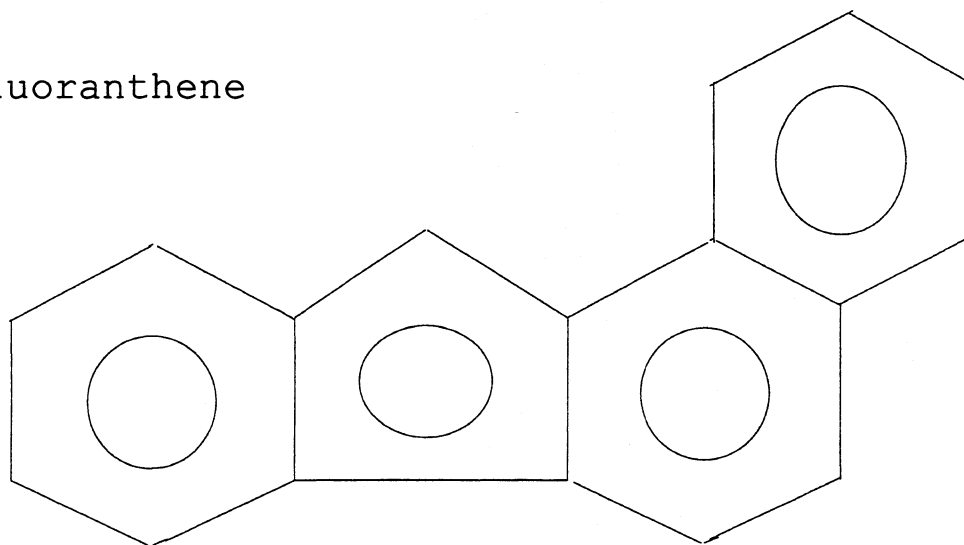
Atrazine



Phenanthrene



Fluoranthene



All organic contaminant reagents were certified at least 95% pure. Glassware used in the experiments was cleaned by presoaking in a water bath (Alconox or Micro cleaning agent) and ashing at 450°C for at least 8 hours.

Batch experiments were conducted in triplicate with soil blanks using 0.5 grams of air-dried, sieved (< 2mm size fraction) soil and twenty ml of simulated stormwater in twenty-five ml borosilicate glass centrifuge tubes with teflon-lined caps. Contaminants were added to the tubes by spiking 10 μ L of a stock solution containing 100,000 μ g/L of the contaminant dissolved in Optima acetonitrile to the centrifuge tube wall. After allowing this spike to evaporate, simulated stormwater was added and allowed to equilibrate. The necessary equilibration time was determined to be approximately 21 hours. After this time had elapsed and the dissolved concentrations of all contaminants were 100 μ g/L, soil was added. Tubes were then covered, capped, wrapped in foil and placed in a horizontal shaker (Fisher model 236) operating at room temperature and 120 revolutions per minute. When the experimental batch time was reached, tubes were

removed from the shaker and their contents vacuum filtered (20 to 25 psi) using a disposable, borosilicate glass pipette to transport the sample to an anodized aluminum Anotec filter (0.02 μm) which had been ashed for 14 hours at 450°C.

Filtrates were collected in glass test tubes and was stored in foil-capped, glass scintillation vials in the dark at 4°C until analysis.

Dissolved concentrations were measured by direct injection onto a Spherisorb ODS 5U HPLC column (250 mm length and 4.6 mm ID) and analyzed using a Waters HPLC equipped with a Waters 717 autosampler, Waters 600 pump and Waters 991 photodiode array. Aqueous standards were prepared in the same manner as the centrifuge tube samples. A solvent gradient using 100 percent acetonitrile:water (40:60) for 5 minutes to 100 percent acetonitrile over 25 minutes following by acetonitrile:water through 35 minutes was used (SLOH, 1988). To adequately quantify each contaminant, the photodiode array detector was used with peak processing wavelengths of 224, 234 and 248 nm for atrazine, phenanthrene and fluoranthene respectively. Approximately 10 percent of the samples were run

in duplicate and 10 percent were spiked to assess instrument reproducibility and analyte recovery.

Sorbed concentrations were measured directly to allow calculation of experimental mass balance. Batch test tubes and ashed foil (used over the centrifuge tube mouth) were preweighed, as were the disposable pipettes used to remove the soil solution for filtration. The final mass of soil deposited on the Anotec filters was determined by difference from the starting centrifuge tube, foil and soil versus final centrifuge tube, foil and residual soil mass. At the conclusion of filtration, the Anotec filters were removed and placed in 20 ml Qorpac screw-capped jars. A triple sonication extraction using a Branson 8200 sonicator and successive 4 ml additions of Optima hexane was employed. The first sonication was for a duration of one hour, followed by allowing the jars to remain at room temperature overnight. The next two 30 minute sonications occurred with a an intervening period of a few hours. The final 12 ml extract was removed with a disposable borosilicate glass pipette and eluted through another disposable borosilicate glass pipette

packed with sodium sulfate to remove any residual traces of water. These extracts were then stored in glass scintillation vials with foil-lined caps at 4°C in the dark until analysis. Sorbed concentrations were also measured by direct injection onto the same reversed phase silica column. All operating parameters, sample quality control protocols and processing wavelengths were the same as for the aqueous samples. Only the standard matrix differed - "sorbed" standards were made using Optima hexane.

A Shimadzo TOC-500 with autosampler was used to measure DOC. Aliquots (6 ml) of the filtered sample were transferred to autosampler tubes, acidified using 100 μ L of 2N HCl, purged for 4 minutes to remove inorganic carbon and analyzed in triplicate.

2. Metal Contaminant Batch Experiments

Metal contaminant batch experiments were conducted using copper and zinc. These contaminants were chosen to provide a range of sorptive behavior while maintaining experimental

feasibility. Armstrong and Llena (1992) assessed copper as being fairly immobile, whereas zinc was judged to be fairly mobile.

Working zinc and copper concentrations were made by diluting commercially available Atomic Absorption standards. All bottles, filters, petri dishes, filter apparatuses and centrifuge tubes were cleaned by soaking in reagent grade 20% HNO₃ acid for at least two days and rinsed at least 5 times with MilliQ water.

Chemical parameters measured for the batch experiments included pH and DOC as well as dissolved and sorbed concentrations of the added contaminants. Final K_d calculations, however were based on measured dissolved concentrations while sorbed concentrations were calculated by difference between added and dissolved values. Batch experiments were conducted in triplicate using either 0.25 and 0.5 g of soil and 50 ml of simulated stormwater in 60 ml low density polyethylene (LDPE) bottles. Stormwater with premixed metal concentrations was added directly to the LDPE containers, followed by air-dried, sieved (<2 mm size

fraction) soil. Bottles were then placed in a horizontal shaker (Fisher model 236) operating at room temperature and 120 revolutions per minute. At the conclusion of the batch experiment, the bottles were removed from the shaker and their contents vacuum filtered (15-23 psi) using an Eppendorf pipette with a metal-free pipette tip through a 0.4 μm Poretics polycarbonate filter with a polysulfone filter apparatus directly into an ashed glass vial for DOC analysis and into a high density polyethylene (HDPE) scintillation vial for dissolved metals storage. Samples for dissolved analysis were then acidified with 2 ml of trace metal grade acid per liter of sample. A Perkin Elmer Graphite Furnace Atomic Absorption Instrument (GFAA) equipped with an autoanalyzer and Zeeman correction was used for analysis of the dissolved fraction. Approximately 10 percent of the samples were run in duplicate and with recovery spikes.

Sorbed concentrations were determined via extraction of soil deposited on the polycarbonate filters. The pre-weighed filters were removed with teflon-tipped forceps, placed in polystyrene petri dishes and dried overnight at 70°C.

Filters were then reweighed and placed in polypropylene centrifuge tubes. Trace metal grade HCl (1N) was added to the centrifuge tubes in a soil:acid ratio of 1:50 by weight. Tubes were then placed in the horizontal shaker (Fisher Model 236) operating at 120 revolutions per minute and room temperature for 16 hours. Samples were then filtered through a 0.4 μm Poretics polycarbonate filter using the same procedures previously described for the dissolved fraction filtration. The GFAA was used to analyze these HCl solutions. Standards were made with 1 N HCl to minimize matrix effects.

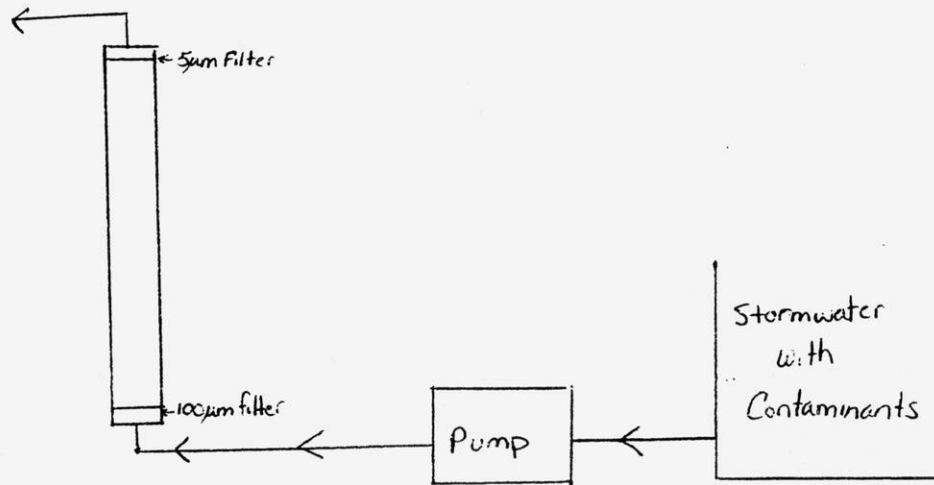
A Shimadzo TOC-500 with autosampler was used to measure DOC using the procedure described above.

D. Column Experiments

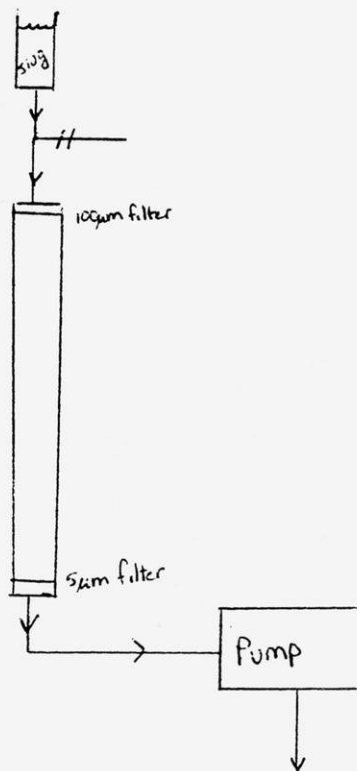
Column experiments were conducted using the appropriate teflon column apparatus (differentiated by method of contaminant introduction: continuous or slug input) as illustrated in Figure 4-3. A Masterflex pump (model 7524-10) with Norprene or C-flex pumphead tubing was used.

Figure 4-3 Column Apparatus

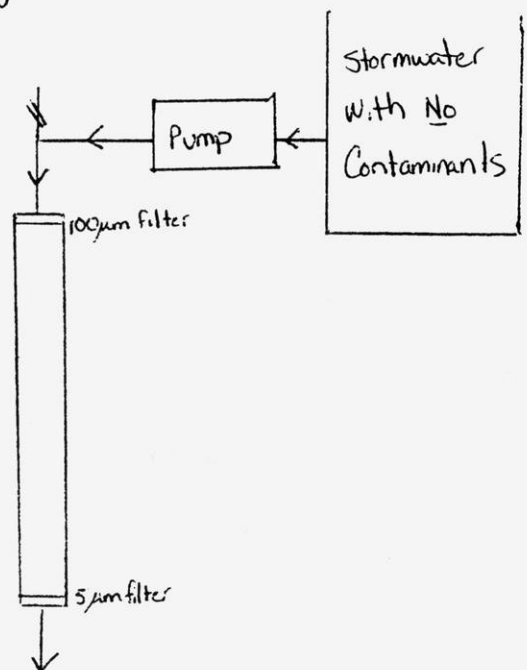
Continuous Input



Slug Input



Slug Elution



The Sparta sand soil was air-dried and sieved prior to drypacking. Frequent mixing was done while packing the columns to prevent any layering effects. Conversely, the St. Charles silt loam column was packed with soil aggregates which remained after minimal air-drying of the soil. The column was packed concurrently as the column was being slowly saturated. This method was found to yield the only operating silt loam column without gross preferential flow or low porosity. All columns were saturated for at least 2 days at flow rates at least one-half of those used during the actual experiment.

Potassium bromide, used as a conservative tracer, was measured using a bromide selective electrode (model 9435) and Orion (model 290A) meter. Tritiated water was also used as a conservative tracer in the St Charles silt loam column. It was measured by dispensing 2 ml of sample into 13 ml of Optifluor scintillation cocktail and counting using a Packard radioactivity detector (model 1900CA).

Several column characteristics were estimated, then compared to measured characteristics. Column length, diameter and mass of soil packed were noted and values of dry bulk

density and estimated porosity were calculated using eq 4-1 and eq 4-2 respectively. In some cases, pore volume (pore volume = ((time)*(flow rate))/estimated total column pore volume) was used to graphically display data. Conservative tracer data were used to determine column effective porosity and pore water velocity. The effective porosity was calculated by dividing the time when one-half of the total mass of the tracer had exited the column by the total column volume. Pore water velocity could then be calculated by the relationship $v = Q/(A/n_e)$ where v is the pore water velocity, Q is the flow rate, A , the cross-sectional column area and n_e is the measured effective porosity.

Measured parameters included column effluent pH, conductivity, DOC, colloid concentrations, and concentrations of major cations as well as zinc and copper. The Orion meter (model 290A) was used to measure effluent pH and an Orion meter (model 160) used for conductivity. TOC was measured directly on samples (6 ml) of column effluent using a Shimadzo TOC 5000 analyzer. DOC was also measured on the Shimadzo TOC 5000 analyzer with procedures previously presented. Colloid

concentrations were measured by serial filtration through 1.0 μm and 0.05 μm Poretics polycarbonate filters. All filters were weighed using a Perkin-Elmer balance (model AD-4 Autobalance), as were control filters used to correct for the effects of temperature and humidity. Concentrations of major cations in the soil effluent were measured using a Perkin Elmer ICP (model Plotsma II). Zinc and copper effluent concentrations were determined by the GFAA.

V. Results and Discussion

A. Organic Contaminants

1. Partitioning in Batch Systems

Pertinent properties of the three soils investigated are listed in Table 5-1. Sparta sand, a sorted glacial outwash which developed under prairie conditions was investigated more thoroughly than the other two soils because of its high infiltration capacity. Batch experiments were performed to elucidate the kinetics of partitioning and also to measure a soil-water distribution coefficient (K_d) for each soil and

contaminant. The K_d values were used in comparing expected transport rates based on equation 5-1.

Table 5-1 Soil Characteristics

Parameter	Sparta Sand	St Charles Silt Loam	Pals Grove Silt Loam
% Sand	89	14	23
% Silt	5	73	57
% Clay	6	13	23
% Organic Matter	1.24	2.3	2.3
% Organic Carbon	0.0073	1.4	1.4
Field Measured ρ_b (g/cm ³)	1.7	1.4	
Estimated Field Porosity	0.35	0.47	

$$v_x/v_c = 1 + (\rho_b/n)K_d \quad (5-1)$$

where

v_x average pore water velocity in the x direction

v_c contaminant velocity in the x direction

K_d distribution coefficient

$$K_d = S/C$$

S = mass of contaminant per unit weight solid

C = concentration of contaminant in solvent

Experiments on the sorption kinetics of atrazine using the Sparta sand showed that equilibrium is probably reached after about 48 hours (Figure 5-1). The average K_d for atrazine was approximately $0.9 \text{ ml/g} \pm 0.8 \text{ ml/g}$, indicating that the mobility of atrazine should be high. As a comparison, predictive equations discussed previously are used to estimate a K_d . Equation 5-2 (which will be referred to as the mineral phase equation) suggested by Armstrong and Llena (1992) predicts a K_d of 1.3 ml/g whereas equation 5-3 (referenced hereafter as the organic carbon equation) gives a K_d of 1.2 ml/g .

$$K_d = K_{oc}f_{oc} + K_{io}f_{io} \quad (5-2)$$

where

K_{oc} = partition coefficient

f_{oc} = fraction of soil organic carbon

K_{io} = inorganic partition coefficient

$$= (S/200) (K_{ow})^{0.16}$$

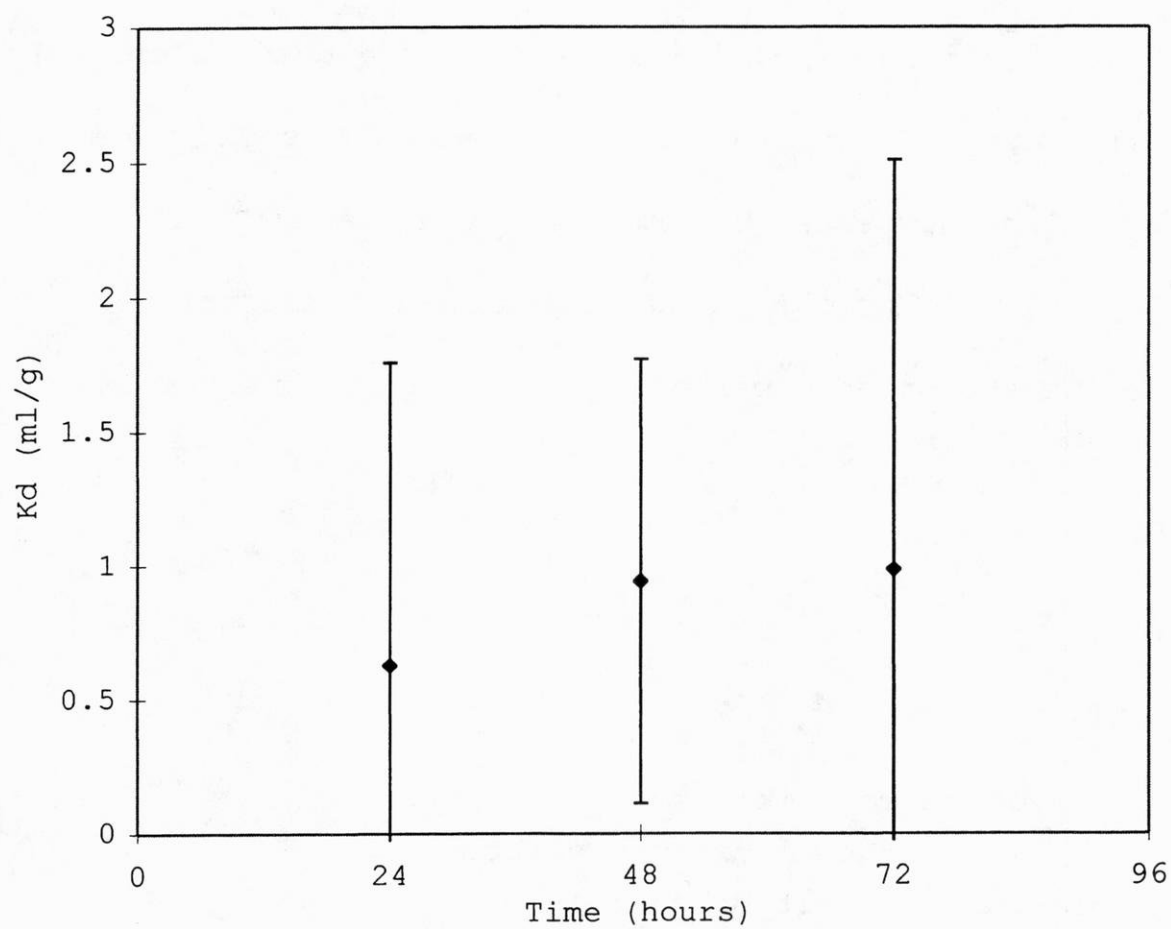
S = soil specific surface area

$$= 0.005(\% \text{ sand}) + 0.4(\% \text{ silt}) + 2(\% \text{ clay})$$

K_{ow} = octanol water partition coefficient

f_{io} = fraction soil inorganic matter

Figure 5-1 Sparta Sand Atrazine Partitioning Kinetics



$$K_d = K_{oc} f_{oc}$$

(5-3)

where

K_{oc} = partition coefficient

f_{oc} = fraction of soil organic carbon

Clearly the relatively large experimental standard deviations preclude precise evaluation of the accuracy of the predicted K_d values, but both are within the experimental K_d range. DOC measurements showed a good correlation to measured atrazine dissolved concentrations (Figure 5-2). Even though atrazine is not very hydrophobic, its correlation to DOC suggests that a fraction of the atrazine is in the form of DOC complexes.

Phenanthrene partitioning seemed to have reached equilibrium after 24 to 48 hours (Figure 5-3). The average K_d for phenanthrene was 51 ± 12 ml/g. Calculated K_d values are 200 ml/g using either predictive equation. No correlation between DOC and phenanthrene K_d was found (Figure 5-4).

Figure 5-2 Sparta Sand Dissolved Atrazine v DOC

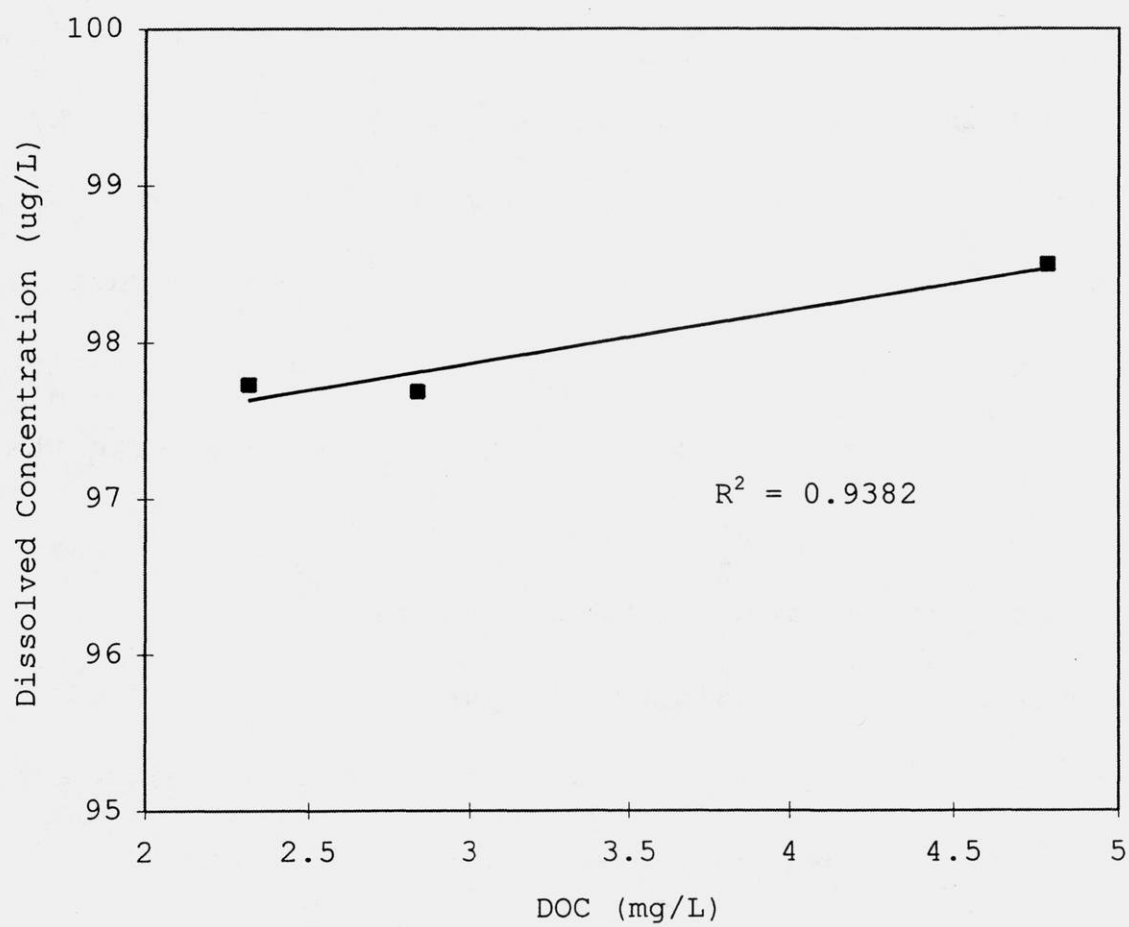


Figure 5-3 Sparta Sand PAH Sorption Kinetics

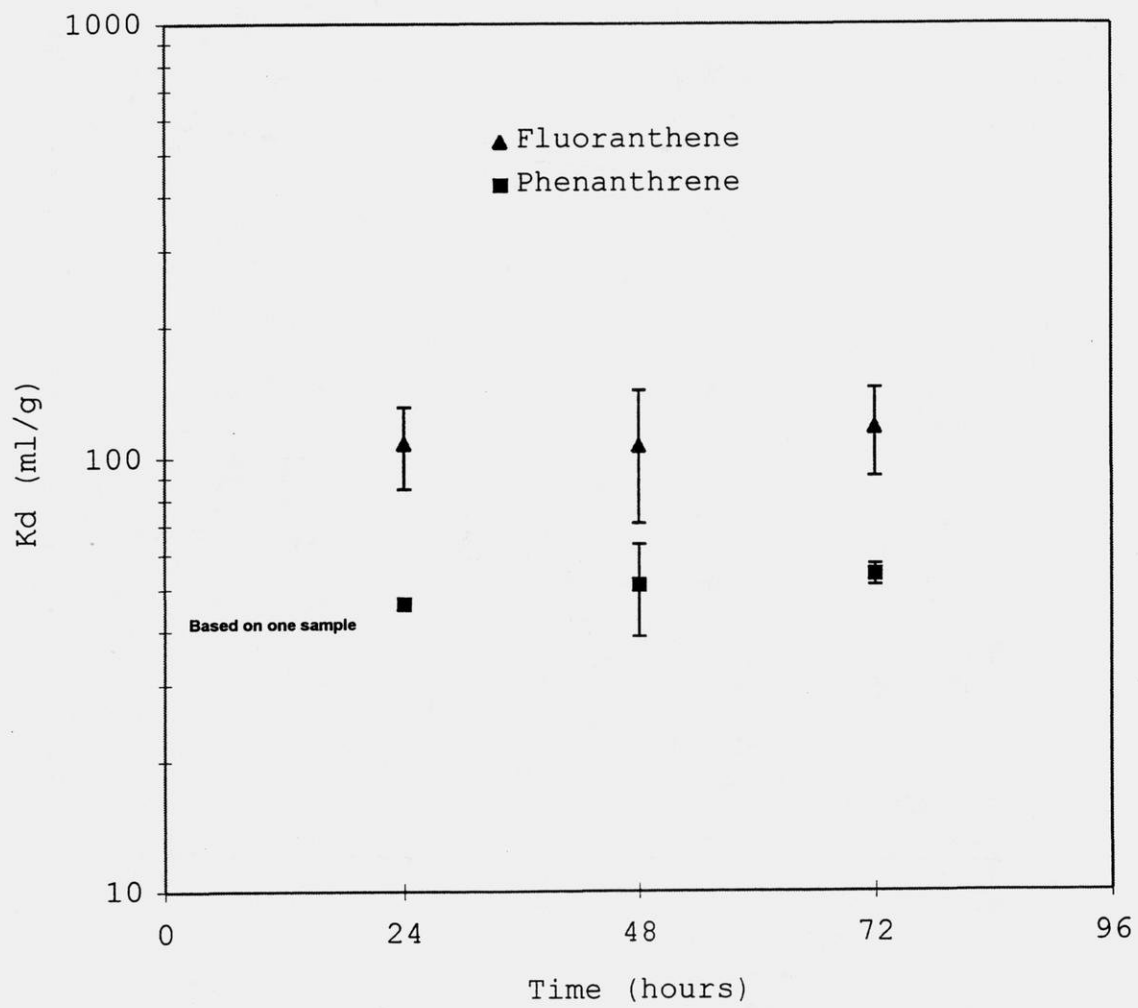
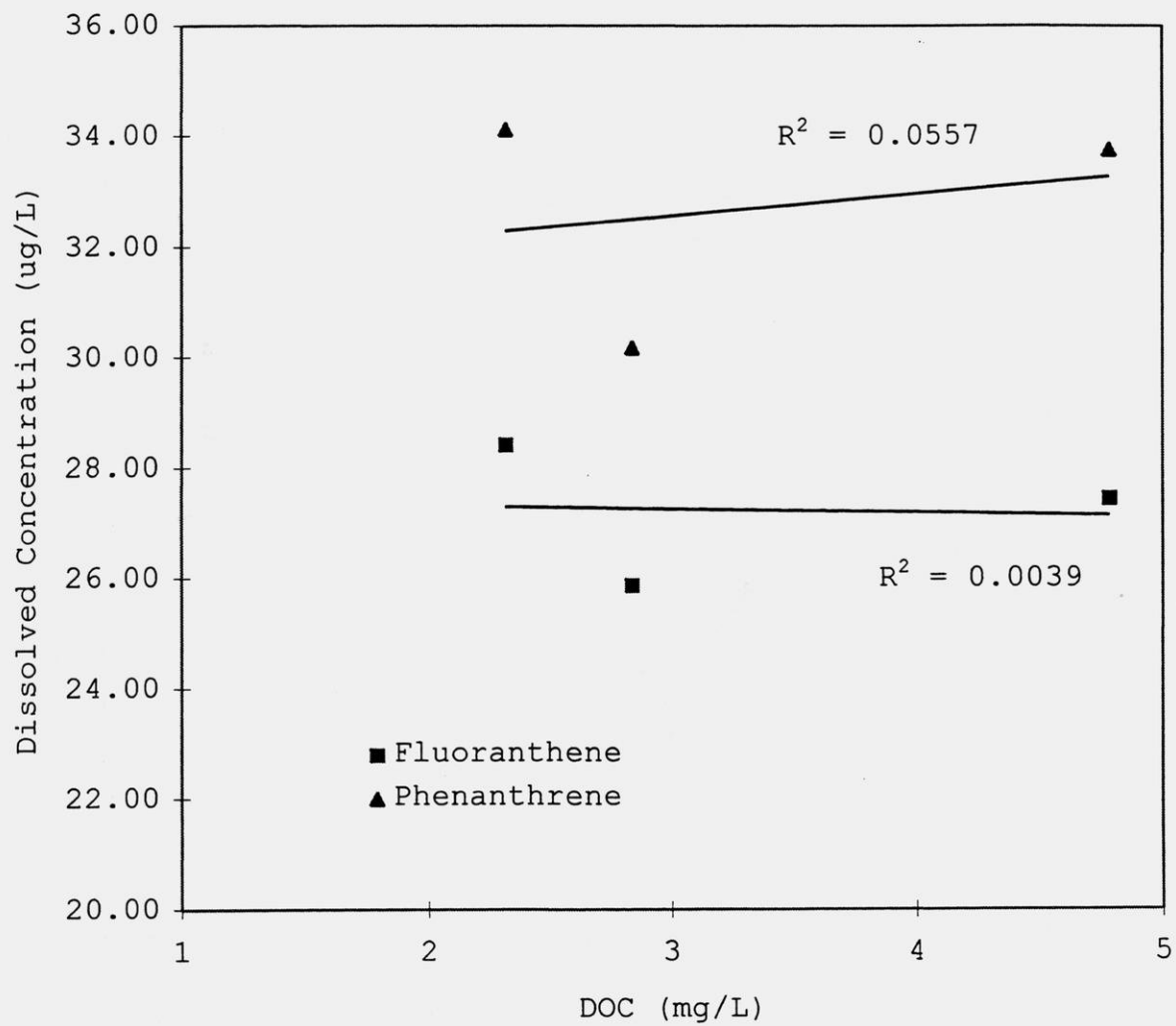


Figure 5-4 Sparta Sand PAH Versus DOC



Clearly, both predictive equations overestimated sorption and therefore underestimated transport times. Other researchers have observed the reduction in sorption of hydrophobic organic contaminants (HOCs) in the presence of other HOCs (Mc Ginley et al., 1993). To test this theory an additional batch experiment was conducted using solely phenanthrene in the stormwater. The results were essentially equivalent to experiments with all contaminants. The overestimation of sorption by both predictive equations translates to an underestimation of contaminant velocity by a factor of about 3.4 as shown below.

$$v_x/v_c x = 1 + (\rho_b/n) K_d$$

Approximations for a sandy soil

$v_x = 0.15 \text{ cm/min}$	$\log K_d = 1.7 \text{ ml/g}$	$v_c x = 6.4\text{e-}4 \text{ cm/min}$
$\rho_b = 1.6 \text{ g/cm}$	$\log K_d = 2.3 \text{ ml/g}$	$v_c x = 1.9\text{e-}4 \text{ cm/min}$
$n = 0.35$		

While this difference seems relatively small, a contaminant advective arrival at the groundwater table would occur after 1.5 years versus 4.9 years for a soil thickness of 5 meters. Although these estimates do not include possible removal by degradation or possible increasing mobility due to decreasing organic carbon content with depth through a soil profile.

Like phenanthrene, fluoranthene equilibrium partitioning appeared to occur within about 24 to 48 hours (Figure 5-3). The average experimental K_d was 100 ± 20 ml/g. Predictive equations gave equivalent estimates of 501 ml/g. Again, both equations overestimated a K_d and therefore underestimated contaminant advective travel times. As indicated by Figure 5-4, dissolved fluoranthene concentration was correlated to DOC concentrations in batch experiments.

In short, even though both predictive equations appeared to satisfactorily estimate an atrazine K_d , they overestimated K_d values for phenanthrene and fluoranthene. However, as discussed in the Background section, K_d values in soils with low organic carbon contents often are not predicted accurately by these equations. It is not surprising then, that K_d values

for phenanthrene and fluoranthene, which are largely based upon organic carbon sorption, show more deviation from predicted values than for atrazine. A desorption experiment was also conducted with the Sparta Sand soil. Figure 5-5 shows that desorption of atrazine occurs within the first few hours. Also, approximately 100 percent of the sorbed atrazine was recovered by desorption, considering experimental standard deviation. Since atrazine is somewhat polar and does not sorb strongly to the Sparta soil these results were expected.

Phenanthrene desorption was slower, reaching a maximum mass desorbed after 48 hours (Figure 5-6). Recovery by desorption of originally added phenanthrene reached 75 percent. The slower desorption than atrazine may be attributed to phenanthrene's hydrophobicity and therefore its "preference" for association with soil organic carbon. The fraction not recovered by desorption, approximately 25 percent of the original added mass, might represent phenanthrene which had penetrated into the soil organic carbon matrix, decreasing desorption into the polar solvent (stormwater).

Figure 5-5 Sparta Sand Atrazine Desorption Kinetics

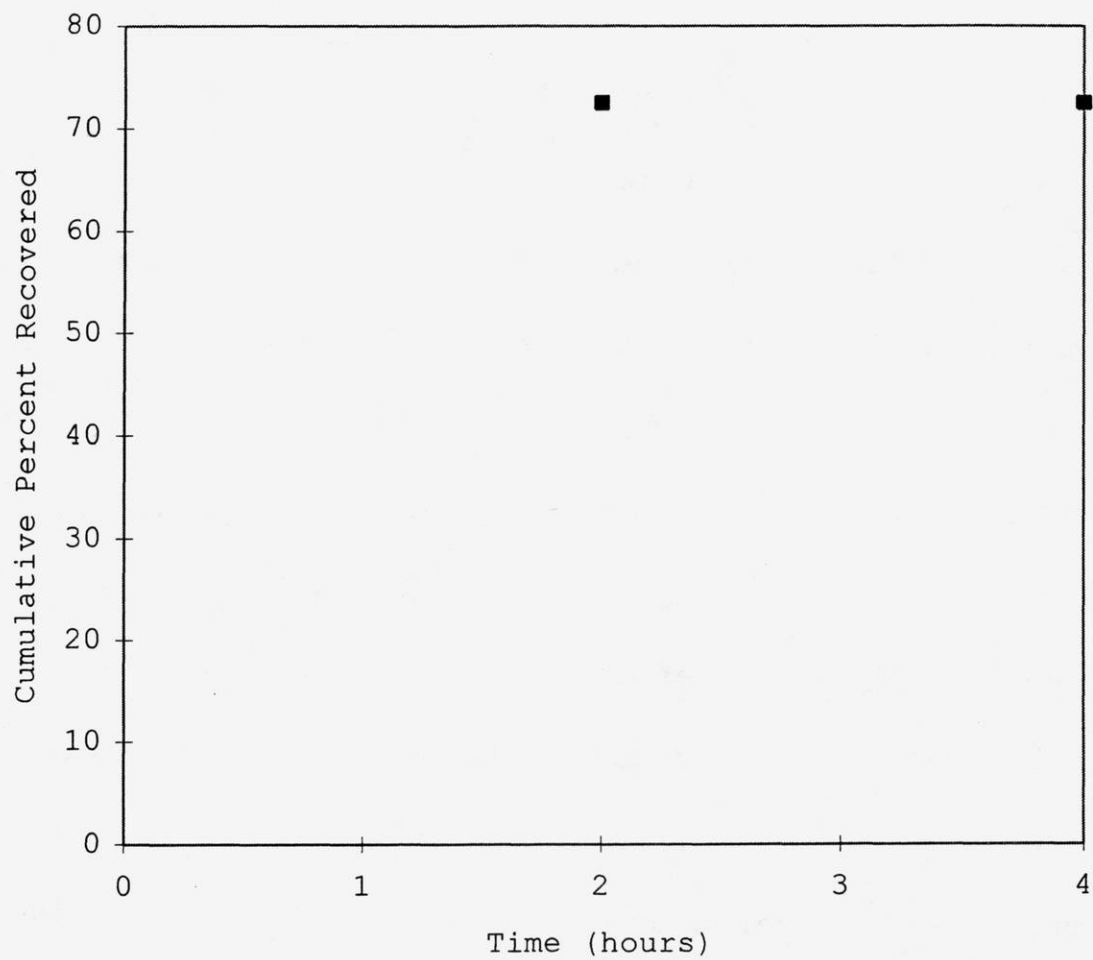
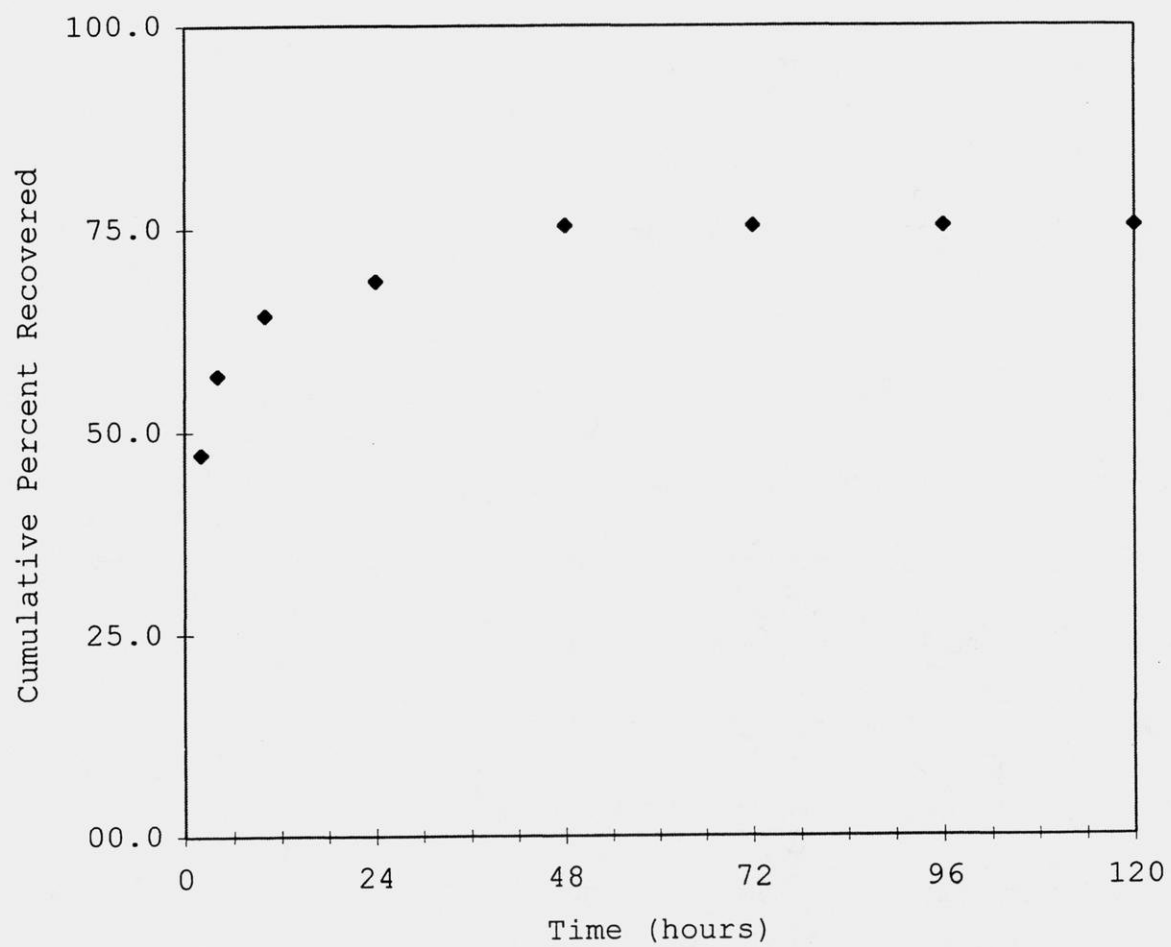


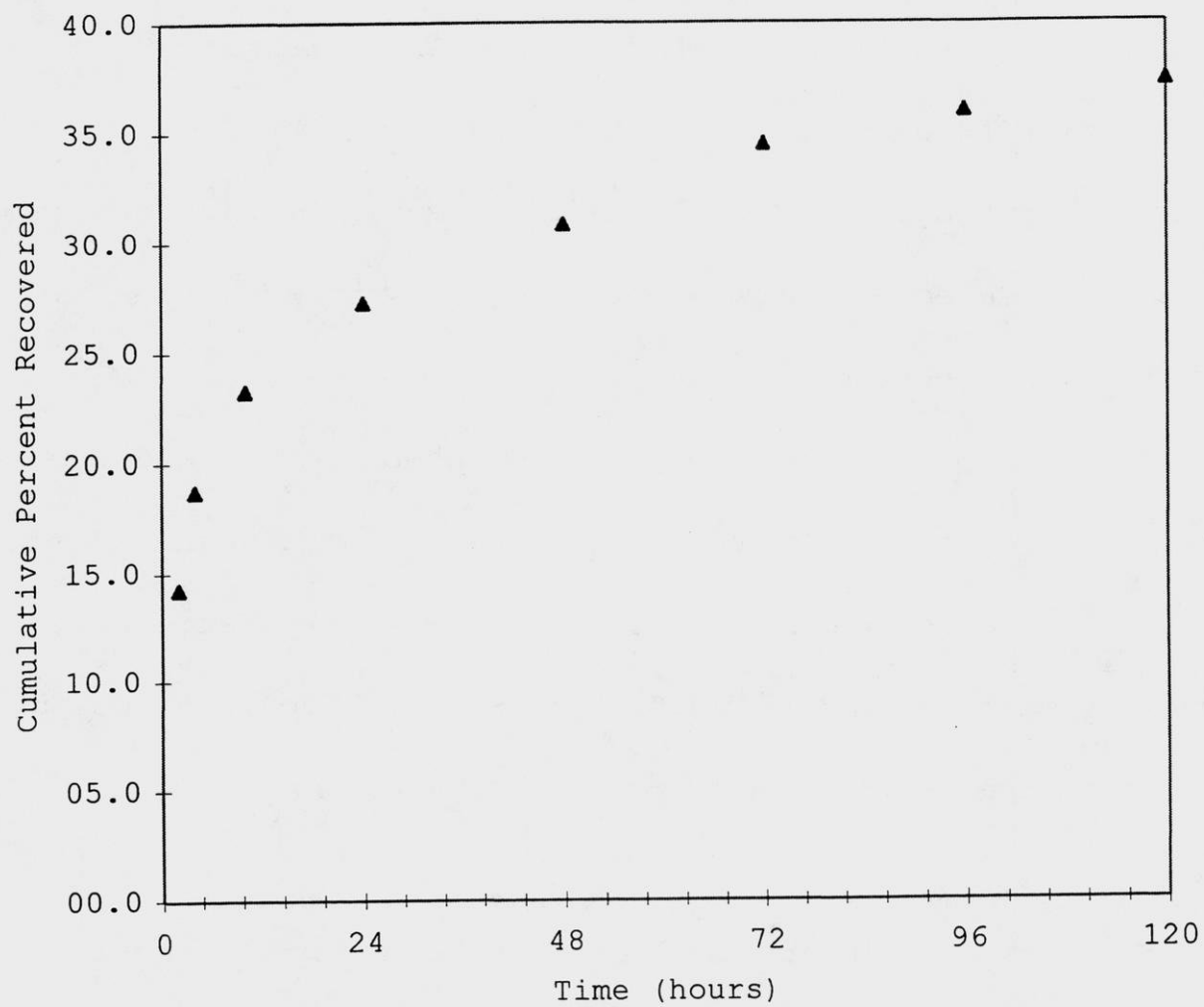
Figure 5-6 Sparta Sand Phenanthrene Desorption Kinetics



Although desorption probably continued after 48 hours, the amounts released into the stormwater were below the detection limit. Continuing desorption could account for at least part of the mass which was not recovered.

Fluoranthene desorption was the slowest (Figure 5-7) of the three organic contaminants, continuing even after 120 hours, when the experiment was terminated. The maximum recoverable mass was much lower than expected, reaching only 30 percent. As the most hydrophobic contaminant studied, fluoranthene desorption into the polar stormwater was expected to be slower. Since the experiment was not conducted past 120 hours, the maximum recoverable mass is unknown. However, since only small increments of recoverable fluoranthene were found after 96 hours, complete desorption seems unlikely. Incomplete recovery of fluoranthene may be due to penetration deep within the structure of the organic matter, making much of the added fluoranthene largely unavailable for desorption.

Figure 5-7 Sparta Sand Fluoranthene Desorption Kinetics



Atrazine partitioning to the St. Charles silt loam was essentially complete within 48 hours (Figure 5-8) although the K_d of 3.0 ± 0.5 ml/g measured after 72 hours is used as an approximate average of the K_d values measured at 24 and 48 hours. Using the mineral phase equation (equation 5-2), a K_d of 2.9 ml/g is calculated. Equation 5-3 (organic carbon equation) gives 2.3 ml/g. Therefore, the K_d predicted by the mineral phase equation gave better agreement with measured partitioning behavior.

Equilibrium partitioning between phenanthrene and the St. Charles silt loam soil appear complete after 48 hours (Figure 5-9). An average measured K_d of 316 ± 100 ml/g range nicely compares with the predicted K_d of 316 ml/g calculated using both the mineral phase and organic carbon predictive equations.

Fluoranthene is observed to reach equilibrium partitioning after approximately 48 hours (Figure 5-9). The measured average K_d of 1000 ± 501 ml/g favorably compares to calculated K_d values of 1000 ml/g using both mineral phase and organic carbon equations.

Figure 5-8 St. Charles Silt Loam Atrazine Partitioning Kinetics

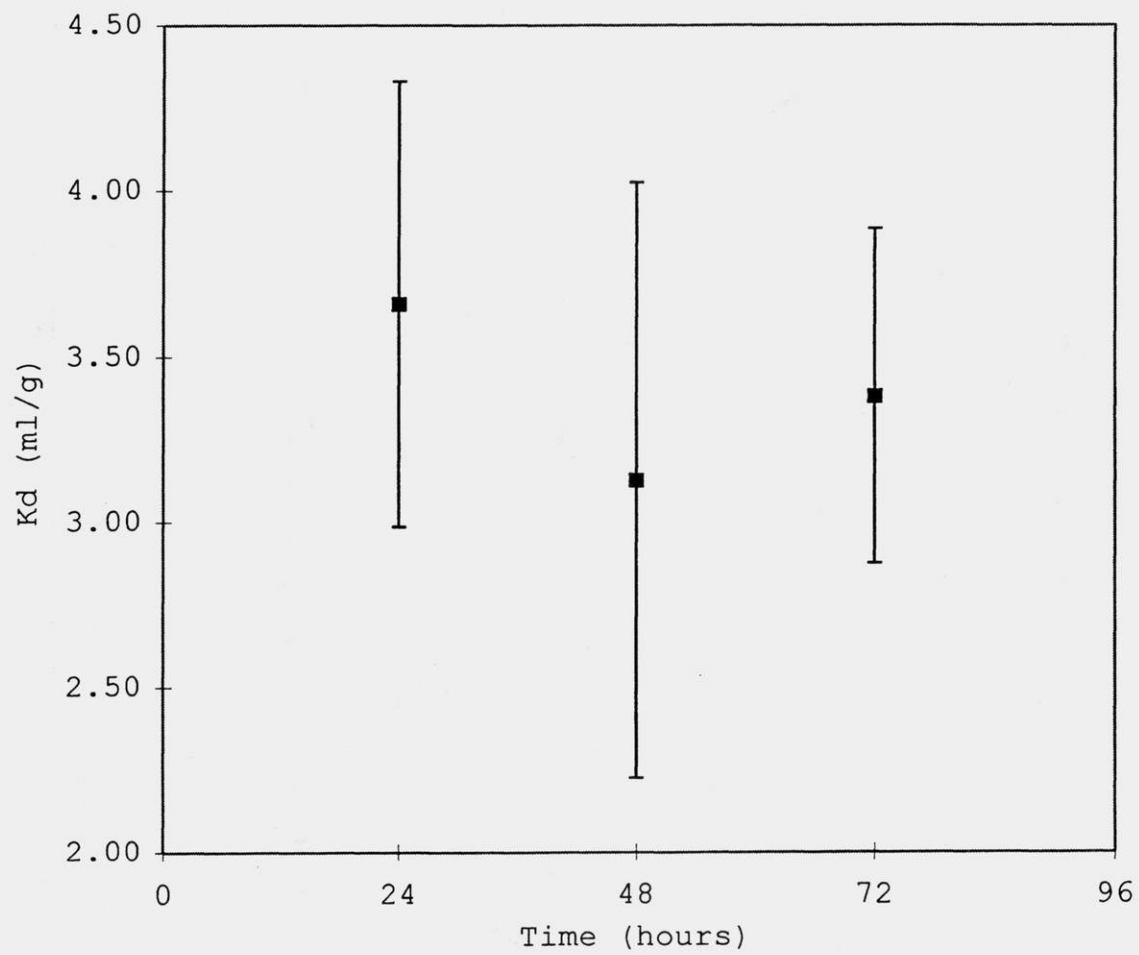
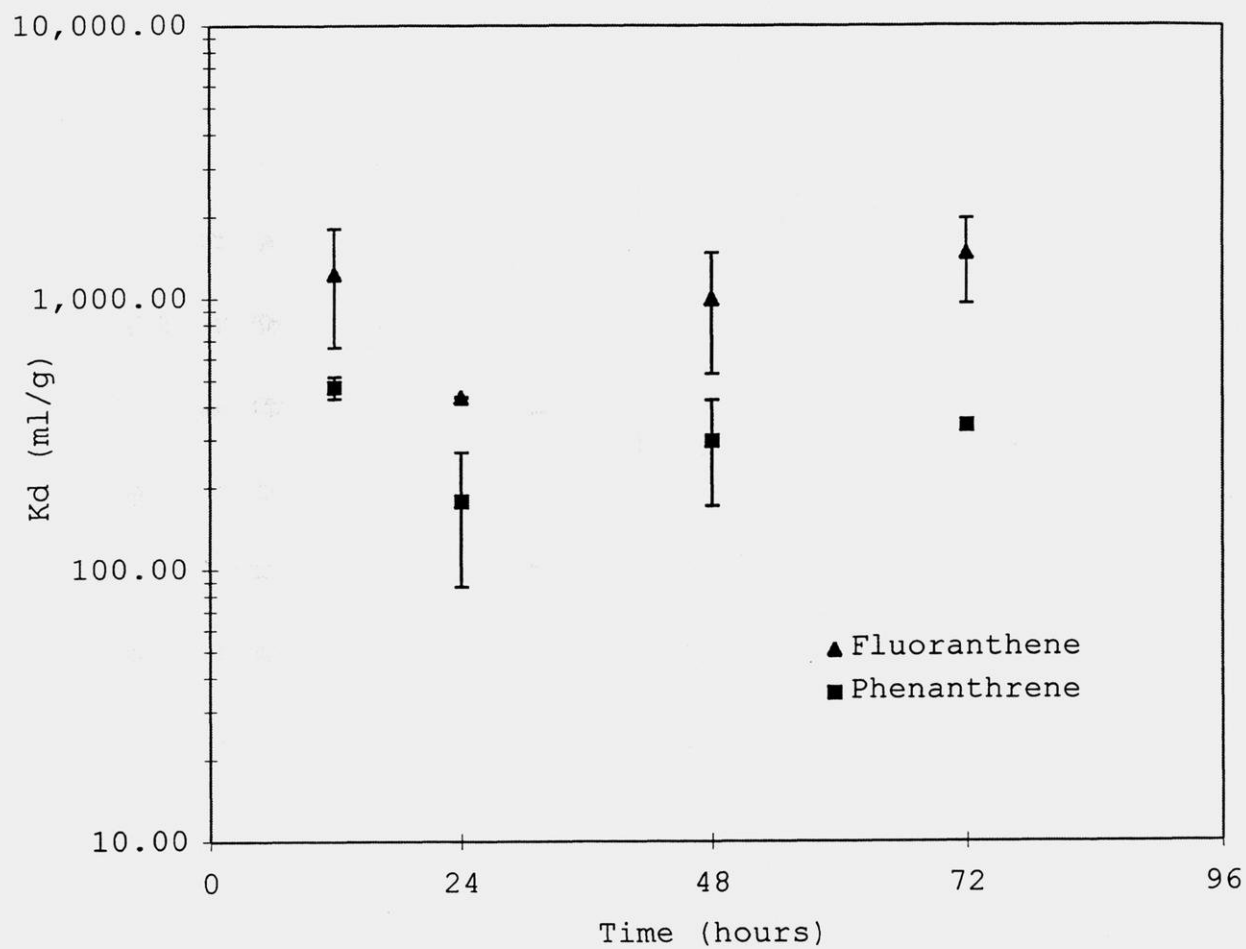


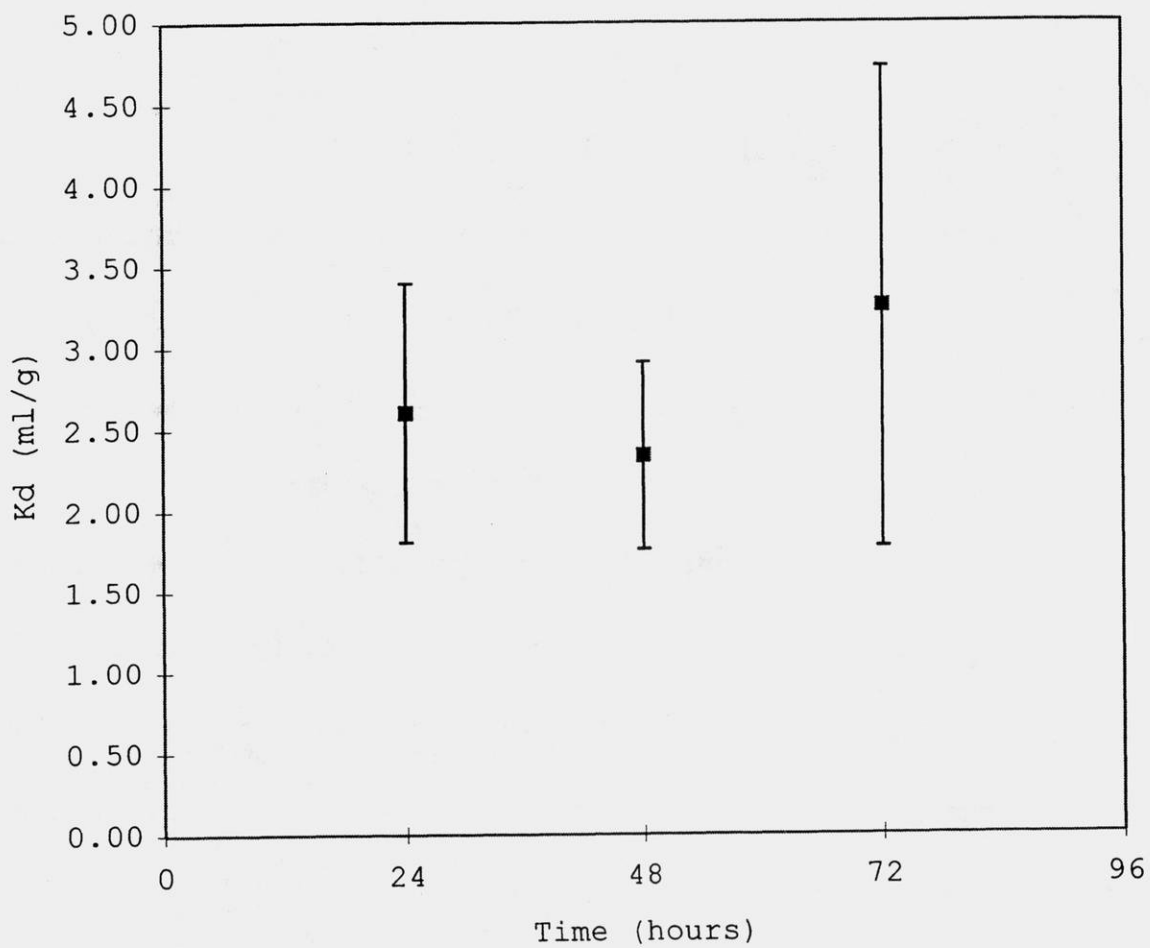
Figure 5-9 St. Charles Silt Loam PAH Partitioning Kinetics



In contrast to the Sparta sand, calculated equilibrium K_d values for the St. Charles silt loam soil using equations 5-2 and 5-3 gave better predictions of the experimentally-derived K_d values. This could be due to a slightly higher organic carbon fraction in the St. Charles silt loam as compared to Sparta sand.

Atrazine partitioning in the Pals Grove silt loam soil reached apparent equilibrium after approximately 24 to 48 hours (Figure 5-10) with an average K_d of 2.3 ± 0.6 ml/g. This compares to the predicted K_d values of 2.3 ml/g (organic carbon equation) and 3.1 ml/g (mineral phase equation). The predicted K_d from the organic carbon equation was a better estimate of measured atrazine partitioning behavior than the mineral phase equation. Perhaps above a minimum fraction of organic carbon, mineral phase sorption is less dominant even for more polar compounds such as atrazine.

Figure 5-10 Pals Grove Silt Loam Atrazine Partitioning Kinetics



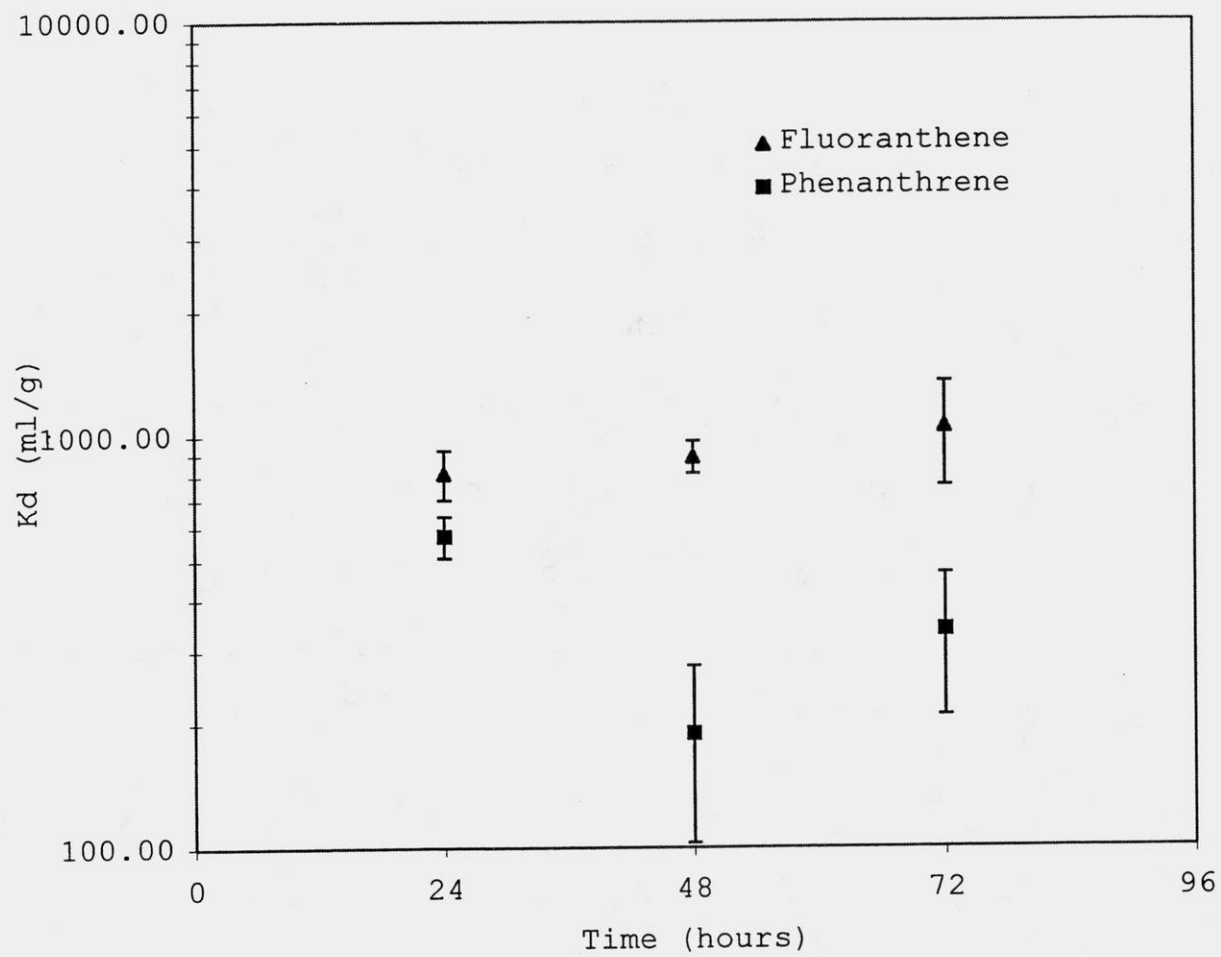
The difference in predictive equation success between the two silt loam soils (St Charles predicted by mineral phase equation versus Pals Grove better predicted by the organic carbon equation) could reflect subtle differences in organic carbon genesis (Seybold, 1993).

Between 24 and 48 hours elapsed before phenanthrene attained equilibrium partitioning (Figure 5-11). The average K_d was 316 ± 126 ml/g. Calculated K_d values were 316 ml/g using either predictive equation.

The 72 hour K_d of 1000 ± 100 ml/g is used as the equilibrium value for fluoranthene sorption (Figure 5-11). The organic carbon and mineral phase equations predicted a K_d of 1000 ml/g. This seems to be a good estimation of observed partitioning.

In general, both eq 5-2 and 5-3 predicted phenanthrene and fluoranthene equilibrium K_d values in the silt loam soils. It should be noted that both equations gave equivalent results for both silt loam soils. This is due to the hydrophobicity of the contaminants and the magnitude of term 1 versus term 2 of the mineral phase equation (eq 5-2)

Figure 5-11 Pals Grove Silt Loam PAH Partitioning Kinetics



Term 1 Term 2

$$K_d = K_{oc}f_{oc} + K_{io}f_{io} \quad (5-2)$$

Phenanthrene and fluoranthene partitioning were not well predicted by either equation for the Sparta sand soil. This is attributed to the soil's low organic carbon content which may invalidate use of either predictive equation (eq 5-2 or 5-3). Calculated atrazine K_d values using both equations were within the experimentally-derived K_d ranges for the Sparta sand. Unfortunately, large experimental standard deviations make a clear comparison of either equations' applicability impossible. Interestingly, the organic carbon equation gave a better prediction of experimental behavior in the Pals Grove silt loam, whereas the mineral phase equation gave a better estimate of observed atrazine partitioning in the St. Charles silt loam. Figure 5-12, illustrating atrazine K_d correlations with the percent silt, clay and organic matter may help explain these observations. As Figure 5-12 shows, atrazine experimental K_d values correlate very well with the soil's percent silt. In addition, since the St. Charles soil has a

higher percentage of silt (73) compared to the Pals Grove silt loam (57), one might expect that the mineral phase equation (eq 5-2) which includes sorptive contributions from silt might better predict atrazine K_d values.

The first soil column experiment on organic contaminant transport was conducted with the Sparta sand soil using a slug input of the contaminants. Column specifications are enumerated in Table 5-2. Figure 5-13 shows the elution history of the potassium bromide tracer inherent to the stormwater mixture. Bromide contained in the contaminant slug travels first through the column. Then bromide contained in the stormwater used to elute the contaminant slug travels through the column. The contaminant slug was pulled through the column using a peristaltic pump, while the stormwater was pushed through the column and column effluent did not contact the pump. Apparently, sorption by the peristaltic pumphead tubing retarded bromide transport.

Figure 5-12 Atrazine Experimental Kd Value Correlation With Soil Characteristics

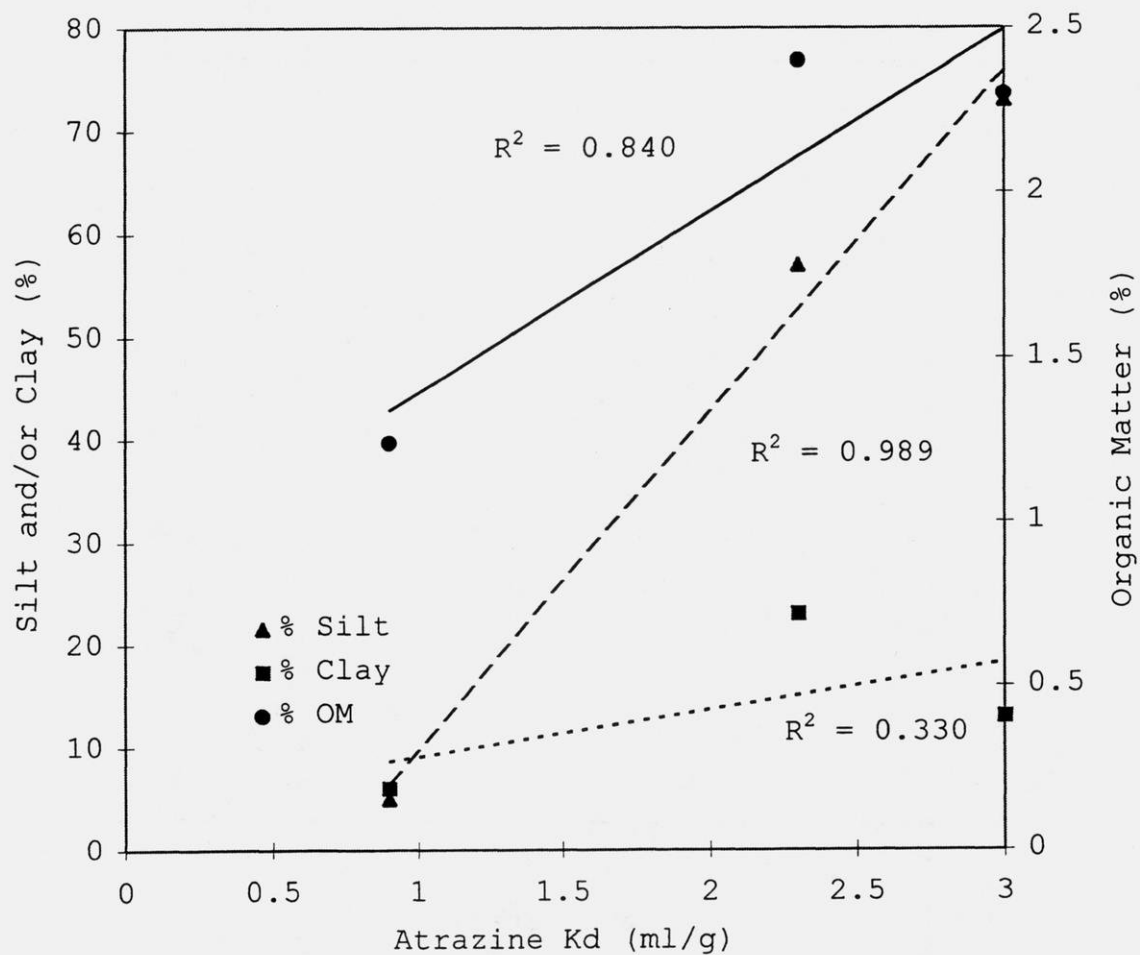
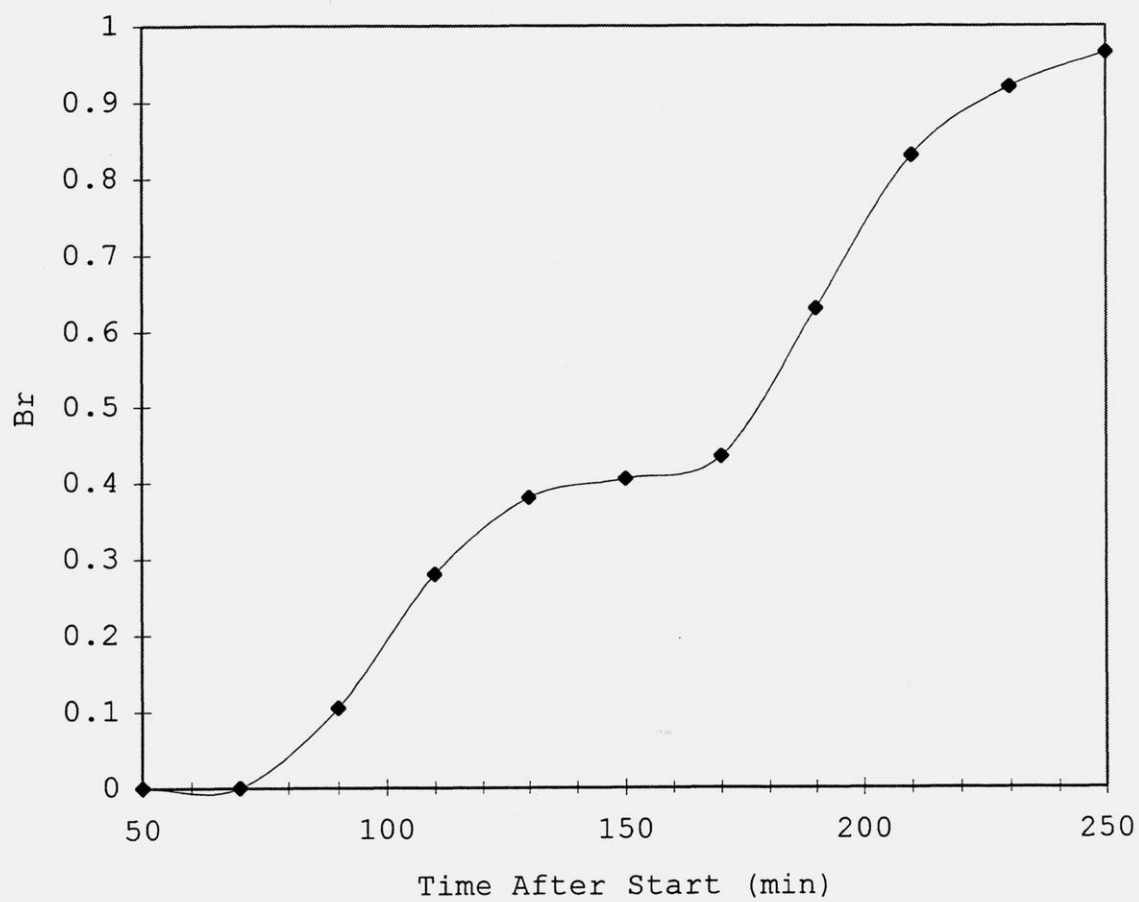


Figure 5-13 Bromide Tracer Concentration History



This caused the discontinuity in bromide concentration. The time when the bromide relative concentration (C/C_0) reached 0.5, was assumed to be the advective breakthrough time for the tracer. Starting at 121 minutes after the start of the experiment, column flow was switched from slug input (which pulled water down through the column and through the peristaltic pumphead tubing) to continuous input of uncontaminated stormwater (pushed through the column so that effluent samples did not contact the peristaltic pumphead tubing).

Table 5-2 Sparta Soil Column Specifications

Length (cm)	11
Inner Diameter (cm)	2.05
Packed Dry Bulk Density (g/cm ₃)	1.4
Estimated Porosity	0.46
Influent Rate (ml/min)	1.0
Pore Water Velocity (cm/min)	0.182
Effective Porosity	0.42
Pore Volume (cm ³)	60.6

Therefore, although some bromide may have remained in the column from the slug input, the majority of bromide at 180.6 minutes (assumed time of tracer advective arrival from Figure 5-13) should have been introduced into the column from continuous input of uncontaminated stormwater. The pore water velocity gleaned from Figure 5-13 was combined with the average K_d measured from the batch experiments to predict the atrazine advective velocity. Predicted advective arrival time at the column exit was 242 minutes. Figure 5-14 shows the concentration history of atrazine in the column effluent. The advective arrival may be graphically determined as the time where one half the mass exits the column. Figure 5-15 shows that the measured advective arrival time was approximately 262 minutes. This agrees fairly well with the calculated arrival time. In fact, the K_d value using the 262 minute arrival time was 1.0 ml/g which is within the experimentally-measured K_d range of 0.9 ± 0.8 ml/g. Although the retardation equation did approximate the advective breakthrough of atrazine, the breakthrough occurred before atrazine had reached equilibrium partitioning (as determined from batch experiments).

Figure 5-14 Sparta Sand Atrazine Concentration History

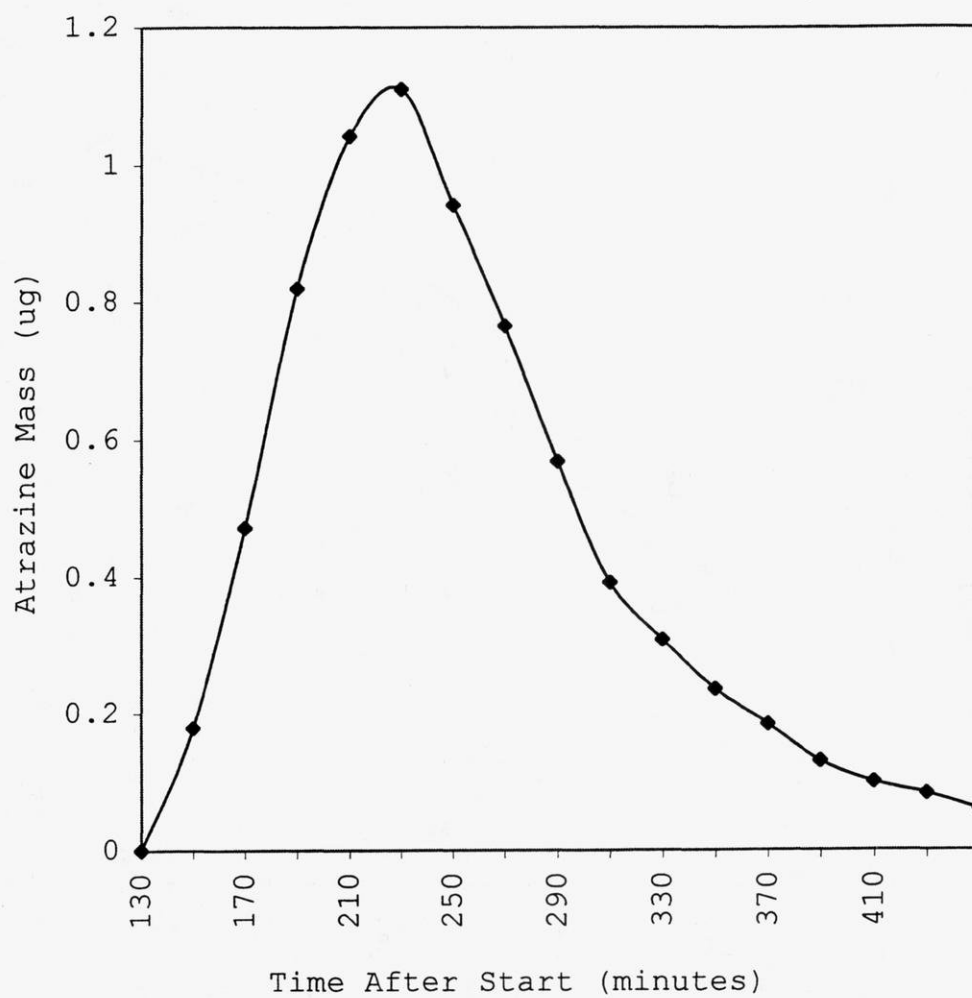
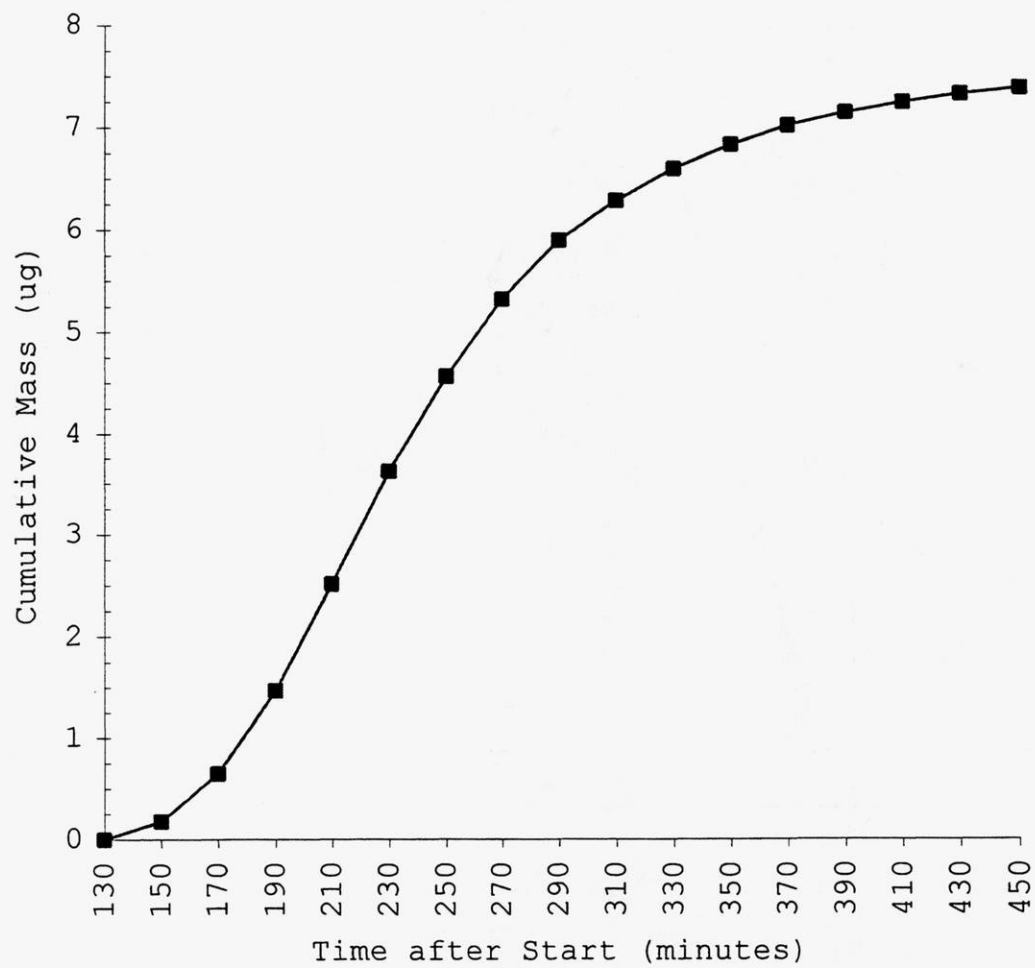


Figure 5-15 Sparta Sand Cumulative Atrazine Mass



Therefore, the retardation equation's assumption of equilibrium partitioning was likely violated and the predictive success was probably due to the relatively low K_d value for atrazine and large experimental standard deviation for the experiment K_d value. Figure 5-15 also illustrates that approximately 20 percent of the added atrazine was not recovered. This could be attributed to loss in dead-end pores and/or elution faster than anticipated due to preferential flow or possibly because of formation of DOC complexes.

Phenanthrene and fluoranthene, applied at concentrations of 100 $\mu\text{g/L}$, were never found in column effluent or in the soil column itself after soil sectioning and extraction. Since only 10 μg of each contaminant was applied to the soil, one explanation for the apparent disappearance of both contaminants involves results from the desorption experiment previously discussed. Only 75 and 36 percent of the total applied mass of phenanthrene and fluoranthene were recovered, respectively. Since column operation was much longer (20 days) than the initial equilibration time (72 hours) for the desorption experiment, both contaminants may have penetrated

into the soil organic matter and become largely unavailable for transport. Also, distribution between dissolved and sorbed masses could have reduced concentrations to values below detection limits. If the sorbed mass remained in the soil in concentrations above our detection limits, the contaminants apparently became unextractable. Another possibility is altered transport, which either carried the contaminants much faster or slower than predicted by batch experiment-measured K_d values and eluded periods of intensive sampling comfortably bracketing calculated arrival times. Colloidal transport may have also helped spread the introduced contaminants to levels below our detection limits. Also, batch experiments have been shown by other researchers to produce sorption values two times lower for PAHs than observed in column experiments (Kilmer et al., 1987).

While the reasons for the disappearance of phenanthrene and fluoranthene remain uncertain, we suspect that slow sorption-desorption kinetics caused the contaminants to slowly spread throughout the column, in effect dispersing the contaminants to concentrations below detection limits.

The other soil column used to study the transport of organic contaminants utilized the St Charles silt loam soil in a continuous input experiment. Table 5-3 lists all relevant column parameters. Because of the possibility of anion exclusion, tritiated water was used in conjunction with bromide as a conservative tracer. Figure 5-16 and 5-17 illustrate concentration histories for both tracers. Although both tracers eluted at approximately the same time, tritium was used for average pore water velocity calculations. Figure 5-16 illustrates that half of the mass of tritium had exited the column at about 95 minutes. Figure 5-18 shows the concentration history of atrazine in the St. Charles silt loam soil. Unfortunately, the start of atrazine breakthrough was not measured, but the atrazine advective front arrived before 886 minutes (Figure 5-18) , cooresponding to a K_d value less than 2.28 ml/g. This is slightly less than the experimentally measured K_d of 3.0 ml/g.

Table 5-3 St Charles Silt Loam Column Specifications

Length (cm)	11.01
Inner Diameter (cm)	2.05
Packed Dry Bulk Density (g/cm ₃)	1.3
Estimated Porosity	0.5
Influent Rate (ml/min)	0.6
Pore Water Velocity (cm/min)	0.070
Effective Porosity	0.65
Estimated Velocity (1PV)	0.091

Figure 5-15 St Charles Silt Loam Column Tritium Data

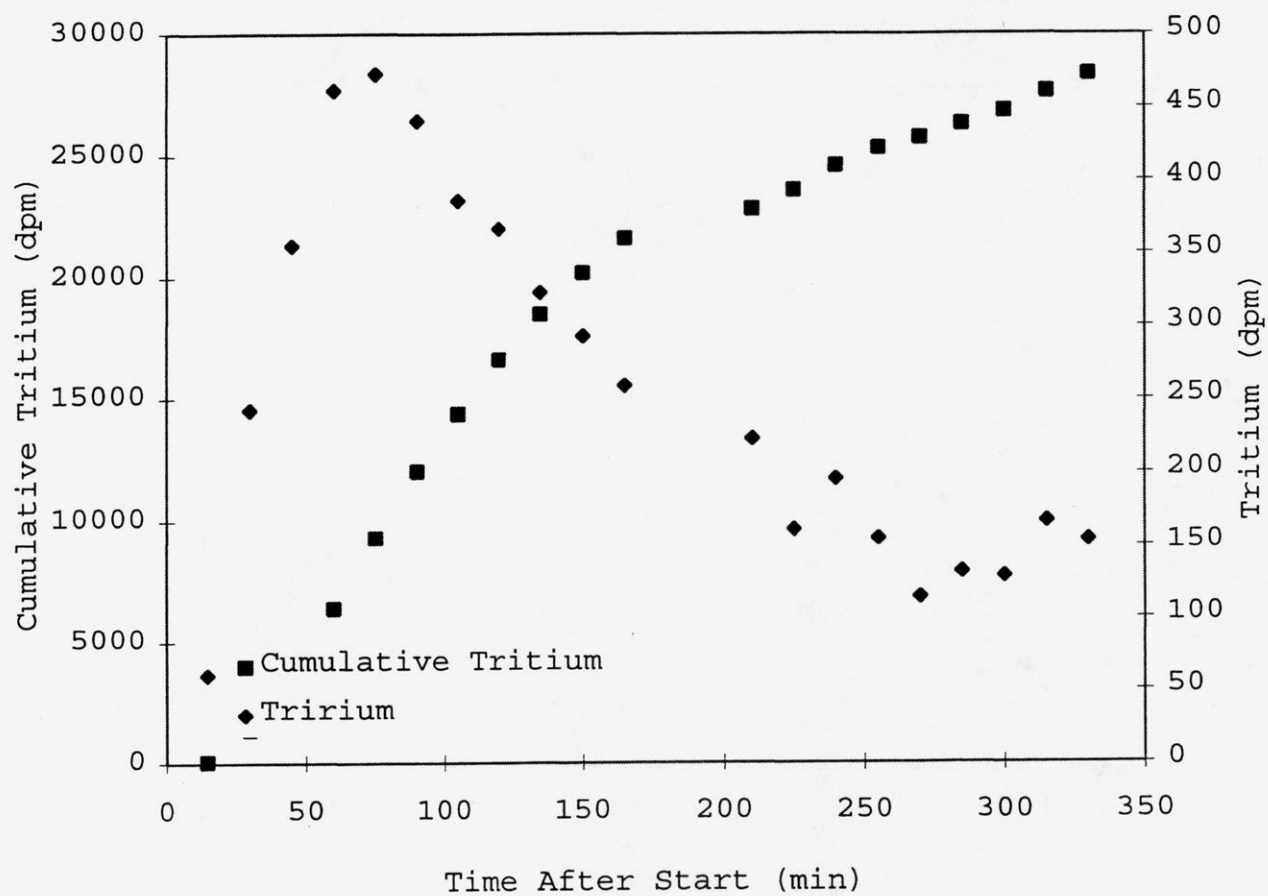


Figure 5-16 St Charles Silt Loam Column Bromide Breakthrough

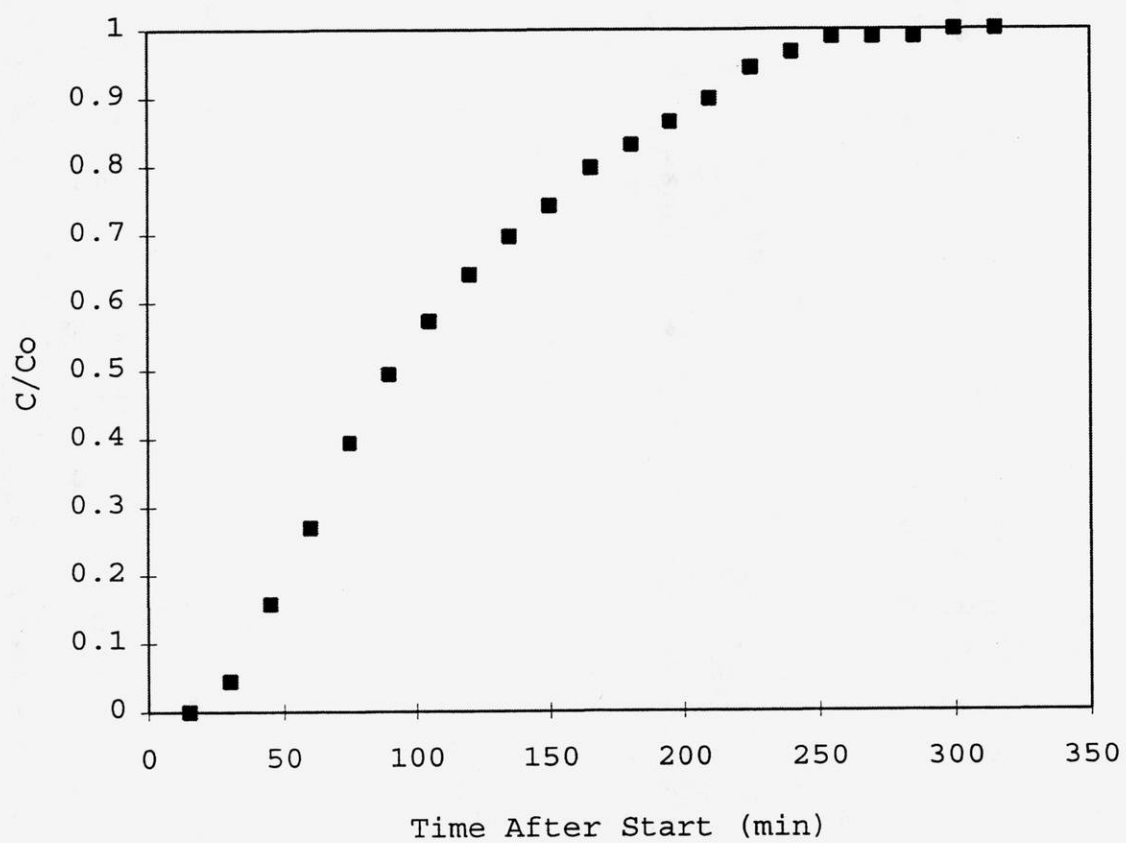
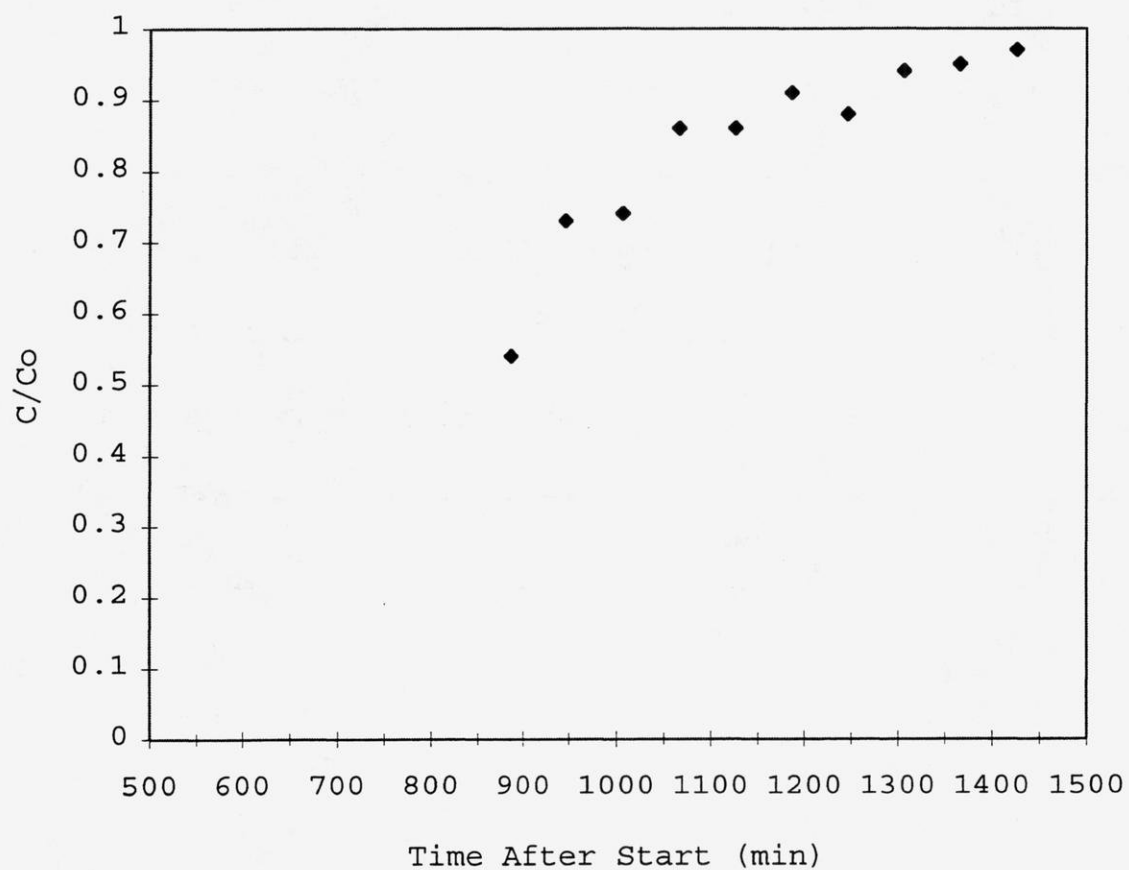


Figure 5-17 St Charles Silt Loam Column Atrazine Breakthrough



This discrepancy may be attributed to nonattainment of equilibrium partitioning or to preferential flow. The asymmetric shape of the tritium concentration profile suggests preferential flow. As previously discussed, one of the retardation equation's assumptions is the lack of preferential flow. Therefore, the predictive error using the retardation equation could arise from the existence of preferential flow. The preferential flow also could have prevented atrazine from reaching soil-water partitioning equilibrium, violating the retardation equation's assumption of equilibrium partitioning. The lack of equilibrium may also be attributed to the constant inflow rate of $0.6 \text{ cm}^3/\text{min}$ which carried atrazine faster than the rate necessary to allow equilibrium partitioning.

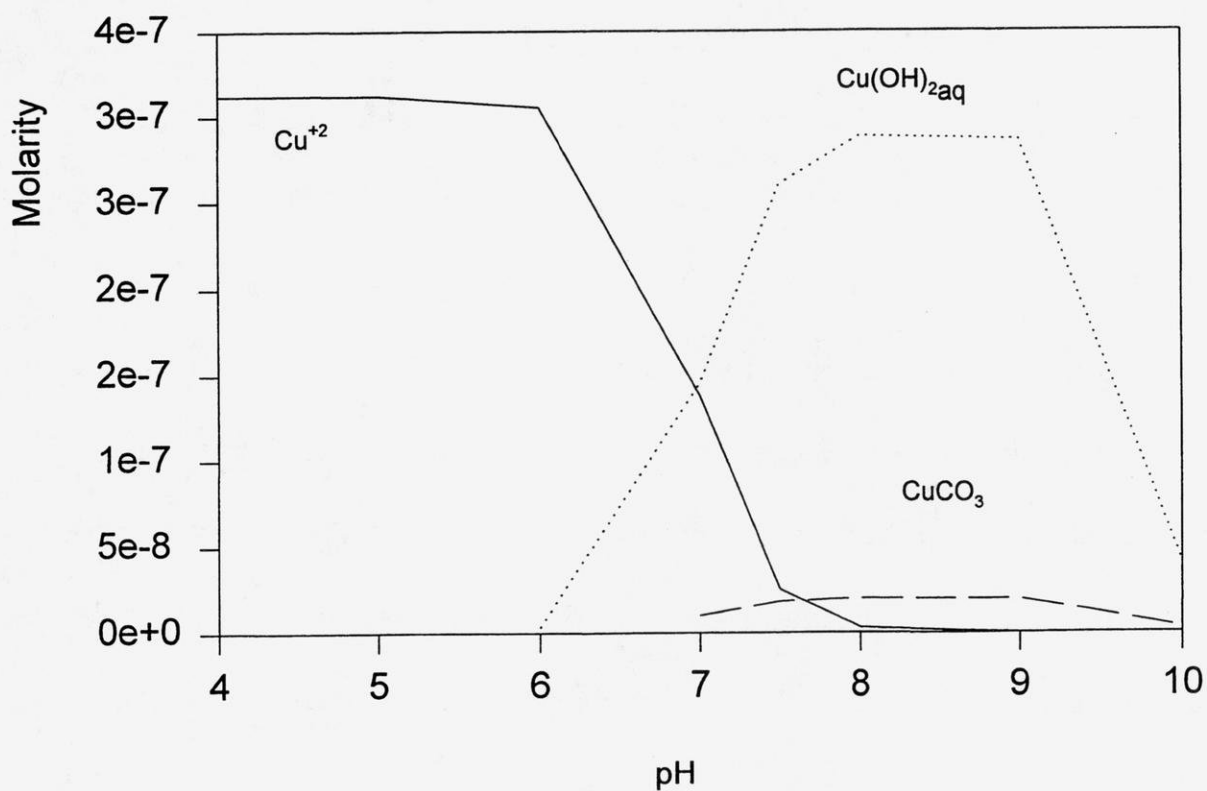
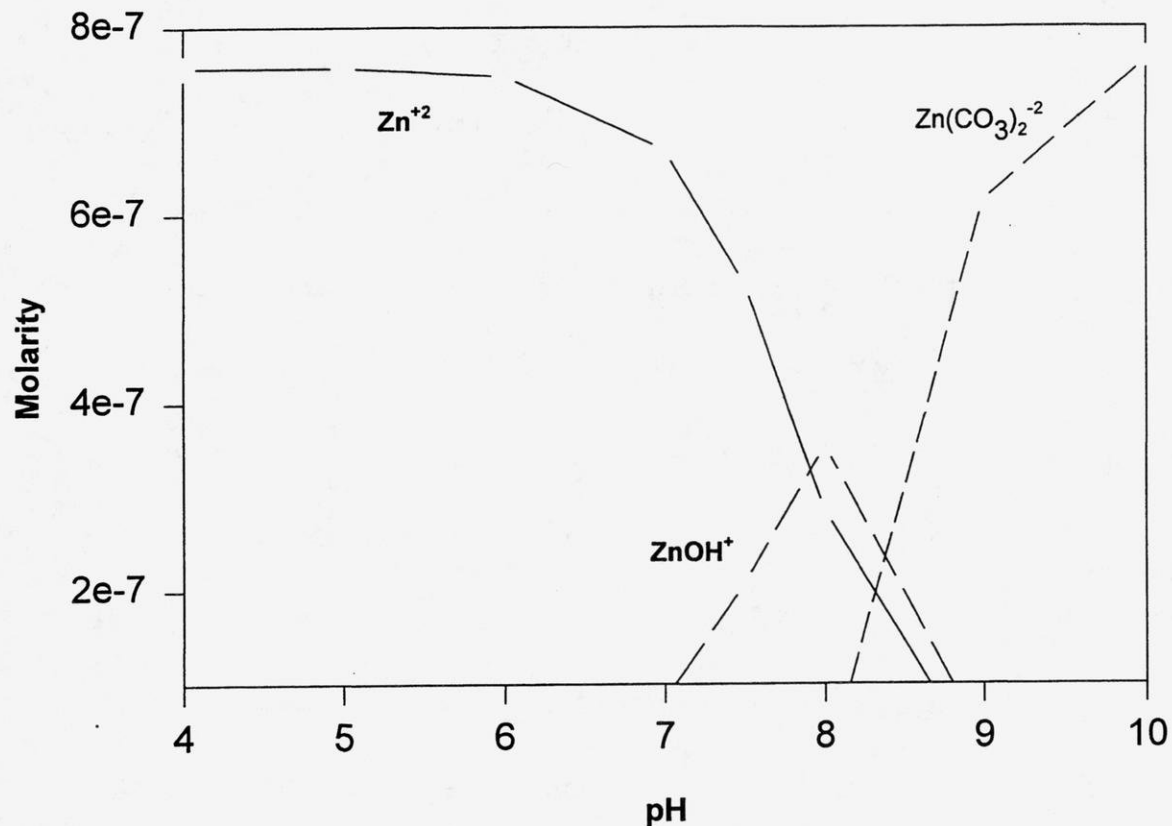
B. Metal Contaminants

1. Partitioning in Batch Systems

As previously discussed, speciation influences the fate of metals in the subsurface. Figure 5-19 shows the predicted speciation of two metals (zinc 50 at μL and copper at μL) using the computer program Minteq version 3.11 (EPA, 1991) in the simulated stormwater mixture over a representative range of pHs. At pH 7.5, the majority of zinc is in the Zn^{+2} form and the majority of copper is in the $\text{Cu}(\text{OH})_2$ form. Speciation is very important, since a given concentration of total metal contains different species or forms of metal, and therefore will sorb differently at a pH of 4.0 than at 7.5. For example, sorption of zinc to a sand soil increased from 15 percent to 100 percent with a pH change from 4.8 to 7.0 (Allen et al., 1993).

Several batch experiments were conducted with the Sparta sand soil. Experiments were done using zinc concentrations of 50 $\mu\text{g/L}$ and 100 $\mu\text{g/L}$ and copper concentrations of 20 $\mu\text{g/L}$ and 40 $\mu\text{g/L}$, respectively. One batch experiment with the Sparta sand was also conducted at the same ionic strength (0.01 M)

Figure 5-19 Zinc and Copper Stormwater Speciation



and pH (7.5) as the other batch experiments, but a hardness of 60 mg/L (versus 40 mg/L). Some batch experiments were also performed with the St. Charles and Pals Grove silt loam soils.

Figure 5-20 shows the kinetics of zinc and copper partitioning (concentrations of 50 $\mu\text{g/L}$ and 20 $\mu\text{g/L}$ respectively) to the Sparta sand soil. It appears that partitioning reached an approximate equilibrium between 48 and 72 hours. The zinc $\log K_d$ value is 3.23 ± 0.12 ml/g, whereas the copper $\log K_d$ value is 3.29 ± 0.07 ml/g. While we do not have models for prediction of K_d values for metals from readily-measurable soil properties, the reported range in measured K_d values for zinc in sandy soils is 0.1 to 8000 ml/g (Sheppard and Thibault, 1990). Partitioning experiments with the colloidal fraction of this soil showed that zinc, at a concentration of 25 $\mu\text{g/L}$, reached equilibrium ($\log K_d = 3.08$ ml/g) after about 36 to 41 hours (Herrin, 1994). Figure 21 illustrates the lack of correlation between the dissolved fractions of zinc and copper (that passing a 0.4 μm filter) and DOC. This lack of correlation to DOC may be due to a very low range in DOC between batch.

Figure 5-20 Zinc (50 ug/L) and Copper (20 ug/L) Partitioning Kinetics

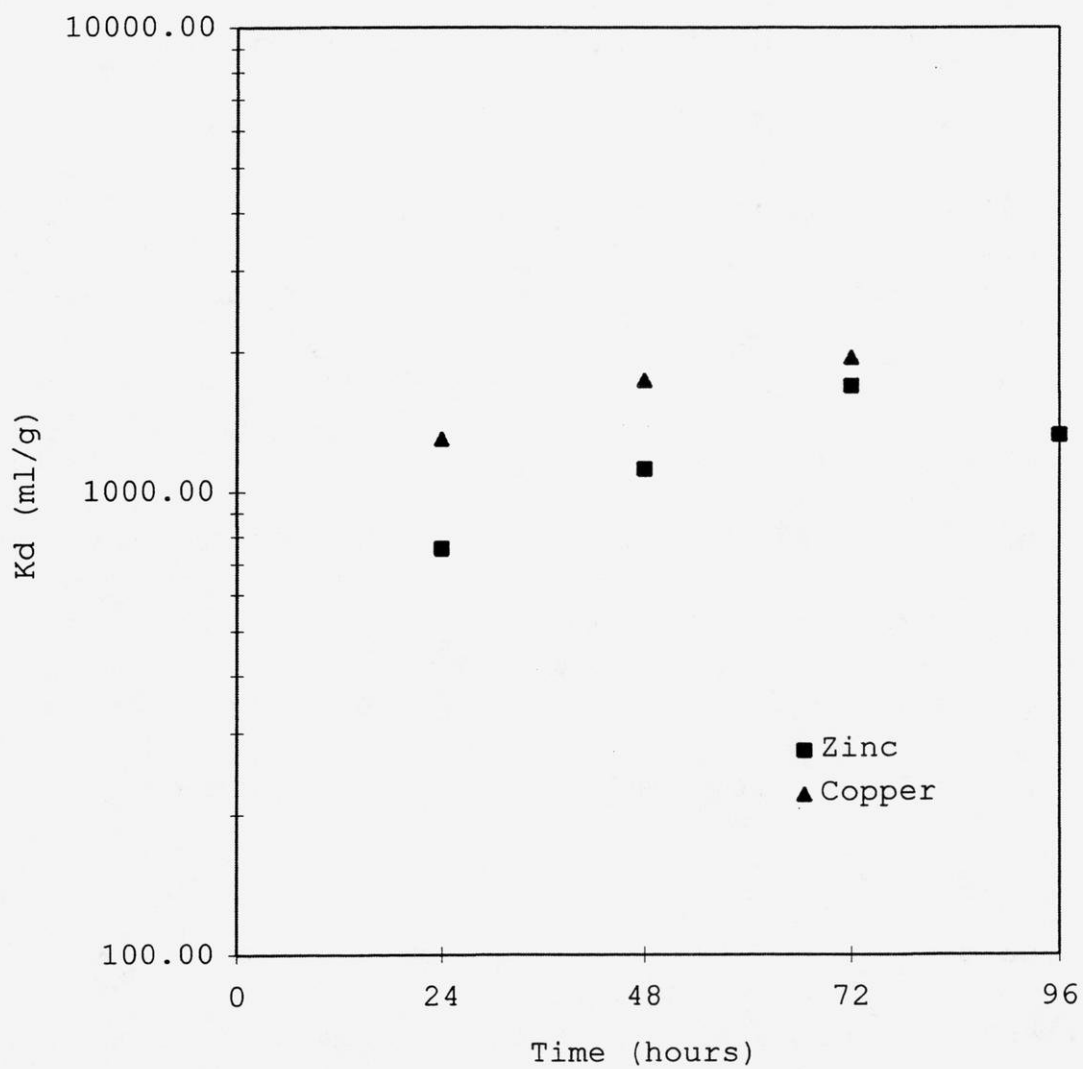
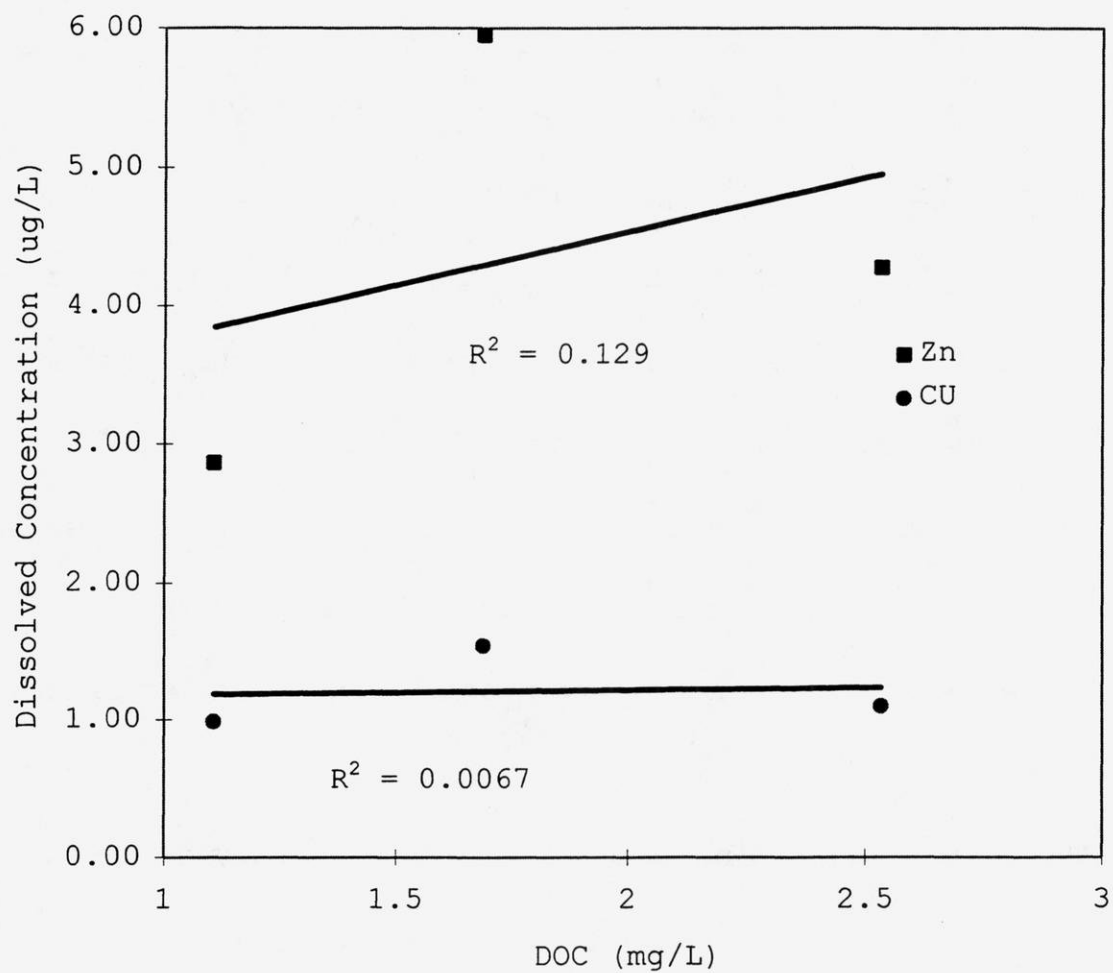


Figure 5-21 Dissolved Zinc and Copper Concentrations Versus DOC

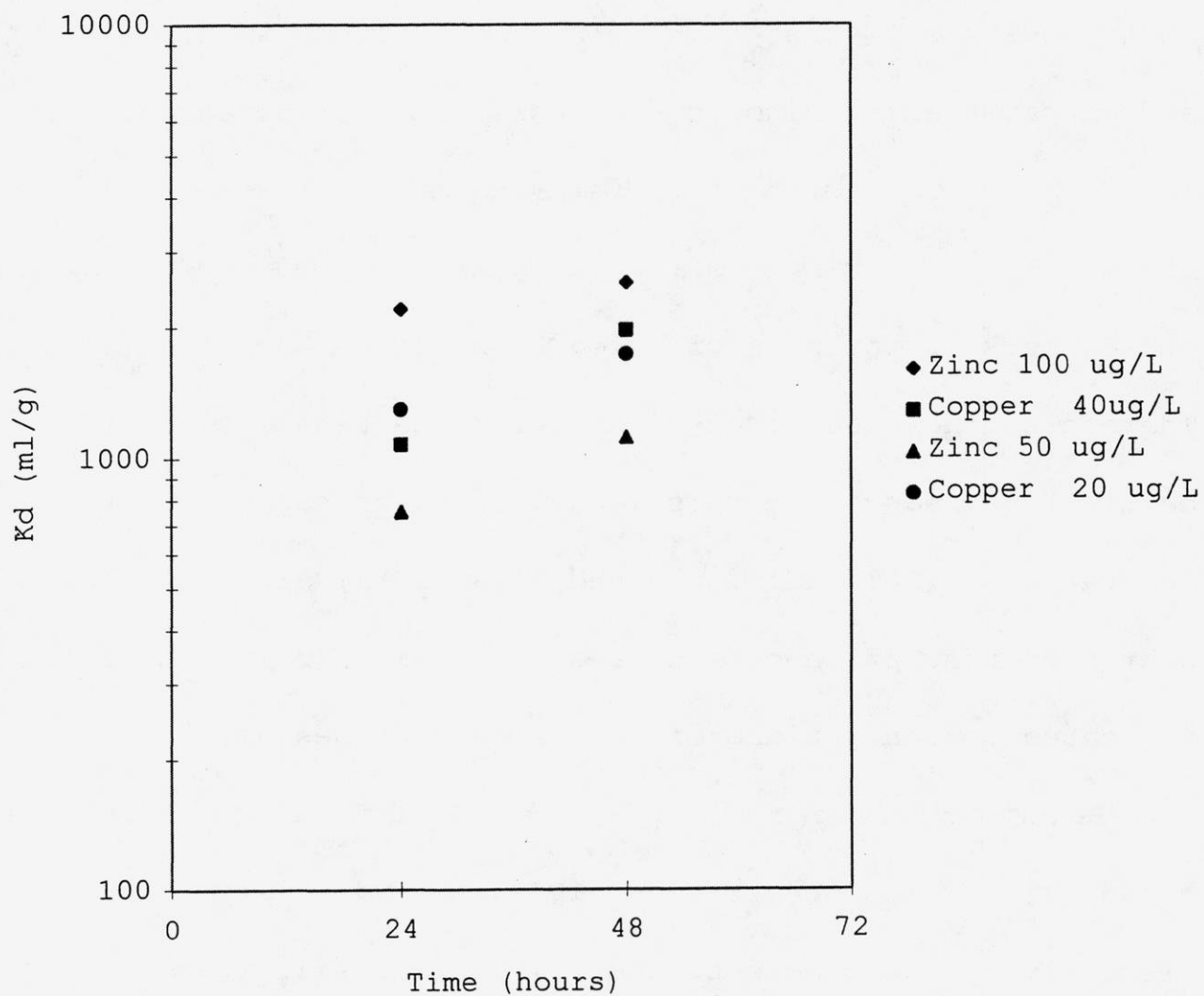


experiments for the Sparta sand soil. A better test of the correlation between dissolved metals concentrations and DOC should be provided by comparisons of the three soils.

Comparisons of the partitioning of high concentrations of zinc and copper (concentrations of 100 $\mu\text{g/L}$ and 40 $\mu\text{g/L}$ respectively) after 24 and 48 hours versus lower concentrations of zinc and copper (50 $\mu\text{g/L}$ and 20 $\mu\text{g/L}$ respectively) show that increased concentrations of both metals led to higher K_d values (Figure 5-22). It was expected that lowered K_d values would be obtained at higher concentrations of metals. Possibly, competition from major cations in the stormwater (calcium, magnesium) for soil sites had a greater influence at lower concentrations of zinc and copper.

To test if zinc and copper sorption was affected by other cations, a 24 hour sorption batch experiment (zinc concentration = 100 $\mu\text{g/L}$ and copper concentration = 40 $\mu\text{g/L}$) was conducted with a stormwater hardness of 60 mg/L .

Figure 5-22 Zinc (100 ug/L) and Copper (40 ug/L) Versus Zinc (50 ug/L) and Copper (20 ug/L) Partitioning



The calcium concentration was increased and the NaCl concentration reduced to maintain an ionic strength of 0.01 M. Results from this experiment compared with the hardness 40 mg/L results show that the K_d values are lower for both zinc and copper when calcium in the stormwater is increased. The log K_d value for zinc was 1.98 ml/g versus 2.97 ml/g, whereas the log K_d for copper value was 2.61 ml/g versus 3.02 ml/g for stormwaters of hardness of 60 mg/L and 40 mg/L, respectively. Therefore, increased concentrations of cations (at least calcium) decreased the sorption of zinc and copper to the Sparta sand. Relatedly, Zhu and Alva (1993) also attributed decreased adsorption of zinc and copper in Florida soils to increased concentrations of calcium and magnesium.

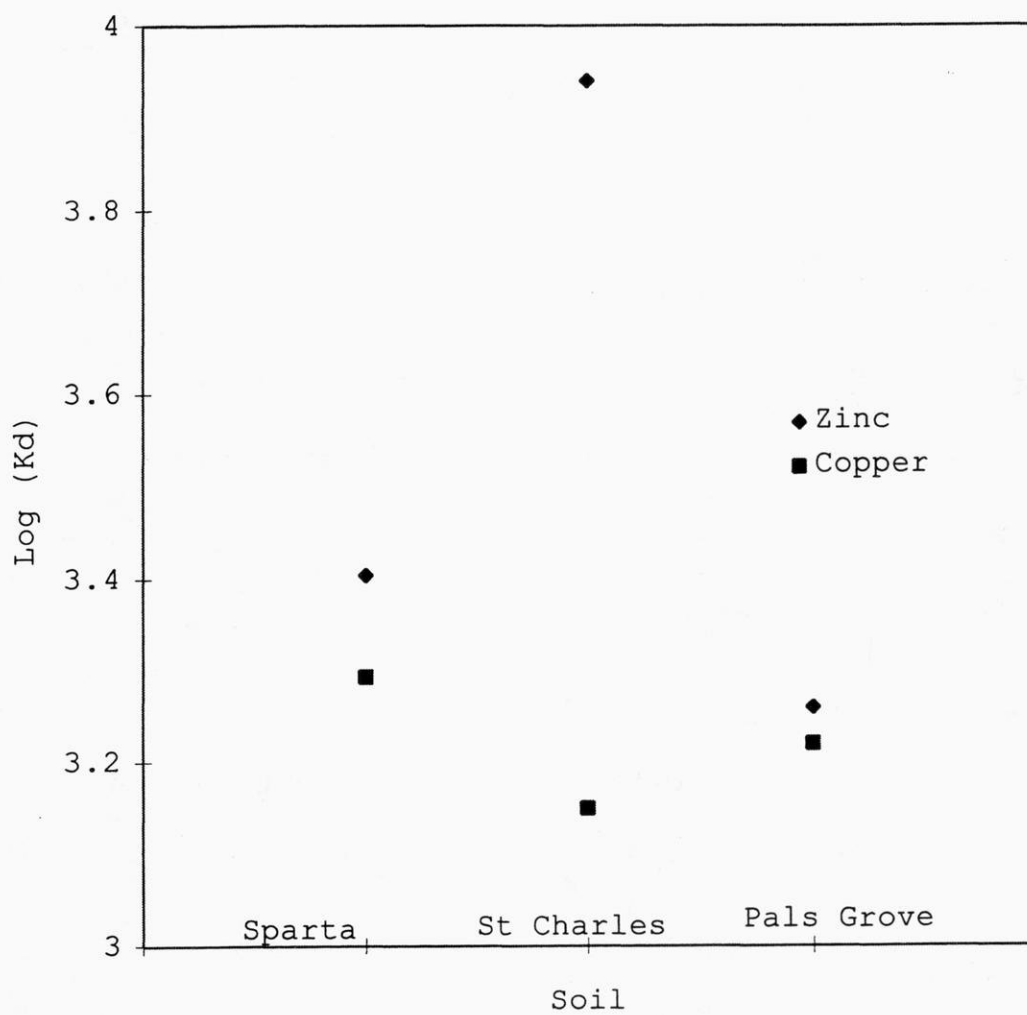
Batch experiments through 48 hours show that both zinc and copper (initial concentrations 100 $\mu\text{g/L}$ and 40 $\mu\text{g/L}$, respectively) sorb more to the St. Charles silt loam than to the Sparta sand with log K_d values 3.94 ml/g for zinc and 3.15 ml/g for copper. This trend was expected because of the St. Charles silt loam's higher CEC (cation exchange capacity) and contents of silt and clay.

Due to their high surface areas, higher amounts of silt and clay could provide a larger number of sorption sites on clay minerals. In addition, the size fraction of soil typically contains nonlayer minerals such as hydrous oxides, amorphous aluminosilicates, (Bohn et al., 1985) and organic matter which can provide sorption sites.

The average 48 hour log K_d values for the Pals Grove silt loam (zinc = 100 $\mu\text{g/L}$; copper = 40 $\mu\text{g/L}$) were 3.26 ml/g for zinc and 3.22 ml/g for copper. These K_d values are within the experimental ranges for the St Charles silt loam, consistent with the similarity between the two soils was expected.

Resulting K_d values from the 48 hour batch equilibration time (zinc = 100 $\mu\text{g/L}$ and copper 40 $\mu\text{g/L}$) are shown (Figure 5-23) for all three soils. While only three soils were studied, the comparisons provide useful information on the relation of K_d values to soil characteristics.

Figure 5-23 Zinc and Copper Kd Values for All Three Soils



Figures 5-24 through 5-28 show correlations between $\log K_d$ values for the metals and various soil parameters.

Zinc sorption (represented by the K_d value) shows the strongest correlation to percent clay content of the soils (Figure 5-24), whereas copper sorption correlates better with the soil's silt content (Figure 5-25). The association of zinc with clay may indicate preference for cation exchange reactions, as supported by lower K_d values with higher concentrations of stormwater matrix cations. Zinc also exhibits specific adsorption to soil iron and aluminum oxides (Zelmanowitz, 1992), present in the clay-size fraction. The correlation of the K_d value for copper with percent silt may be due to the high correlation of silt with soil organic matter (Figure 5-26). Copper forms complexes with dissolved organic matter as well as organic matter on soil surfaces. Copper partitioning also correlates with soil organic matter content (Figure 5-27) as well as the soil's bulk calcium content (Figure 5-28).

Figure 5-24 Zinc Log Kd Value Versus Soil Silt, Clay and Organic Matter

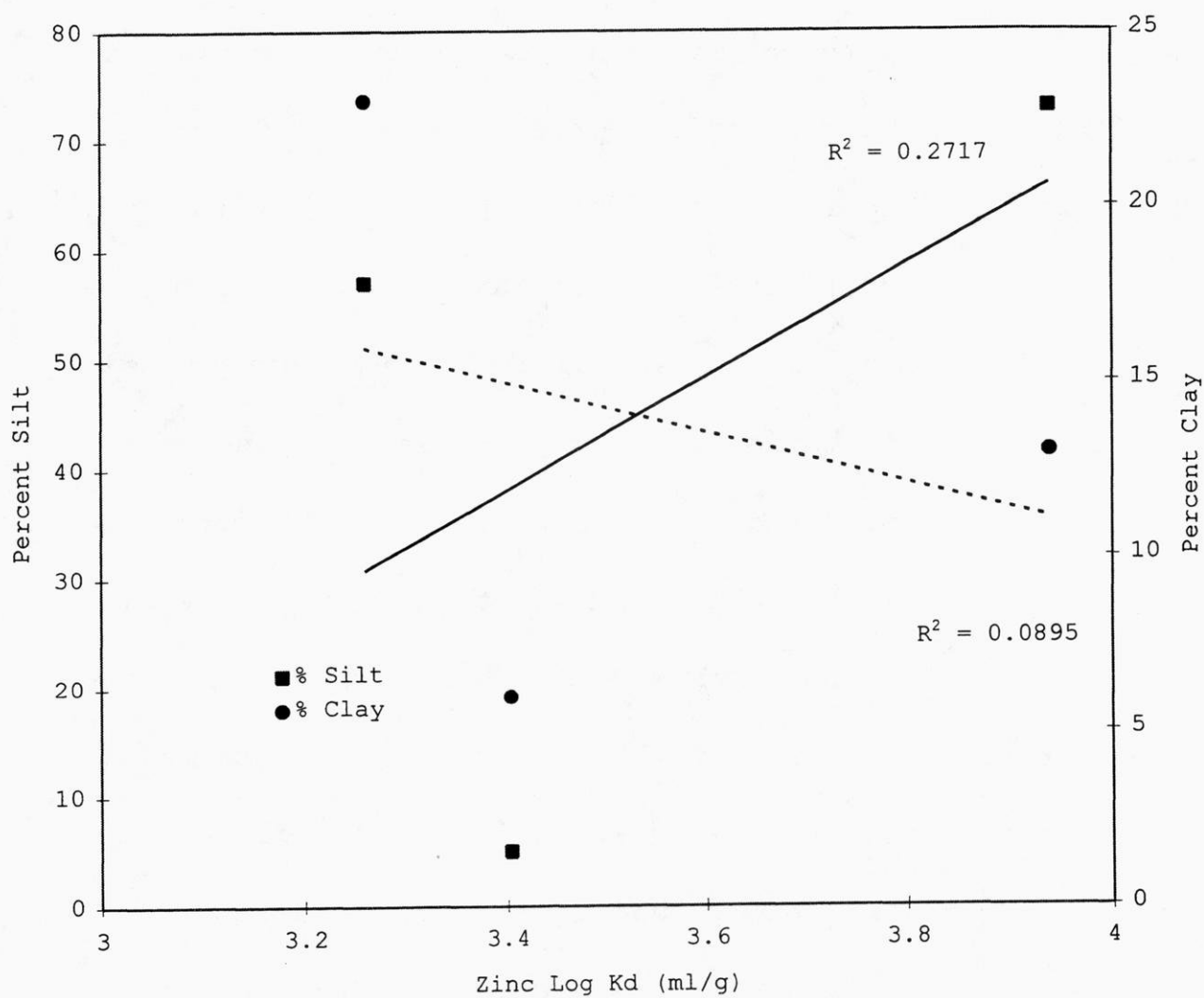


Figure 5-25 Copper Log Kd Value Versus Soil Silt, Clay and Organic Matter

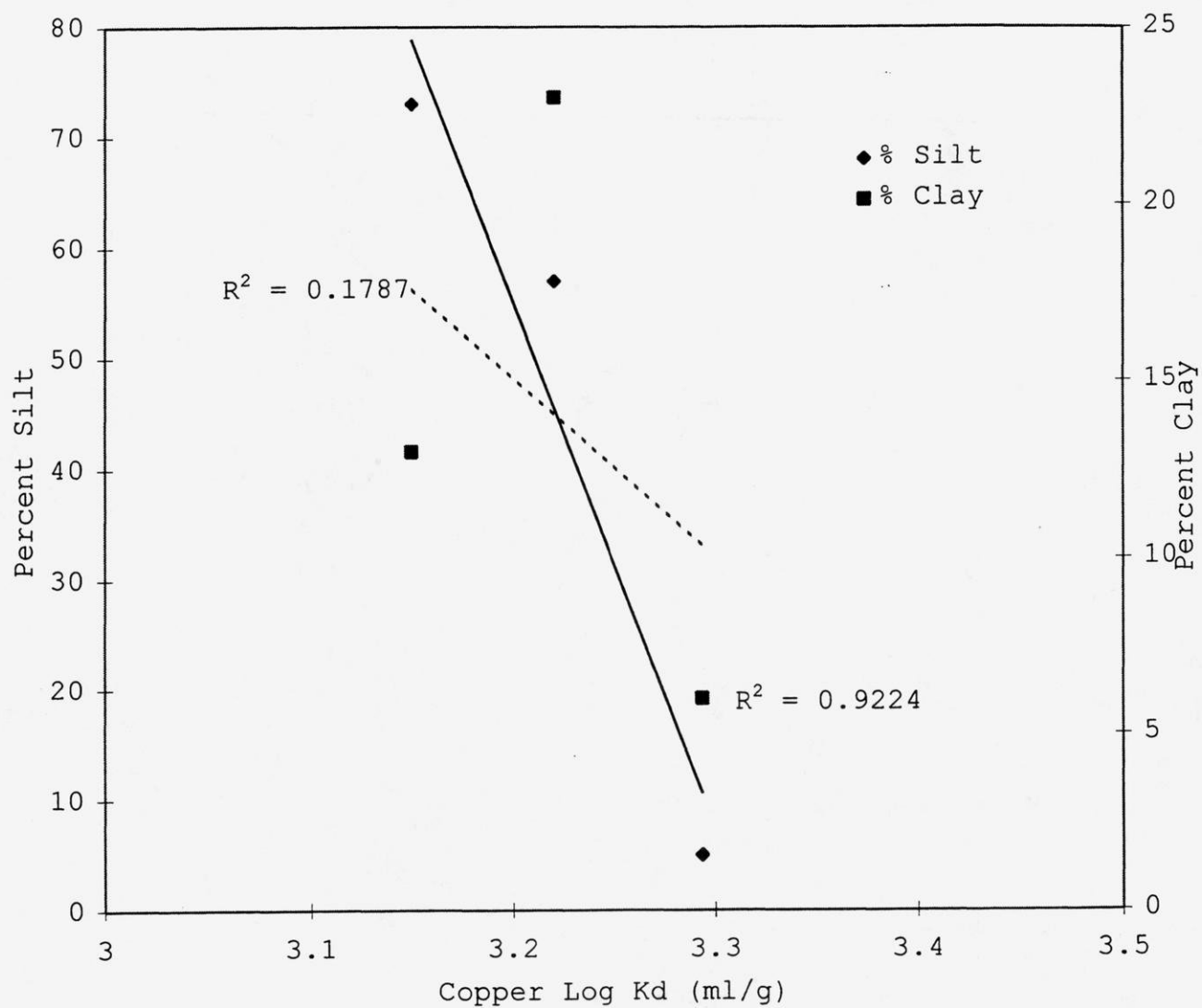


Figure 5-26 Soil Organic Matter and Silt Content

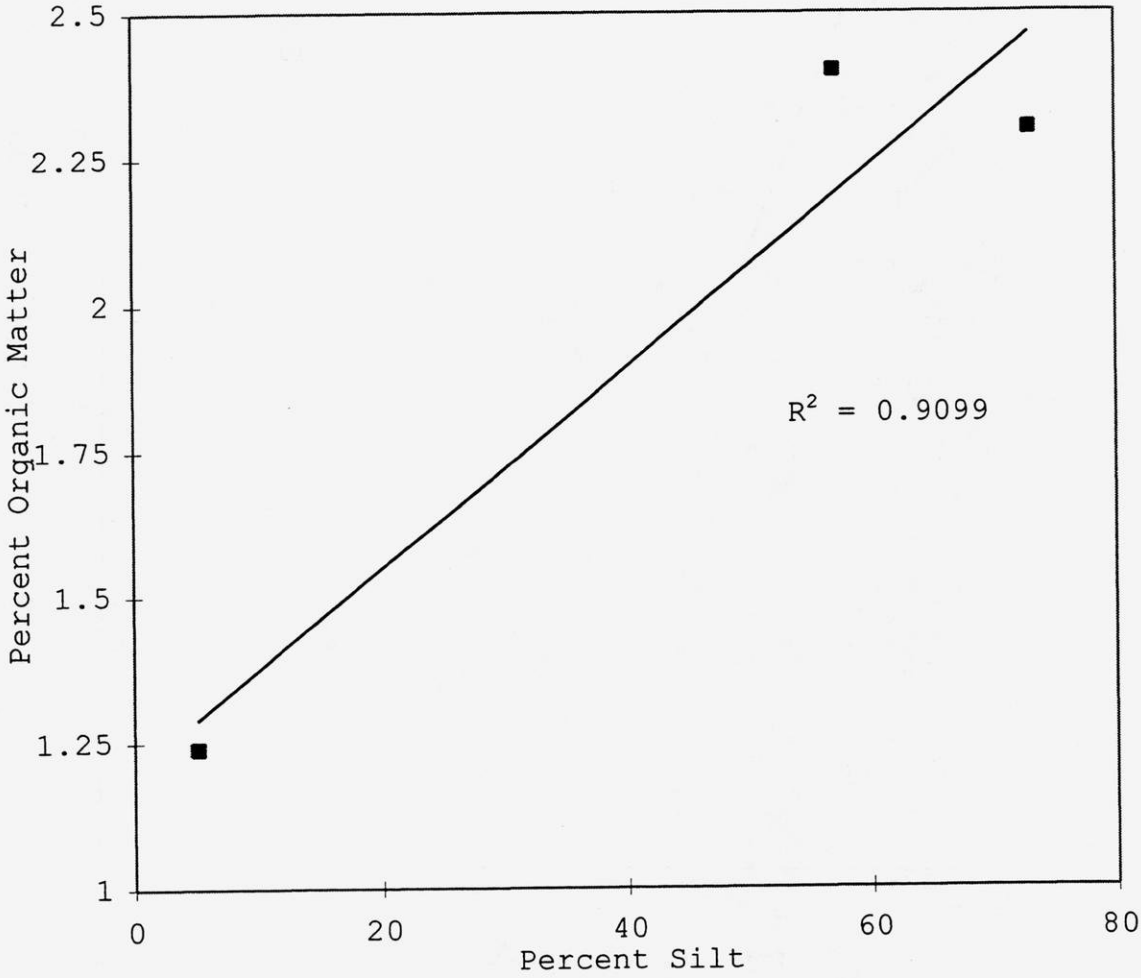


Figure 5-27 Zinc and Copper Log Kd Value Versus Soil Organic Matter

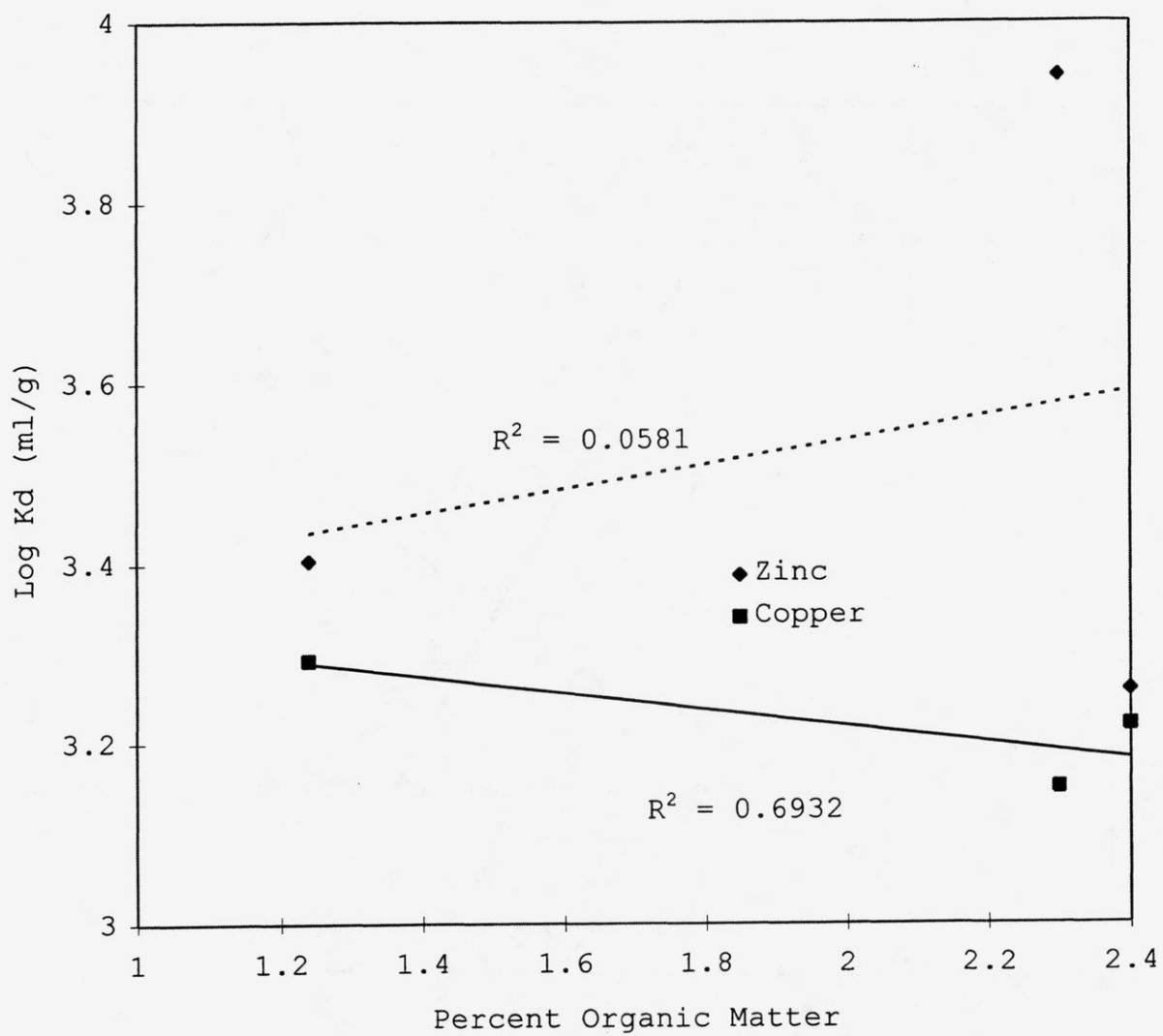
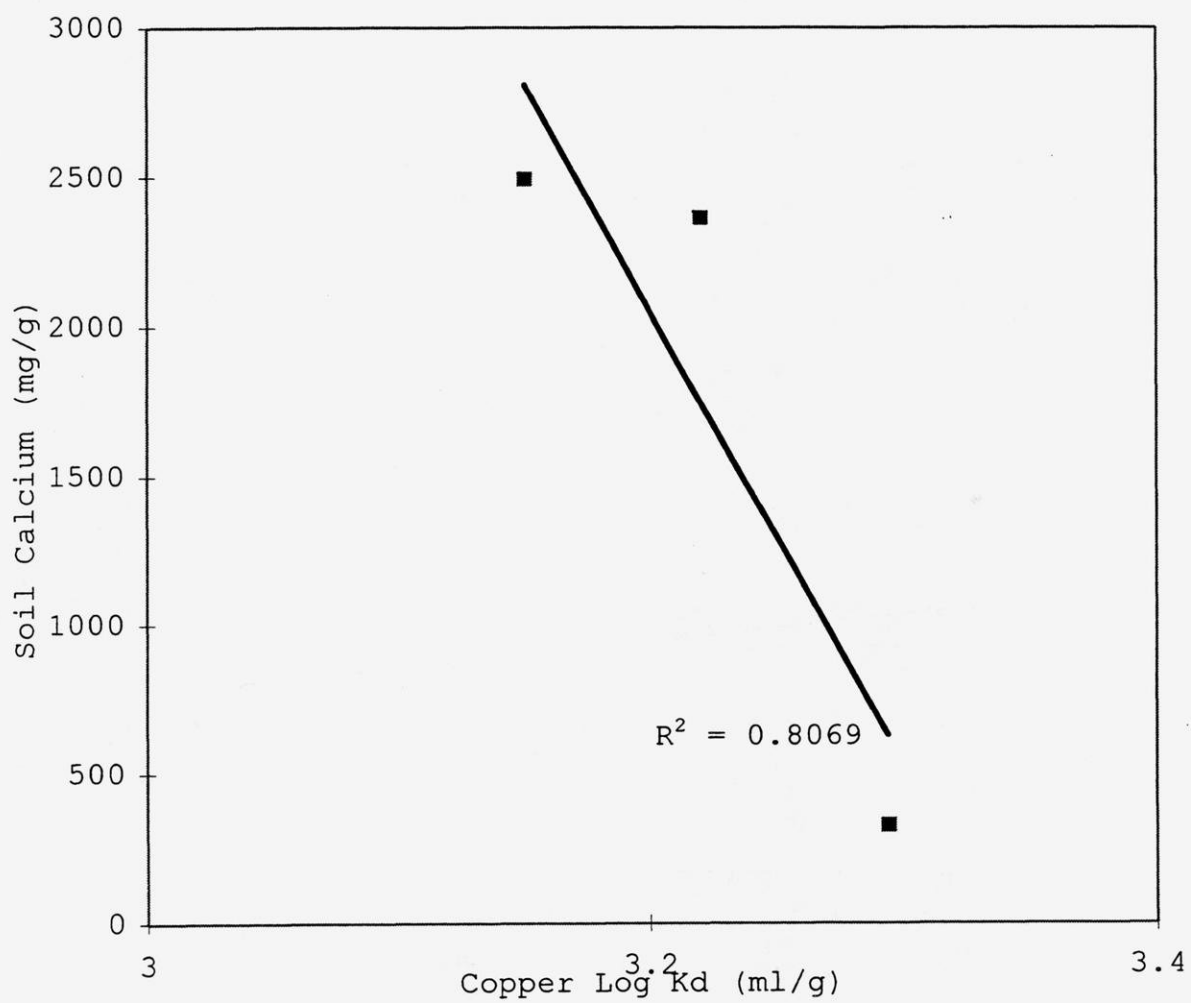


Figure 5-28 Copper Log Kd Value Versus Soil Calcium



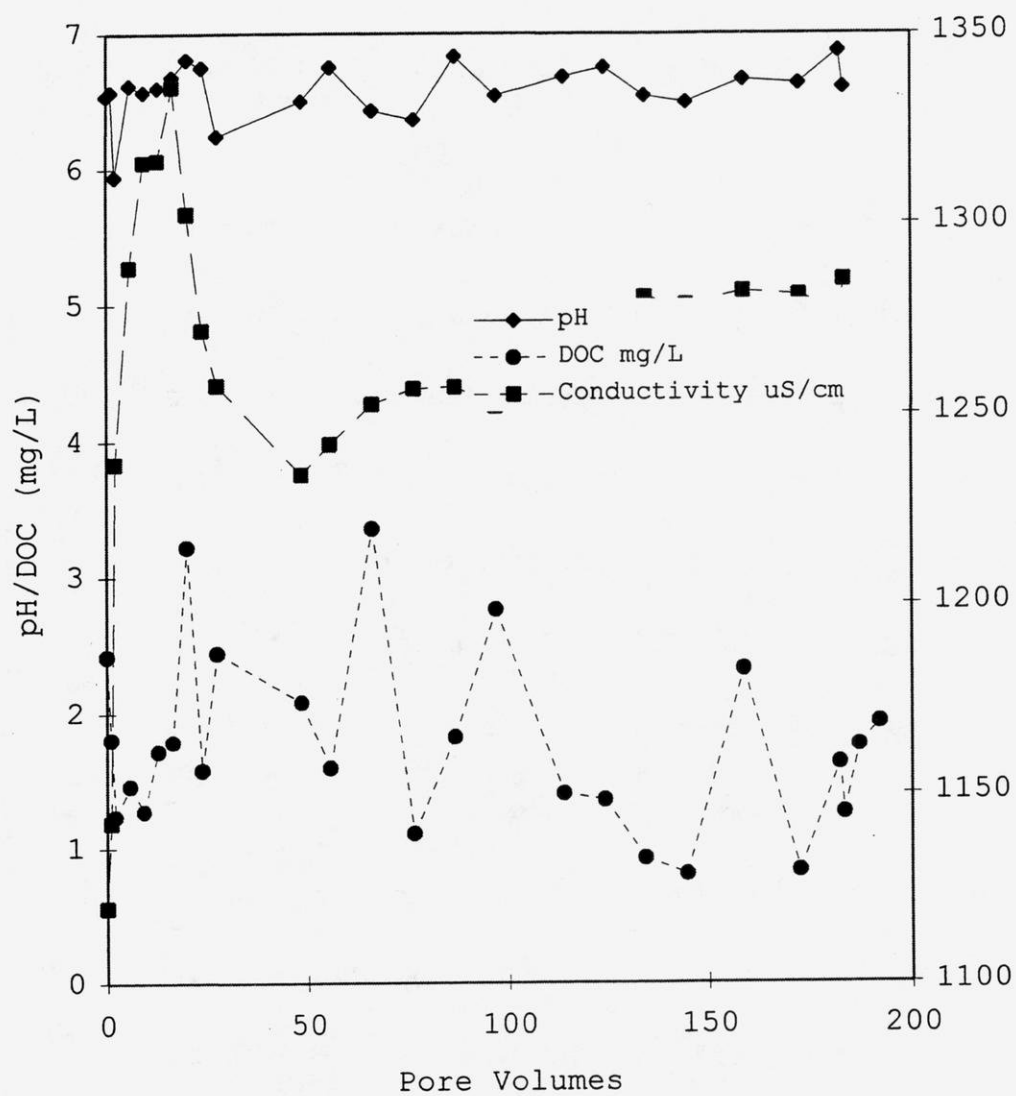
This correlation is thought to represent copper partitioning to calcium carbonate.

2. Partitioning and Transport in Soil Columns

The first soil column was packed with Sparta sand and operated in a continuous input fashion. Unfortunately, copper sorbed over time to the peristaltic pumphead tubing used in the experiment, so no data for copper transport could be obtained. Table 5-4 lists pertinent column details as well as relevant soil parameters. Column parameters such as pH, DOC, conductivity, colloid generation, selected major cations in the column effluent as well as effluent concentrations of zinc and copper were measured during the experiment. At the conclusion of the experiment, the column was sectioned and subjected to a 16 hour extraction with 1.0 N HCl for measurement of zinc and copper sorbed by the soil.

Figure 5-29 shows the variation in pH, DOC and conductivity throughout the experiment.

Figure 5-29 Sparta Sand Continuous Input Column pH, DOC, and Conductivity



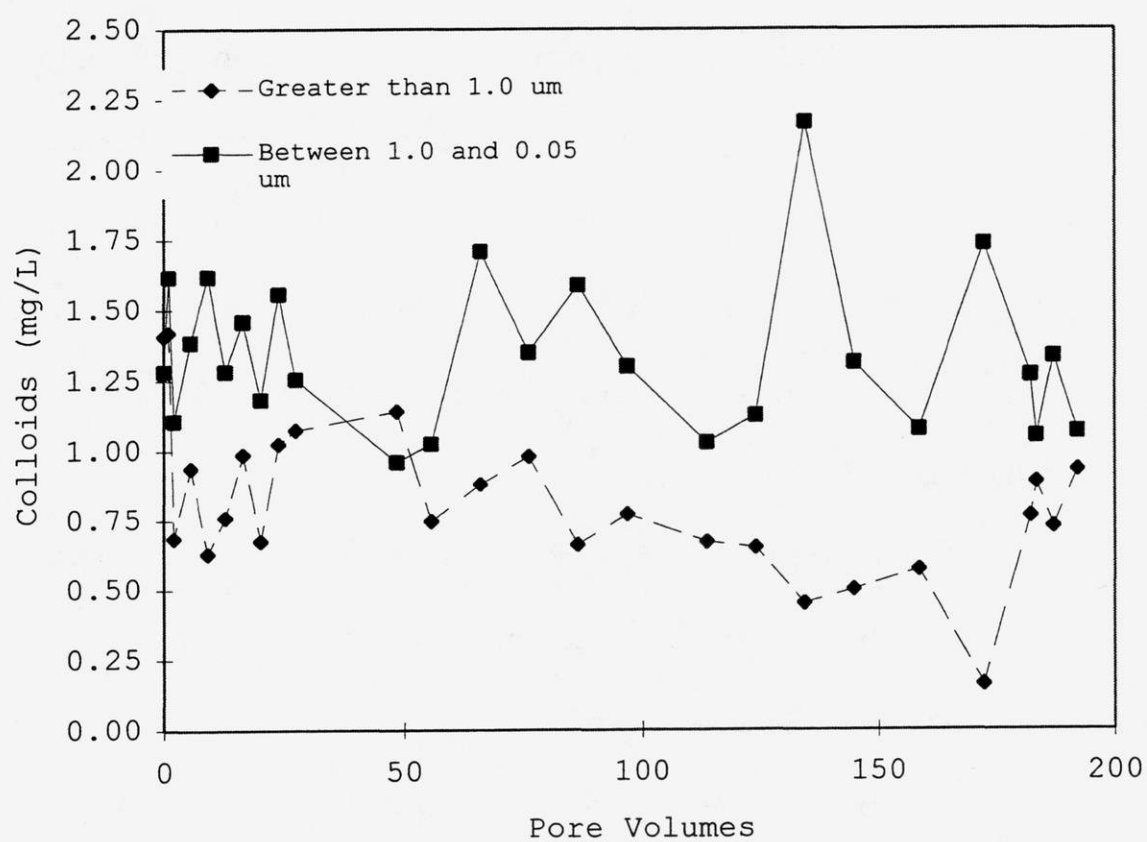
The general trend of increasing pH through time might be attributed to the decreasing buffer capacity of the soil. DOC production appeared variable without any clear trends during the experiment. The noticeable spike in conductivity after approximately 30 pore volumes, is probably due to cation exchange.

Table 5-4 Sparta Sand Continuous Input Column

Characteristic	Value
Length (cm)	24.6
Inner Diameter (cm)	2.05
Packed Dry Bulk Density g/cm ₃	1.4
Estimated Porosity	0.46
Influent Rate cm ³ /min	1.0
Pore Water Velocity cm ³ /min	0.165
Effective Porosity	0.46
Pore Volume cm ³	150

Colloid generation (Figure 5-30) remained variable but higher than measured in groundwater samples from the same aquifer (0.3 ml/L ;measured for a size range of 0.03 μm to 1.0 μm ;Armstrong et al., 1992). In the packed column, the average particle concentration in the size fraction greater than 1.0 μm was 0.79 mg/L with a standard deviation of 0.28 mg/L, whereas the fraction between 0.5 μm and 1.0 μm was 1.27 mg/L with a standard deviation of 0.35 mg/L. Steady increases in column backpressure during the experiment were indicative of effluent filter (5 μm pore size opening) clogging. Soil structure disturbances during the packing process probably caused the high colloid concentrations. Effluent concentrations of iron, manganese, magnesium, calcium, sodium (analyzed with the ICP) and zinc and copper (analyzed by the GFAA) were also measured during the experiment. Iron and manganese (measured to signal reducing conditions) were at or below instrument detection levels.

Figure 5-30 Sparta Sand Continuous Input Column colloid Production



Calcium, magnesium, and sodium (all present in the stormwater) were measured to assess cation exchange and whether if an equilibrium between influent and effluent concentrations could be reached. Figure 5-31 shows the concentrations of calcium, magnesium and sodium during the experiment. The massive release of all three cations at and before pore volume 5.5 is likely a result of cation exchange reactions. Calcium and magnesium approximate their influent concentrations for most of the experiment ($\text{Ca} = 10000 \mu\text{g}$, $\text{Mg} = 3800 \mu\text{g}$). Sodium effluent concentrations were about 6 times higher than influent concentration (approximately $10000 \mu\text{g}$) throughout the experiment.

Figure 5-32 illustrates effluent concentrations of zinc and copper. With the exception of the peak in copper concentrations at pore volume 104 (possibly due to sample contamination), both zinc and copper concentrations dropped dramatically during the early stages of the experiment and continued to slowly decline. The initial high concentrations of both metals released was from release from the soil due to cation exchange.

Figure 5-31 Sparta Sand Continuous Input Column Effluent Calcium, Magnesium and Sodium

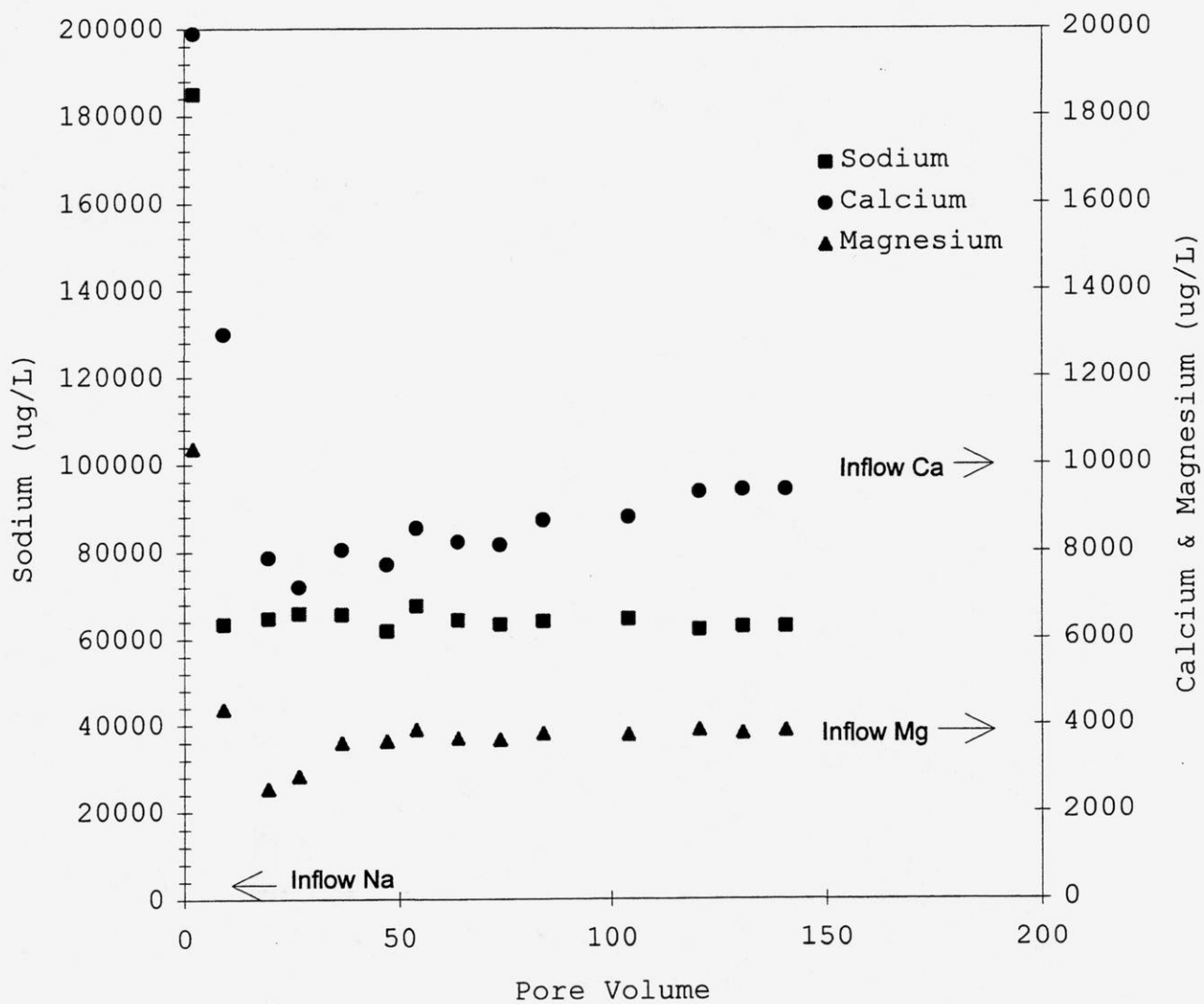
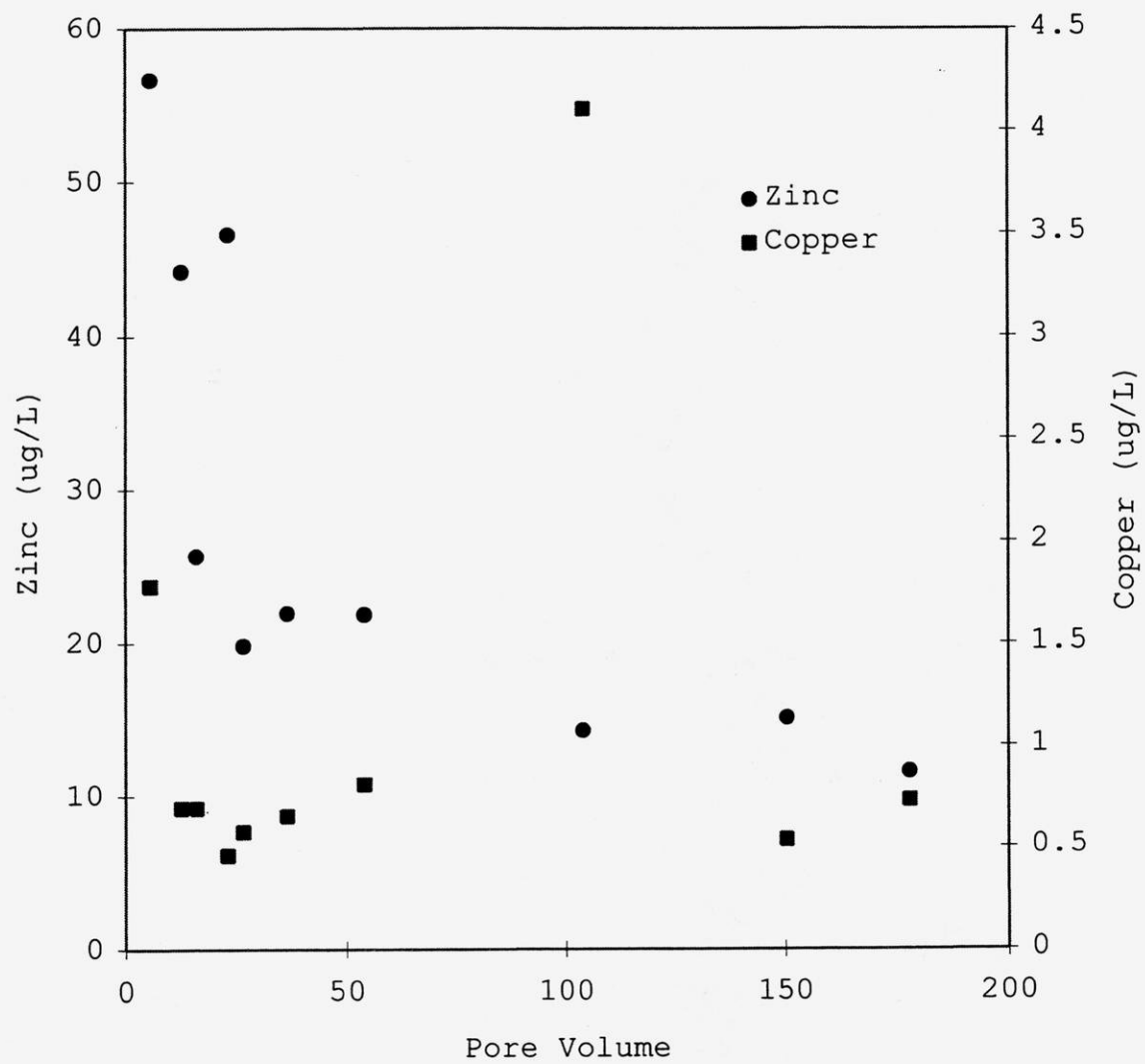


Figure 5-32 Sparta Sand Continuous Input Column Effluent Zinc and Copper



All soils have a natural exchangeable fraction of ions which should be considered in the context of stormwater infiltration. If stormwater matrix cations, or complexing ligands, move through the soil a fraction of "natural" soil trace metals can be released through ion exchange reactions or desorption into soluble complexes.

As previously discussed, the average pore water velocity is determined graphically from conservative tracer data. In this case, the average pore water velocity was determined to be 0.165 cm/min (Figure 5-33). Using this velocity, measured K_d value range, and the retardation equation, zinc is predicted to move 0.7 to 1.23 cm in 20.4 days under the flow rate of 1.0 cm³/min. Figure 5-34 of the cumulative mass of zinc recovered illustrate that the zinc advective front traveled 0.16 cm through the column. This transport would correspond to a K_d value of 4.00 ml/g (back calculated using the retardation equation). The discrepancy in transport predictions could be attributed to differences in sorption conditions in batch experiments versus soil columns.

Figure 5-33 Sparta Sand Continuous Input Column Conservative Tracer

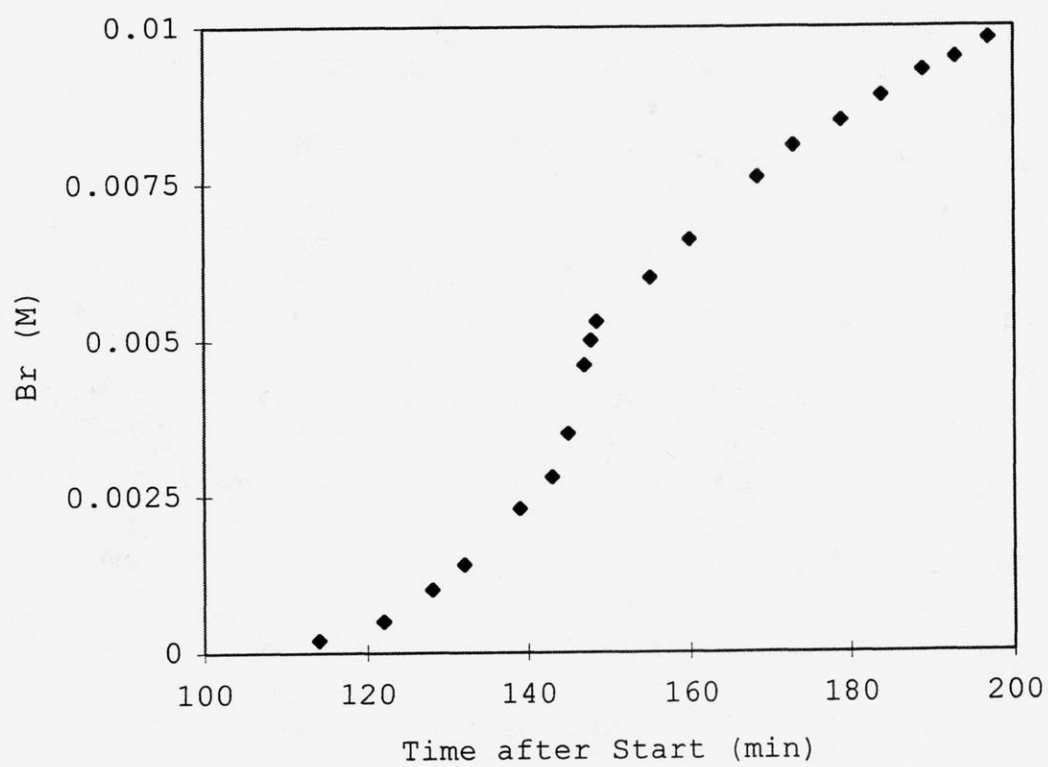
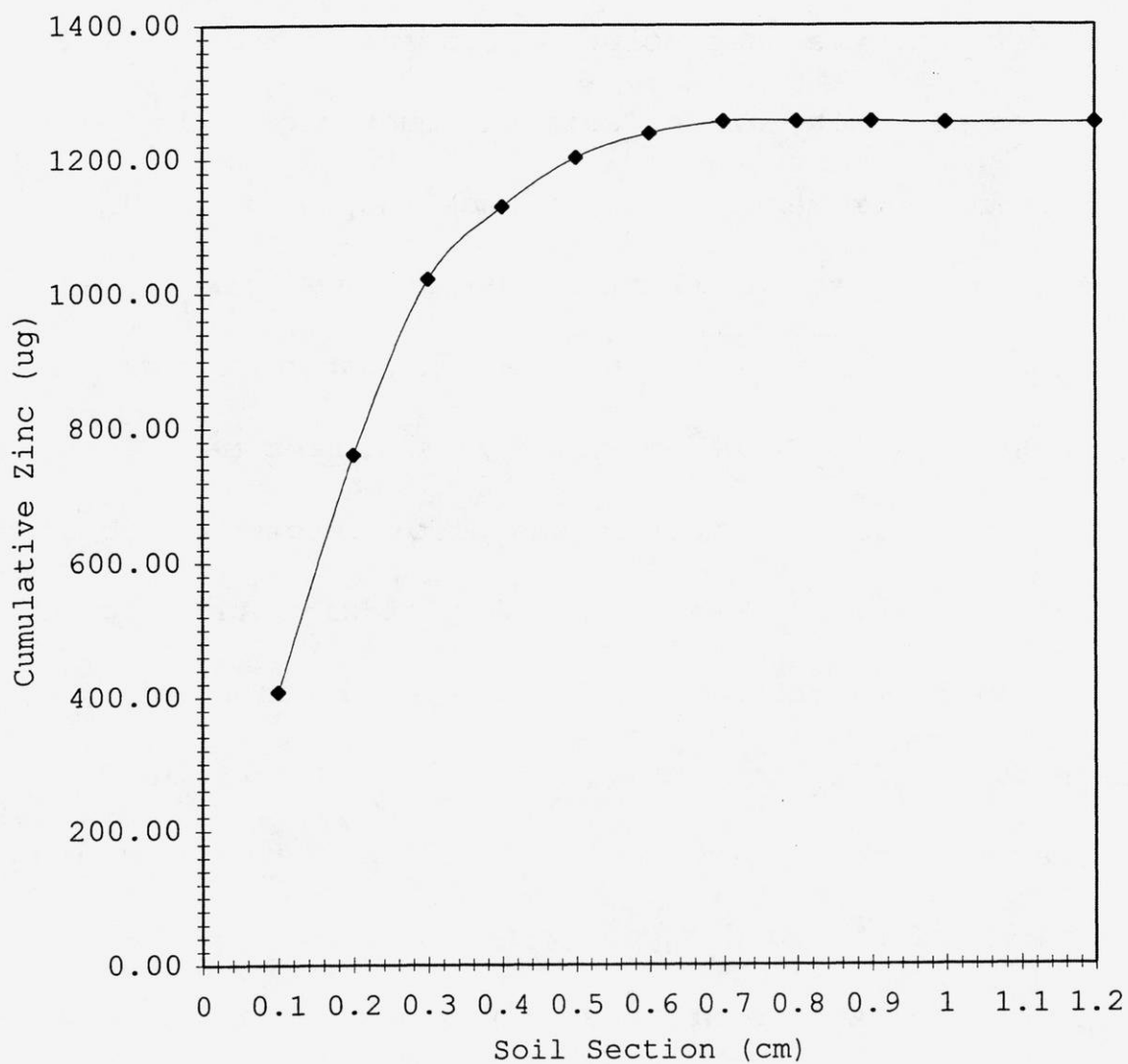


Figure 5-34 Sparta Sand Continuous Input Zinc Transport



The soil:solution ratio in batch experiments was 0.5 g:50 ml whereas, using 0.46 as the effective porosity, in the soil column the soil:solution ratio was approximately 1.85 g:0.61 ml. Therefore, at the same solution concentration, the amount of zinc added per unit mass of soil was much higher in batch than in column experiments. With increasing sorption, K_d tends to decrease. Thus, actual K_d values would tend to be lower in batch than column experiments, and column transport rates based on batch system K_d values would be underestimated.

A slug input of contaminants was also performed with the Sparta sand. The slug input about 10 μg of zinc and 4 μg of copper. As with the column using a continuous input of contaminants, pH, DOC, conductivity, colloid generation, selected major cations in the column effluent as well effluent concentrations of zinc and copper were measured. At the conclusion of the experiment, the column was sectioned and subjected to a 16 hour extraction with 1.0 N HCl.

Table 5-2 Sparta Soil Column Specifications

Length (cm)	11
Inner Diameter (cm)	2.05
Packed Dry Bulk Density (g/cm ₃)	1.4
Estimated Porosity	0.46
Influent Rate (ml/min)	1.0
Pore Water Velocity (cm/min)	0.182
Effective Porosity	0.42
Pore Volume (cm ³)	60.6

Figure 5-35 shows the changes in pH, DOC and conductivity during the experiment. As observed in the first Sparta sand column, pH slowly rose during the experiment. Again, this could signify a decrease in soil buffering capability. An initial spike in conductivity was observed which may be attributed to ion exchange reactions. DOC varied during the experiment without a clear pattern. Colloid generation was higher than in the first column (Figure 5-36), perhaps due to the nonreproducibility of the packing technique and/or soil heterogeneity.

Figure 5-35 Sparta Sand Slug Input Column Effluent pH, DOC, and Conductivity

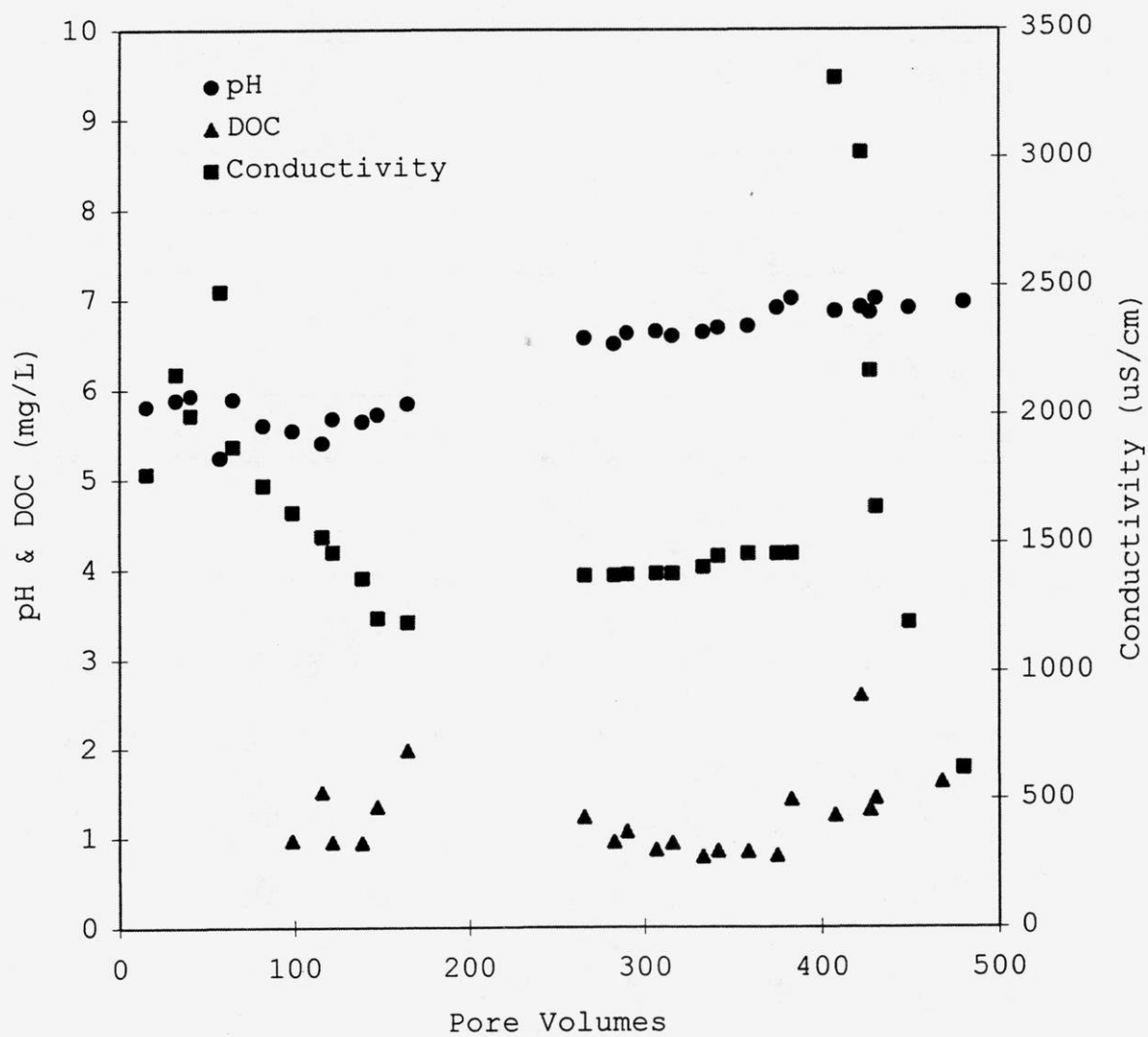
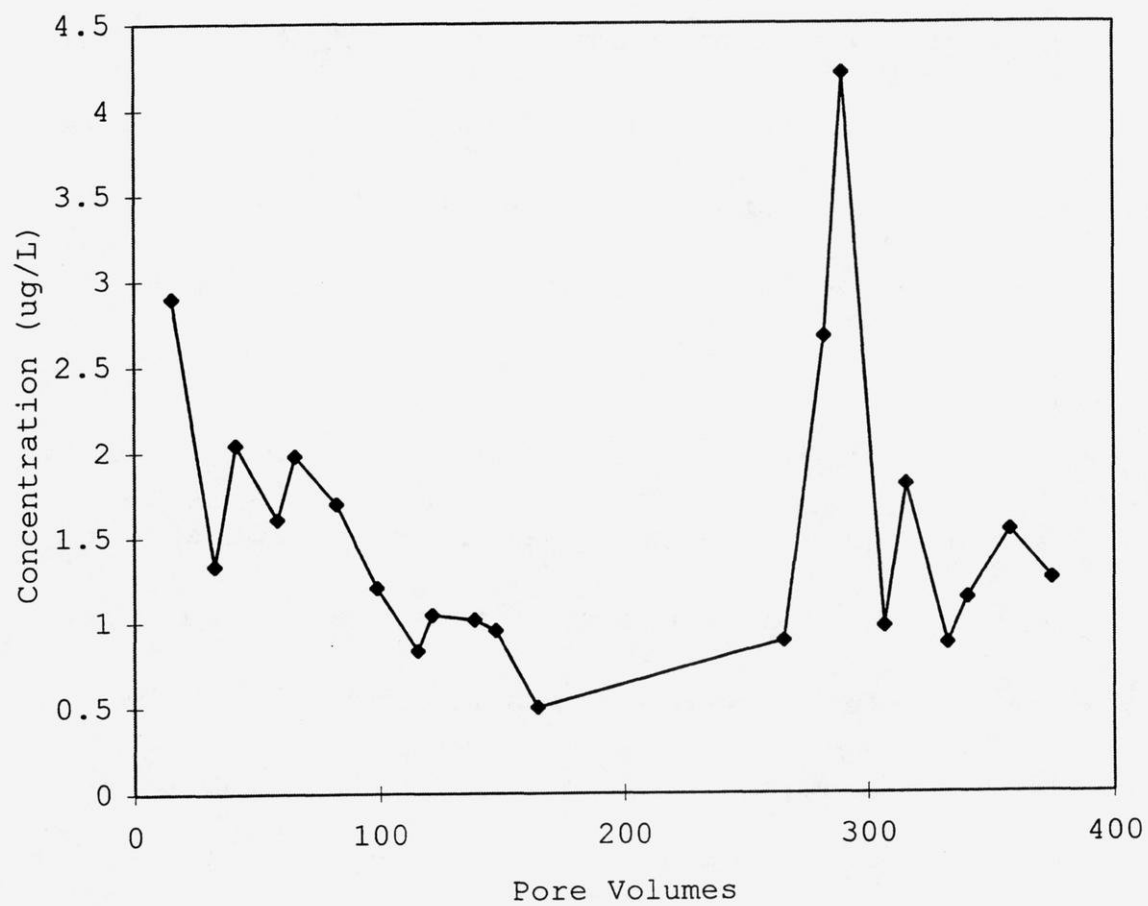


Figure 5-36 Sparta Sand Slug Input Column Colloid Concentration
(Between 1.0 μm and 0.05 μm)



Effluent concentrations of the calcium, magnesium and sodium (Figure 5-37) show the same general trend as the first column. Initial high concentrations were followed by lower concentrations, eventually approximated influent stormwater matrix concentrations over time.

Zinc and copper effluent concentrations showed the same trend as the first column of initially high effluent concentrations, decreasing through time (Figure 5-38). The peak after 200 pore volumes may have been due to sample contamination.

Figure 5-39 shows the distribution of zinc and copper in the column at the end of the experiment. High zinc and copper concentrations at the top of the column may have been a result of the stormwater slug pH which might have been less than 7.5. The pH of the remaining slug volume after column input was measured with pH paper to be approximately 7.0 or higher. The possibility of a lower pH would explain an initial release of "native" zinc and copper which only traveled a short distance before the pH was buffered. The lowered pH theory is also supported by comparison of Figure 5-29 to Figure 5-35.

Figure 5-37 Sparta Sand Slug Input Column Effluent Calcium, Magnesium and Sodium

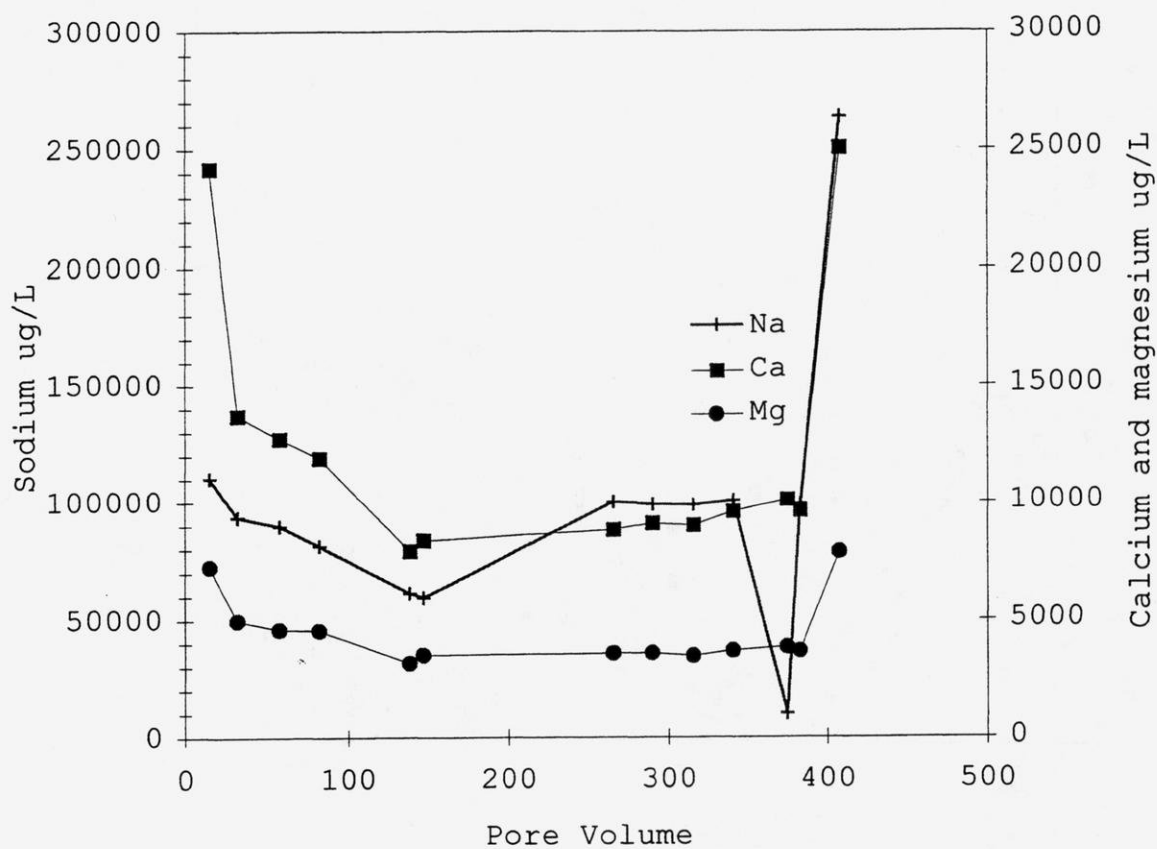


Figure 5-38 Sparta Sand Slug Input Column Effluent Zinc and Copper

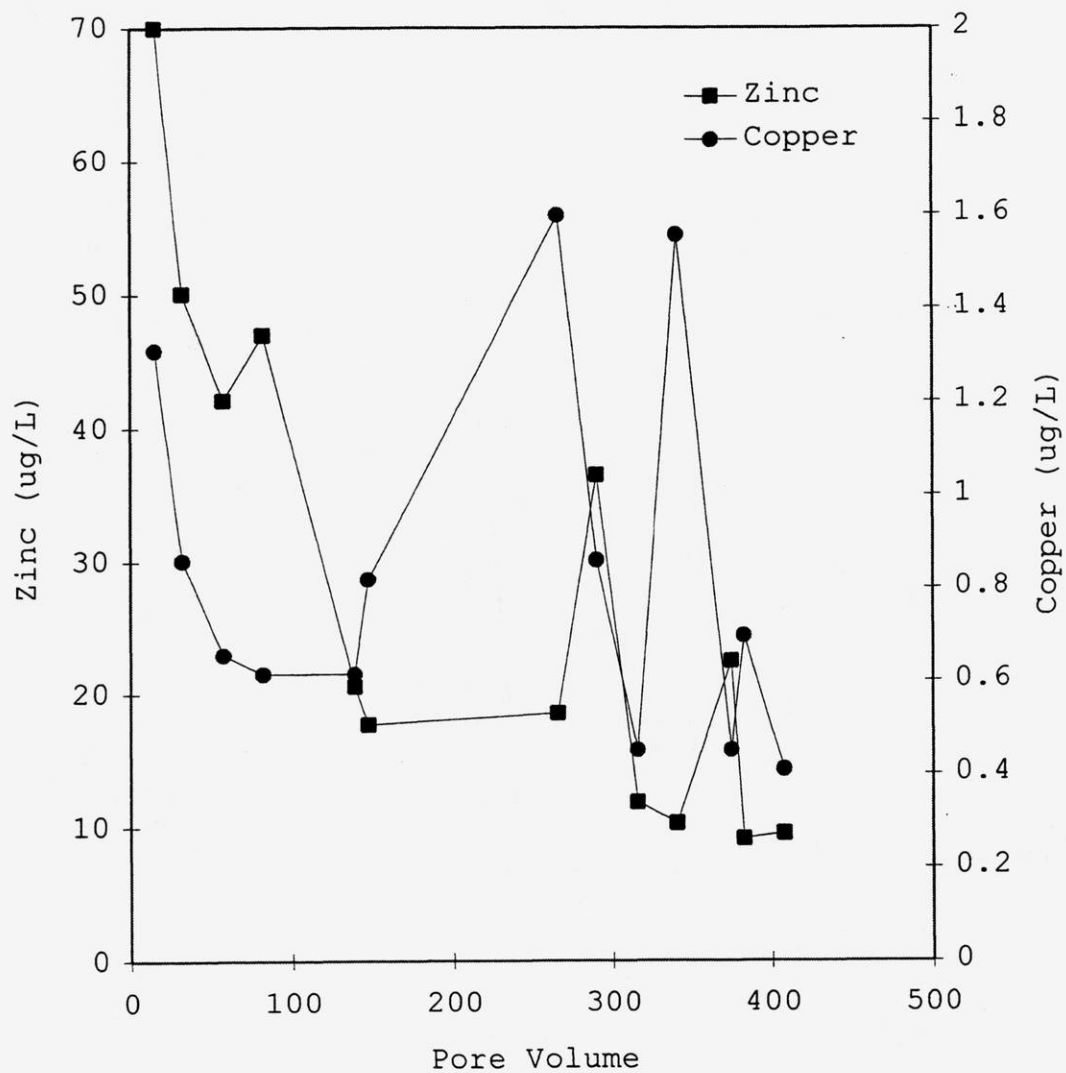
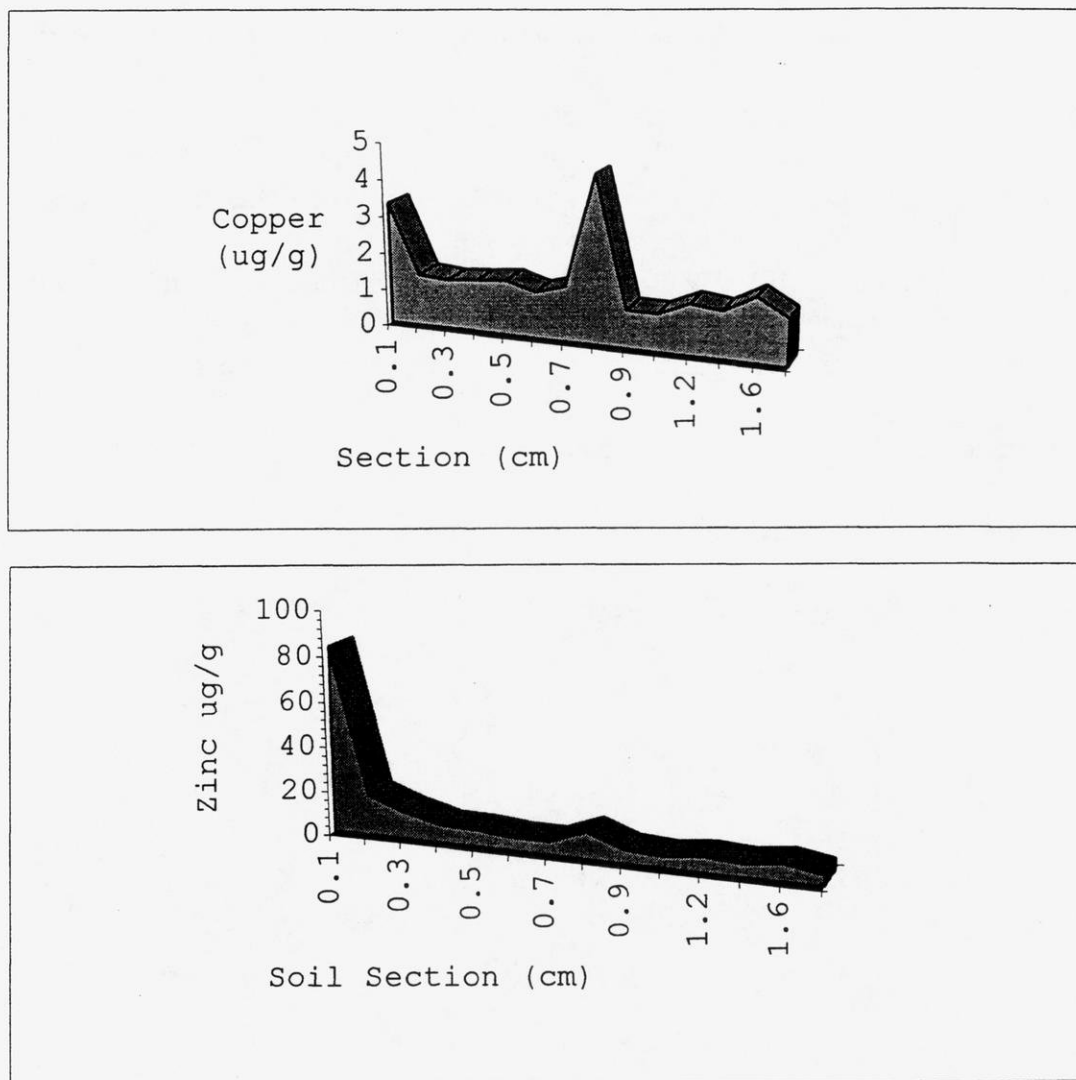


Figure 5-39 Sparta Sand Slug Input Column Zinc and Copper Transport



The initial effluent pH of column 1 was essentially above 6.0, whereas initial pH for column 2 was below 6.0.

Using the batch-measured 48 hour K_d values for zinc and copper and the retardation equation, zinc is predicted to travel 0.5 to 0.6 cm and copper 1.0 to 0.6 cm through the column. Copper transport, probably due to the larger standard deviation of the K_d value, is predicted by the retardation equation. Conversely, zinc transport is underestimated by the retardation equation. However, until a firm explanation for the high zinc and copper concentrations in the first soil section is found, any use of the retardation equation would be suspect.

VII. Conclusions

1. An ideal infiltration basin (i.e., no preferential transport, adequate depth to groundwater) could substantially attenuate contaminants. However, unless removed by a reaction such as precipitation or biodegradation reduces contaminant mass, the contaminant will eventually reach the groundwater table.
2. The retardation equation provides a useful framework for comparative assessments of mobility during infiltration as related to soil and contaminant chemical properties (K_d) and soil physical characteristics (bulk density, porosity). However, the retardation model should not be used for simulation of actual transport at a field site because the model does not account for several important factors and processes important in contaminant transport. The model does not account for some important removal and/or retention (degradation, irreversible sorption or precipitation) and may greatly overestimate contaminant transport. Also, the model is applicable only to systems where contaminant retention is controlled by reversible sorption reactions, i.e., local equilibrium.

3. Contaminant retardation may be substantially greater than predicted by the retardation equation. While agreement between observed and predicted mobility was fair for a moderately sorbed organic compound (atrazine), no mobility assessment could be made for more highly sorbed chemicals (phenanthrene and fluoranthene) since they were undetectable in our soil columns.
4. The K_d value for the specific soil contaminant system is the largest source of error in the retardation model. Several interrelated factors contribute to uncertainty in the K_d : 1) the assumption of equilibrium for the contaminant-soil adsorption-desorption reaction as the contaminant migrates through the soil may be invalid; 2) slow desorption rates may cause the contaminant to migrate more slowly than expected; 3) K_d values measured in batch equilibration systems may differ from actual K_d values in soil columns due to differences in soil dispersion, particle size distribution, surface area, and available sorption site density.
5. Stormwater matrix compositions (major anions and cations; DOC) is highly variable and can have an important influence on contaminant mobility. The simulated stormwater used in this study does not reflect variability in composition and associated contaminant behavior encountered at field sites.

6. When used to assess potential mobility, the retardation equation should be modified to account for decreasing organic carbon fractions with depth found in natural soil profiles and other changes in soil properties.
7. Organic contaminant predictive equations suggested by Armstrong and Llena (1992) did not adequately predict K_d values for PAHs in soils with low fractions of organic carbon. This is an important limitation of these equations.
8. All assumptions of the retardation equation must be met before using the equation as a predictive tool. It is unlikely that all the assumptions will be at an actual field setting.

VIII. Recommendations for Future Research

1. Appropriate field studies should be conducted to fully characterize stormwater matrix constituents, especially DOC and colloidal concentrations.
2. Field studies should also include bacteria and virus concentrations, viable lifespan and potential to transport contaminants.
3. Laboratory methods other than the standard batch technique should be developed to measure more realistic K_d values.

4. The retardation equation may be more useful (qualitatively) if expanded to account for partitioning in soils with low organic carbon or decreasing organic carbon with depth. Equation expansion could also include the effects of DOC and colloids on transport.
5. At minimum an equation which includes the effects of dispersion should be used for predictive modeling.

References

- Armstrong, David E. 1991. Urban Stormwater Infiltration: Assessment and Enhancement of Pollutant Removal. Proposal to the Wisconsin Department of Natural Resources.
- Armstrong, David E., Shafer, Martin M., Dean, Kirk E., 1991. Role of Mobile Colloids in the Transport of Chemical Pollutants in Groundwaters. Technical Completion Report
- Armstrong, David E., and Reynaldo Llena. 1992. Stormwater Infiltration: Potential for Pollutant Removal. Project Report to the United States Environmental Protection Agency, Region V. Chicago Illinois.
- Bannerman, Roger T., Rick Dodds, David Owens and Peter Hughs. 1992. Sources of Pollutants in Wisconsin Stormwater. Report to the United States Environmental Protection Agency. Region V Chicago Illinois.
- Barkdoll, Michael P., Donald E. Overton and Roger Betson. 1977. Some Effects of Dustfall on Urban Water Quality. Journal of the Water Pollution Control Federation.
- Brusseau, Mark L. and P. Suresh C. Rao. 1991. Influence of Sorbate Structure on Nonequilibrium Sorption of Organic Compounds. Environmental Science and Technology. Vol 25 No 8.
- Boyd, Stephen A., Sun, Shaobai. 1990. Residual Petroleum and Polychlorobiphenyl Oils as Sorptive Phases for Organic

Burglsser, Christa S., Miroslav Cernik, Michal Borkovec and Hans Sticher. 1993. Determination of Nonlinear Adsorption Isotherms from Column Experiments: An Alternative to Batch Studies. Environmental Science and Technology. Vol 27 No 5

Chiou, C.T., Peters, L.J. and Freed, V.H., 1979. A Physical Concept of Soil-Water Equilibria for Nonionic Organic Compounds. Science, 206:831-832.

Dao, T.H. and T.L. Lavy. 1978. Atrazine Adsorption on Soil as Influenced by Temperature, Moisture Content and Electrolyte Concentration. Weed Science Vol 26 Issue 3.

Dean, Lyn E. 1993. Colloids From Intact Soil Columns: Production and Organic Chemical Sorption. Masters Thesis. Water Chemistry Program. University of Wisconsin Madison.

Domenico, Patrick A. and Franklin W. Schwartz. 1990. Physical and Chemical Hydrogeology. John Wiley and Sons Publ. New York, New York.

Doner, H.E. 1978. Chloride as a Factor in Mobilities of Ni(II), Cu(II), and Cd(II) in Soil. Soil Sci. Soc. Am. J. Vol 42.

Dragun, James. 1988. The Soil Chemistry of Hazardous Materials. Hazardous Materials Control research Institute. Silver Spring, Maryland.

Drever, James I. 1988. The Geochemistry of Natural Waters. Prentice Hall Inc. New Jersey

Dunnivant, Frank M., Phillip M. Jardine, David L. Taylor and John F. McCarthy. 1992. Cotransport of Cadmium and Hexachlorophenol by Dissolved Organic Carbon through Columns Containing Aquifer Material. Environmental Science and Technology Vol 26.

Eaganhouse, Robert P., Berndt R.T. Simoneit and Isaac R. Kaplan. 1981. Extractable Organic Matter in Urban Stormwater Runoff. 2. Molecular Characterization. Environmental Science and Technology Vol 15 No 3.

Eaganhouse, Robert P. and Isaac R. Kaplan. 1981. Extractable Organic Matter in Urban Stormwater Runoff. 1. Transport Dynamics and Emission Rates. Environmental Science and Technology Vol 15 No 3.

Freeze, R.A. and J.A. Cherry. 1979. Groundwater. Prentice Hall Publishers. Englewood Cliffs, New Jersey.

EPA 10/80 Ambient Water Quality Criteria for Polynuclear Hydrocarbons.

Gamerding, Amy P., Ken C.J. Van Rees, P. Suresch, C. Rao and Ron E. Jessup. 1994. Evaluation of in-Situ Columns for Characterizing Organic Contaminant Sorption during Transport. Environmental Science and Technology Vol 28.

Gamerding, A.P., R.J. Wagenet and M.Th.van Genuchten. 1990. Application of Two-Site/Two Region Models for Studying Simultaneous Nonequilibrium Transport and Degradation of Pesticides. Soil Sci Soc AM J vol 54.

Grundl, Tim and Greg Small. . Mineral Contributions to Atrazine and Alachlor Sorption in Soil Mixtures of Variable Organic Carbon and Clay Content. Department of Geosciences and Center for Great Lakes Studies, University of Wisconsin, Milwaukee.

Herrin, Russell T. 1994. Production and Metal Sorption Characteristics of Soil Colloids. Masters Thesis. Water Chemistry Program. University of Wisconsin Madison.

Karickhoff, S.W., Brown D.S. and Scott, T.A., 1979. Sorption of Hydrophobic Pollutants on Natural Sediments and Soils. Chemosphere, 10:833-846.

Kilmer J.W., R.A. Minear, C.W. Francis. 1987. Adsorption Studies Evaluating Codisposal of Coal Gasification Ash with Wastewater Sludge Containing Polycyclic Aromatic Hydrocarbons. ORNL/TM 2786, Oak Ridge National Laboratory. Oak Ridge, Tennessee.

Klemetson, Stanley L. 1985. Factors Affecting Stream Transport of Combined Sewer Overflow Sediments. Journal of the Water Pollution Control Federation Vol 57 No 5.

Lee, Linda S., P. Suresh C. Rao and Mark Brusseau. 1991. Nonequilibrium Sorption and Transport of Neutral and Ionized Chlorophenols. Environmental Science and Technology Vol 25.

Meylan, William, Phillip H. Howard and Robert S. Boethling, 1992. Molecular Topology/Fragment Contribution Method for Predicting Soil Sorption Coefficients. Environmental Science and Technology Vol 26 No 8.

McCarthy, John F., Thomas M. Williams, Liyaun Liang, Phillip M. Jardine, Louwanda W. Jolley, David L. Taylor, Anthony V. Palumbo and Lee W. Cooper. 1993. Environmental Science and Technology Vol 27 No 4.

Michelbach, S. and C. Wohrle. 1992. Setteable Solids in a Combined Sewer System - Measurement, Quantity, Characteristics. Water Science and Technology Vol 25 No 8.

Prey, Jeffery, Laura Chern, Steve Holaday, Carolyn Johnson, Terry Donovan and Percy Mather. 1994. The Wisconsin Stormwater Manual Part One: Overview. Wisconsin Department of Natural Resources Bureau of Water Resources Management Nonpoint Source and Land Management Section.

Rogge, Wolfgang F., Lynne M. Hildemann, Monica A. Mazurek, Glen R. Cass and Bernd R.T. Simoneit. 1993. Sources of Fine Organic Aerosol, 3. Road Dust, Tire Debris, and Organometallic Brake Lining Dust: Roads as Sources and Sinks. Environmental Science and Technology 27, 1892-1904.

Schillinger, John E. and John J. Gannon. 1985. Bacteria Adsorption and Suspended Particles in Urban Stormwater. Journal of the Water Pollution Control Federation.

Seybold, Cathy. 1992. PhD Thesis. Soil Science Program. University of Wisconsin Madison.

Shaw, Byron H., and James D. Berndt. 1990. An Assessment of the Impact of Stormwater Disposal Wells on Groundwater Quality. Report to the Wisconsin Department of Natural Resources, Bureau of Water Resources Management Groundwater Section.

Sims, Judith L., Ronald C. Sims and John E. Matthews. 1990 . Approach to Bioremediation of Contaminated Soil. Hazardous Waste and Hazardous Materials. Vol 7 No 2.

Snoeyink, Vernon L., and David Jenkins. 1980. Water Chemistry. John Wiley and Sons. New York

Spurlock, Frank C. and James W. Biggar. 1990. Effect of Naturally Occurring Soluble Organic Matter on the Adsorption and Movement of Simazine [2-chloro-4,6-bis(ethylamino)-s-triazine] in Hanford Sandy Loam. Environmental Science and Technology Vol 24.

Stumm, Werner and James T. Morgan. 1981. Aquatic Chemistry. John Wiley And Sons. New York

United States Geological Survey. 1994. Stormwater-Runoff Data from National Pollutiont-Discharge-Elimination System Monitoring for Madison, Wisconsin. Open File Report 94-***.

Valocchi, Albert. 1989. Nonequilibrium Adsorption During Reactive Contaminant Transport Through Heterogeneous Aquifers. Final Technical Report University of Illinois.

W & H Pacific. 1992. Compost Storm Water Filter System. Technical Summary.

Wilber, William G. and Joseph Hunter. 1979. Distribution of Metals in Street Sweepings, Stormwater Solids, and Urban Aquatic Sediments. Journal of the Water Pollution Control Federation Vol 51 No 12.

Wood, J.M., 1985. Effects of Acidification on the Mobility of Metals and Mettalloids: An Overview. Environmental Health Perspectives. Vol 63.

Xian, Xingfu and Gholamhoss In Shokohifard. 1989. Effect of pH on Chemical Forms and Plant Availability of Cadium, Zinc and Lead in Polluted Soils. Water, Air and Soil Pollution. Vol 45.

Zhu, B. and A. K. Alva. 1993. Differential Adsorption of Trace Metals by Soils as Influenced by Exchangeable Cations and Ionic Strength. Soil Science Vol 155 No 1.

Zelmanowitz, Sharon. 1991. The Ability of Subsoils to Attenuate Metals in Coal Pile Leachates. PhD Thesis. Water Chemisrty Program. University of Wisconsin Madison.

89073804635



B89073804635A

Water Resources Center
University of Wisconsin - MSN
1975 Willow Drive
Madison, WI 53706

Water Resources Center
University of Wisconsin - MSN
1975 Willow Drive
Madison, WI 53706

DEMCO

Smead

UPC 80559
No. R129-S

HASTINGS, MN



89073804635



b89073804635a